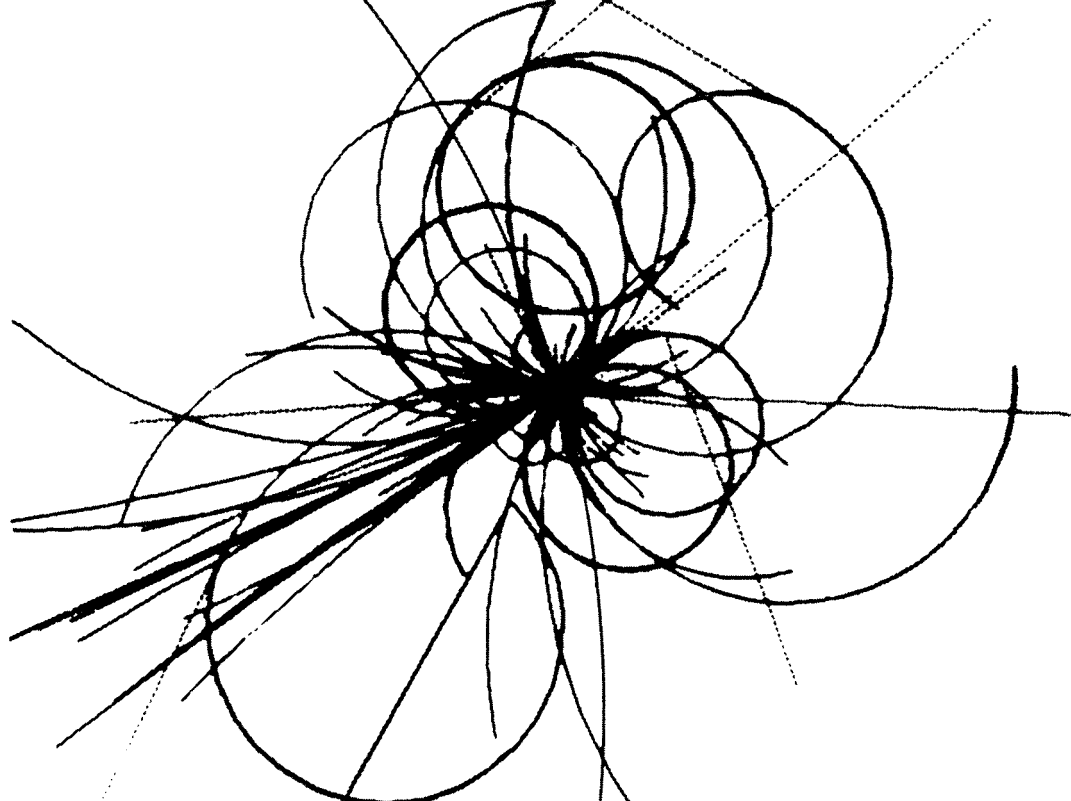


The Superconducting Super Collider



Non-Linear Finite Element Analysis of the SSC Superconductivity Magnet

M. Zaslawska

April 1987

DISCLAIMER

This report was prepared as an account of work sponsored by an agency of the United States Government. Neither the United States Government nor any agency thereof, nor any of their employees, makes any warranty, express or implied, or assumes any legal liability or responsibility for the accuracy, completeness, or usefulness of any information, apparatus, product, or process disclosed, or represents that its use would not infringe privately owned rights. Reference herein to any specific commercial product, process, or service by trade name, trademark, manufacturer, or otherwise does not necessarily constitute or imply its endorsement, recommendation, or favoring by the United States Government or any agency thereof. The views and opinions of authors expressed herein do not necessarily state or reflect those of the United States Government or any agency thereof.

DISCLAIMER

Portions of this document may be illegible in electronic image products. Images are produced from the best available original document.

SSC--126

DE90 014038

NON-LINEAR FINITE ELEMENT ANALYSIS OF THE SSC SUPERCONDUCTIVITY MAGNET

including the effects of cool down, operation, quench,
pre-assembly loads, and Lorentz Forces

M. Zaslavsky

April 1987

SSC Central Design Group*
Lawrence Berkeley Laboratory
Berkeley, California 94720

* Operated by Universities Research Association for the U.S. Department of
Energy

MASTER
DISTRIBUTION OF THIS DOCUMENT IS UNLIMITED

TABLE OF CONTENTS

	<u>Page</u>
I. Introduction	1
II. Model Description.	3
III. Analytical Verification.	5
IV. Method of Analysis	8
V. Material Description	12
VI. Loading Conditions	13
VII. Results.	21
VIII. Comparison with Experimental Results	45
IX. Future Work.	51

Appendices

I. Material Description	A-1
II. Loading Conditions -- Input to NIKE.	A-9
III. Secondary Results.	A-24
IV. ORION Output	A-31

I. Introduction

A two-dimensional plane strain model (using primarily quadrilateral elements) of the SSC magnet (cold mass) as shown in Fig. 1 was developed to determine the stresses and deflections under a variety of conditions. Cool down from room temperature to 4.35 K and the effects of quench in the coils were calculated using the computer code TACO -- a finite element heat transfer code. Pre-assembly loads, energization to 6.6 tesla, pressure due to liquid helium, Lorentz Forces on the copper plated beam tube, were incorporated in NIKE2D -- a 2-D vectorized implicit finite element code. The model for material behavior was treated as thermo-elastic plastic which required material properties as a function of temperature. The programs were run remotely on the Cray computers in Livermore via the Vax computers at Berkeley.

The Lorentz Forces on the copper plating on the inside of the beam tube, which consists of a thin-walled tube subjected to a $\cos\theta$ load, was verified by use of a closed form solution. This solution was also compared to one obtained using beam elements instead of quadrilateral elements. Additional verification of the model was performed analyzing the pre-assembly loads and thermal loads. The code NIKE2d incorporates the temperature results from TACO for each node as function of time. NIKE then calculated the displacements and stresses for the nodes and the elements respectively. ORION, a post-processor, was then used to plot time histories and contours. Both steel and aluminum collars were evaluated.

As a means to experimentally measure the stress in the coil, a section of the collar at the pole adjacent to the coil is replaced by a strain gauged "insert" sensitive to the stress in the circumferential direction. LBL uses an aluminum insert for both steel and aluminum collars and BNL uses a steel

insert in steel collars and an aluminum inserts in a aluminum collars.
Numerous NIKE calculations were made to complement the measurements made by
using the inserts.

II. Model Description

The model is a plane strain model, i.e., a two dimensional model whose length is sufficient to assume that the strain in the length direction, (ϵ_x) is approximately zero. Since the heat transfer/thermodynamic equations are independent of stress, they can be solved independently. Therefore, in the cool down operation, a specified set of nodes representing specific locations change temperatures (300 K to 80 K, 80 K to 4.35 K) and one solves for the temperature everywhere else as a function of time using a finite element code called TACO (a two dimensional finite element heat transfer code).¹ The output of TACO is the nodal temperatures as a function of time. NIKE² which is the structural analysis code requires the same identical model to that utilized by TACO. NIKE requires the temperature at a specific time (produced by TACO) and selects the material properties associated with that temperature including the thermal coefficient of expansion/ contraction. NIKE then proceeds to calculate the deflection at each node and the stress for each element. The model used by NIKE must therefore be exactly the same model used by TACO. The boundary conditions for the heat transfer and structural analysis are obviously different, but every node and element in TACO must be the same as that in NIKE.

The quarter of the cold mass was modeled because of symmetry and as a consequence the computer time is significantly reduced over having to model the entire cold mass. The boundary conditions for TACO and NIKE are obviously different, but permit the use of 1/4 section.

The mesh which consists of the nodes, their location, and the elements which are made up of a set of nodes and a material number. The mesh is generated through use of a code called MAZE,³ (an Input Generator). It is

unfortunate, but all these codes were put into the MFE Library over two years ago and subsequently ignored until now. As a consequence, corrections discovered at LLNL using these codes were not incorporated into the MFE Library. In addition, NIKE was updated some thirty times in the past two years without documentation. Therefore, in order for us to use these codes, extensive verification analysis was performed consistent with QA,⁴ which we will discuss later. However, it should be noted that the version of MAZE, NIKE, ORION⁵ we use are not in the MFE Library, but in our private directory; we have a version which we have checked out and consistently use that version. The MFE Library of engineering codes is being updated, but it still has not been completed.

In producing the model, each part or component must be described separately. In addition, each part must contain a sufficient number of elements such that the solution converges. A finite element analysis is an approximation. In order to insure that the solution converges, the number of elements are doubled until no differences in the solution are obtained. We have found therefore, that the beam tube requires 30 elements circumferentially and 3 elements thick in a quarter section to capture the response. The beam tube is three elements thick which is the minimum in order to capture bending. Another area of caution is the aspect ratio which is the length of the element compared to its width. If the loading was purely radial, the aspect ratio would not be important. The aspect ratio was varied from 30/1 to 1/1 and no differences were observed between 10/1 and 1/1. Maximum stress was therefore achieved with an aspect ratio of 10/1.

There are four types of slide lines in the code. They are: sliding only, tied, sliding with voids or separation, and sliding with separation and

interface friction. It is the last type of slide lines -- sliding with separation and interface friction which characterize the results presented in this report and models reality.

The final model consists of a 1/4 section, 18 different materials, 753 nodes, 497 elements, 25 slide lines consisting of 205 slave nodes and 227 master nodes. The geometry and loading permits the using only 1/4 section, which in-turn reduces the computation computer time without loss in accuracy.

III. Analytical Verification

In order to perform verification, the problem was decomposed into basic elements and hand calculations and/or other codes were utilized.

The beam tube loading due to Lorentz forces as a result of eddy current was taken as a separate problem. In this case, a closed form analytical solution was developed consistent with similar analysis performed by others¹⁷. Complex methods using shell theory, degenerate to this solution because the Lorentz forces are a $\cos \theta$ force distribution. NIKE3D,⁶ a totally different code than NIKE, was also utilized, using beam elements as distinct from the quadrilateral elements used in NIKE; excellent agreement was achieved. Therefore, at least 2 independent methods verified the solution obtained by NIKE. Increasing the number of elements circumferentially or through the thickness did not change the results. The NIKE3D calculations required only 30 beam elements in lieu of the 300 quadrilateral elements because of the sophisticated properties of a beam element (10 beam elements circumferentially). This is mentioned because in future work, it will be necessary to go to 3D to capture the cooling and quench phenomena in the longitudinal direction and beam and shell elements can be used to reduce running time. Unfortunately, beam or shell elements are not available in NIKE2D.

The thermal stress determination of cold mass assembly can be decomposed to a series of concentric shells coupled with the Lame' equations. The thermal stress, σ , was expressed as $E\alpha\Delta T$ where α is the coefficient of thermal expansion/contraction and ΔT is the temperature change. NIKE reads the temperature associated with each node as a function of time. The strain, ϵ is $\alpha\Delta T$ where $\epsilon = \Delta l/l$ and Δl is the change in length. E is the modulus of elasticity over temperature T_2 , T_1 , ΔT . This is the method by which NIKE calculates the stress and displacement except that it iterates the solution so that the boundary conditions are met, and it solves the stress for each element. The thermal stress calculation using NIKE was isolated from some of the other effects such as prestress so that a direct compression was made between NIKE and simple hand calculations; excellent agreement was also achieved in this example. In this manner, the code was verified as far as thermal stress computations. TACO, which calculates temperature is one code that has not changed much the last ten years and has adequate documentation. Nevertheless, there are a number of checks which can be performed. One is the steady state calculation, which has an obvious result. Another is performing hand calculations decomposing components of cold mass as concentric shells. The third approach to verify TACO is by comparing it to another code. That code is TOPAZ⁷ which was written independently of TACO. Except, TACO was used to verify TOPAZ, since the latter is more recent. NIKE calculates the deflection at each node, then calculates strain, using properties of materials, it then calculates the stress. In an analogous manner, this operation can be done by hand. Using Lame's equations and knowing the inside and/or outside pressure, one can calculate the radial and circumferential stress using thick walled or thin walled theory. In the above manner, all aspects of the problem can be verified. What the computer presents is the

simultaneous application of all the boundary conditions on a complex geometry consisting of numerous parts composed of complex temperature dependent material properties.

The method used in NIKE to determine when two parts have come together or have separated is based on the convergence tolerance on displacement and the convergence tolerance on energy. The default or recommendation of the author of the code is 0.001 and 0.010 respectively. The convergence tolerance was increased by a factor of 10 and the same results were obtained. When the tolerance was increased, convergence was obtained in two or three iterations. With the default value, convergence was obtained in 44 iterations. However, that was only in the beginning of the calculation where the temperature changed quickly on cool down. After the initial significant change, the number of iterations needed to converge was one or two. The results show that convergence is obtained and is not sensitive to convergence tolerance on displacement or energy for the range investigated.

IV. Method of Analysis

The method used to perform the analysis has not changed since its inception last April. Time consuming has been the problem to obtain a suitable verifiable set of computer programs which are compatible. The computer codes MAZE, TACO, NIKE, ORION, need to be compatible as not all versions of the programs will be accepted. For example, the version of ORION (which is the post-processor) in the MFE library is not compatible with the version of NIKE (structural mechanics code) in our private directory. Therefore, a compatible version was obtained from SANDIA and is in our directory. The MFE library of engineering codes is being updated, however it yet has to be done as of this date.

The following procedure is used to obtain a solution.

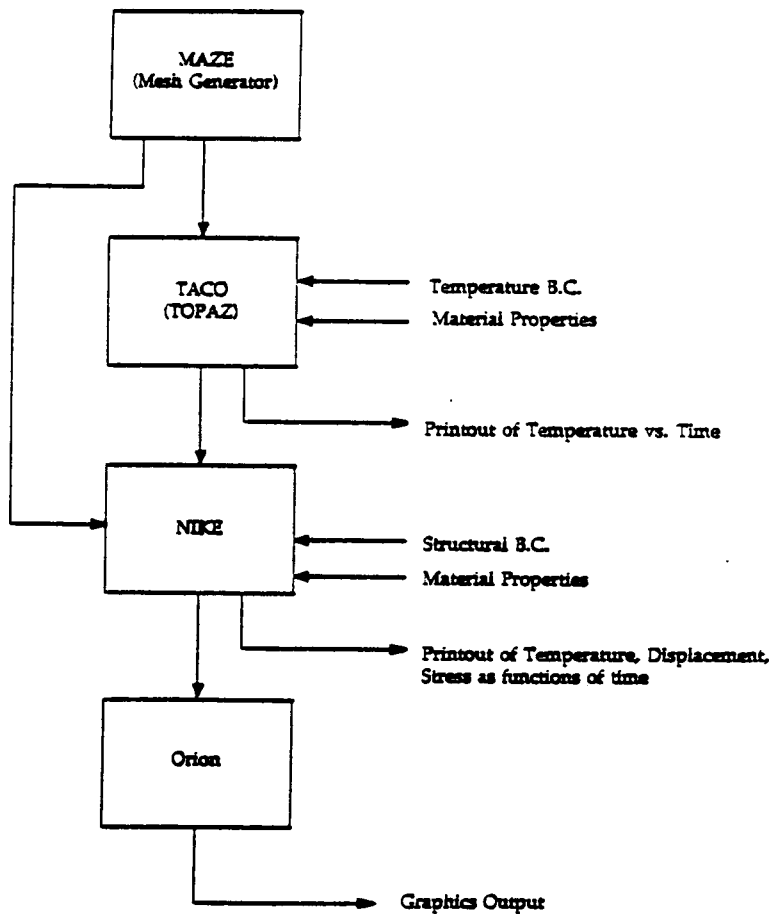


Fig. 1. Procedure.

MAZE is the computer program which is used to develop the geometry, the nodes, elements, slidelines. This geometry is used for both TACO and NIKE. TACO requires material properties and boundary conditions and the output is the temperature at each node as a function of time. The output comes in the form of a printout and a plot-file. The plot-file is used as an input to NIKE. NIKE requires material properties additional from that of TACO. Boundary conditions in the form of displacement, pressure, load, stress as a function of time makes up the input file. In the execution of NIKE, the plot file from TACO is called out in order to couple NIKE to temperature. The output of NIKE at each time specified are the normal and shear stresses and the principal stresses for each element and the deflections and temperature for each node.

ORION provides the graphics output in any of the standard forms -- principal stress, yield stress, etc. versus time. In addition to stress, displacement and temperature can be plotted. A print out is also available at each time step. ORION will calculate different types of strains from the displacement. Examples of ORION output are given in the Appendix.

The computer program MAZE translated the cross-section of the dipole magnet, Fig. 2A, including the details given in Fig. 4B to the mesh given in Fig. 3.

The programs are on the C&D Cray computers in Livermore and in private directories (FILEM). The terminal is in Berkeley which is then connected to the MFE system in Livermore. The programs are run remotely and the output file transmitted to Berkeley as described above. The Berkeley terminal ties into the VAX computers at Berkeley which then tie into Livermore (MFE Net).

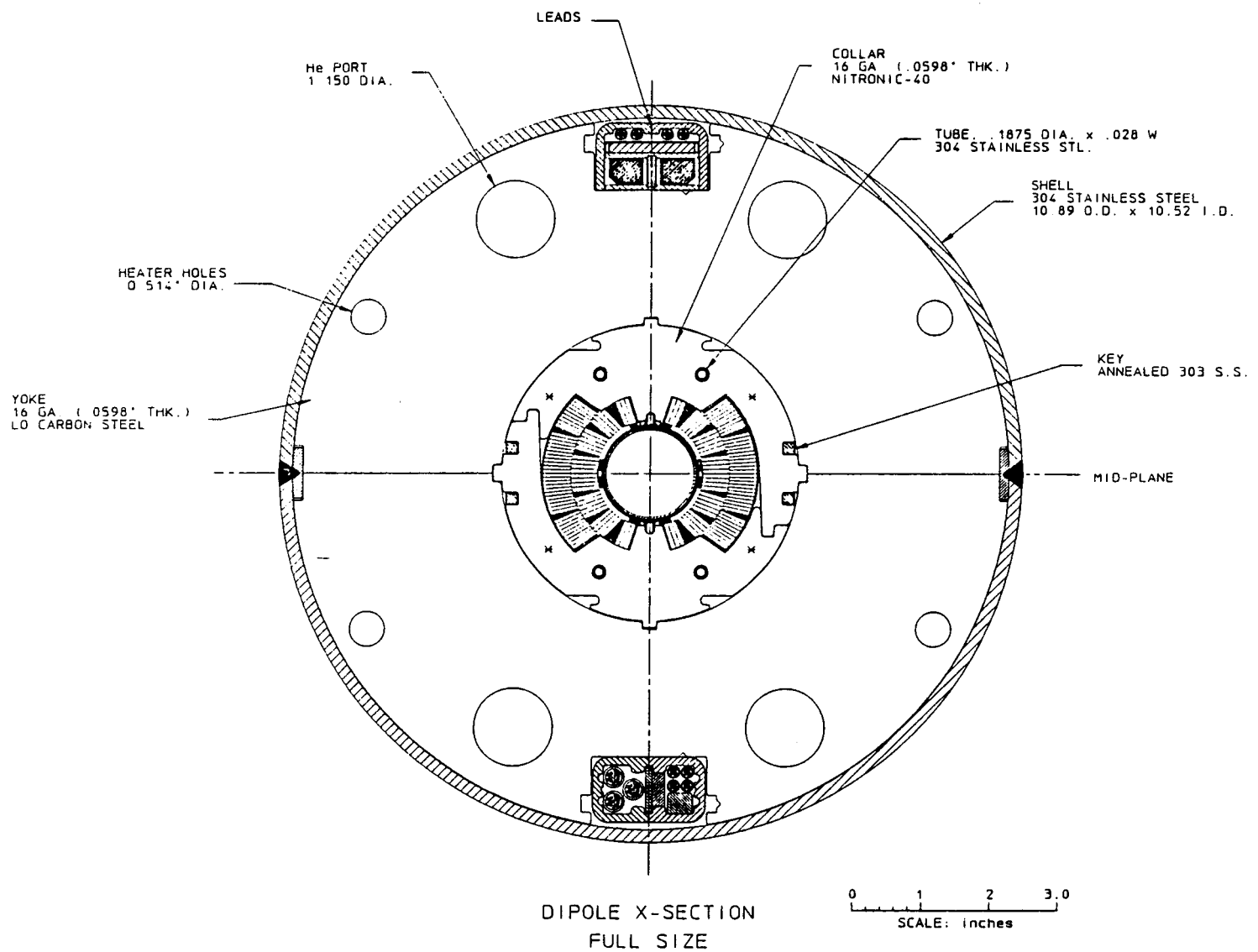


Fig. 2. Cross Section - Dipole

STRUCTURAL QUENCH/STEADY STATE OPERATION - AL. COLLAR 4-2-87

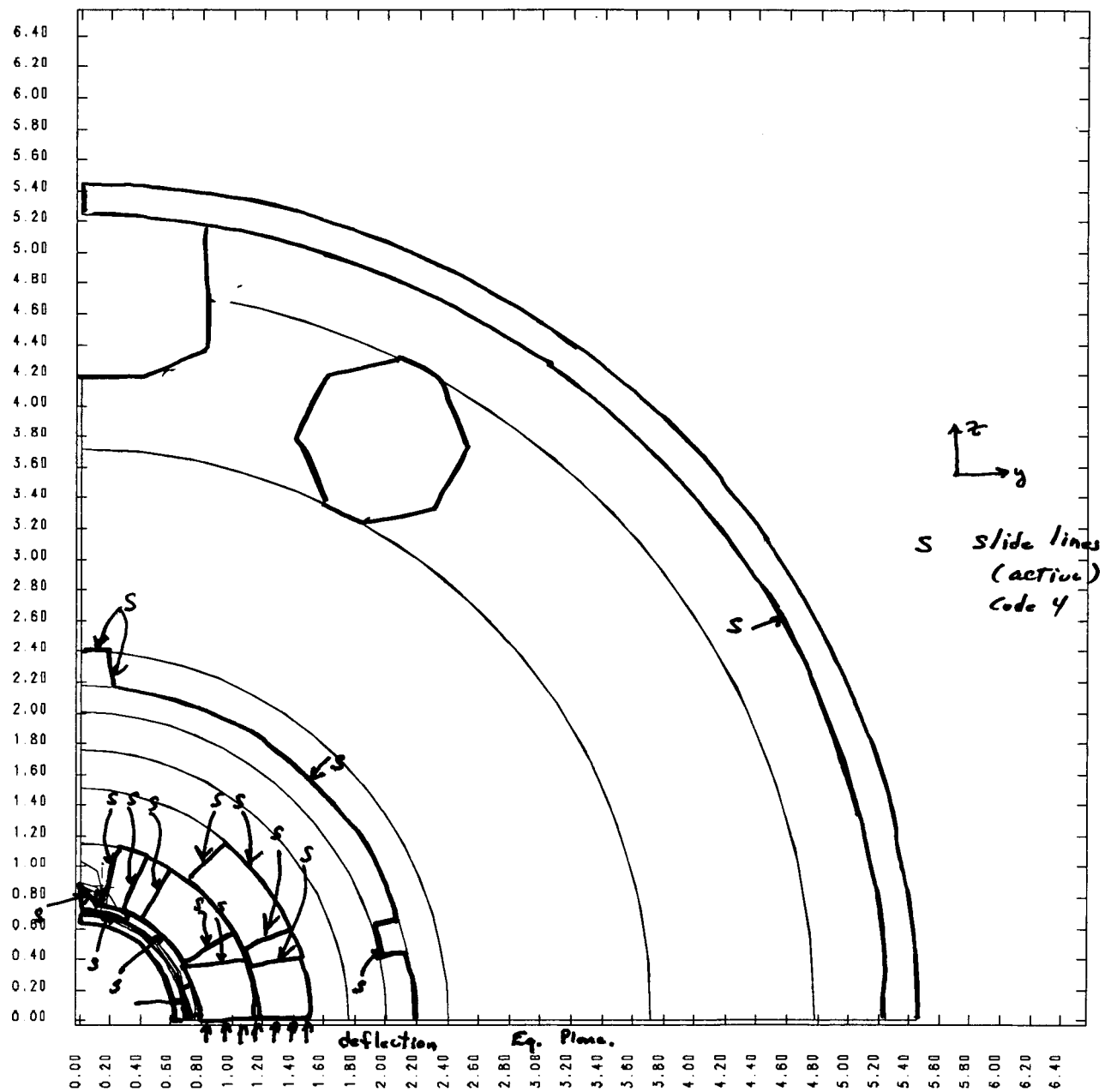


Fig. 3. Model showing components and slide lines (active).

V. Material Description

The cold mass contains some 18 different materials. Some of the material properties required by TACO and NIKE were difficult to obtain and subject to discussion. In the case of the coil, a sensitivity analysis was performed on the properties of the coil to determine the influence of uncertainty on the results. In varying the material properties of the coil, the model was changed from thermo elastic plastic to orthotropic. In TACO, the model selected was isotropic and the properties temperature dependent. The problem is non-linear because the problem is transient with temperature dependent properties. Density, specific heat, and thermal conductivity are required for each temperature in TACO. Since this is not a dynamic problem, density is not utilized. For NIKE, a thermo-elastic-plastic model is used requiring density (again not of importance), Young's modulus, Poisson's ratio, coefficient of thermal expansion, and if allowed to go plastic, yield stress and plastic hardening modulus, (all) as a function of temperature. For the thermo-orthotropic elastic case, the modulus, Poisson's ratio, coefficient of thermal expansion/contraction, all in the three (3) directions, shear modulus in the plane formed by first two axes, and the relationship between the three material axes and global or local coordinate systems, are required. The units must be consistent and consistent with the mesh. Therefore, BTU, inches, K, lbs, seconds, were selected, since the mesh was developed in "inches" and we think in terms of "psi". See Appendix I for tables on material properties.

VI. Loading Conditions

There are two types of loading -- thermal loading and structural loading, and both types are identified in the cold mass. The thermal aspect of the analysis has to be run first. The structural analysis incorporates the affect of the thermal stresses and displacements, plus any other additional structural loads. Since two different collars are being evaluated, steel and aluminum, two separate thermal calculations were required irrelevant of the fact that the models differ slightly. The model with the Al collar contains no clearance between the collar and the yoke, whereas the model with the steel collar does contain a clearance. The effects of cool down, quench, and warm up were calculated.

The cool down occurs in two stages (Fig. 5A). From 300 K to 80 K and from 80 K to 4.35K. The cool down occurs in the helium port and annulus around the coil. Here liquid helium is injected at a specified rate. For cool down, the temperature at the nodes around the helium port and annulus are specified since TACO has difficulty in handling liquid solid heat transfer problems. In NIKE, the helium is described as an element. Temperature ramp down from 300° K to 80 K and from 80 K to 4.35 K is artificial. In order to capture the pressure exerted by the helium in the annulus during quench, a pressure of 40 atms (600 psi) is placed on the surfaces around the annulus. This is a conservative number selected from various analyses and shall be verified experimentally during the next long magnet tests.

On quench (Fig. 5B), the temperature of the coil increases from 4.35 K to 300 K in \sim 600 ms.⁸ The temperature profile in Fig. 5B (solid lines) were obtained from analysis that did not consider heat transfer from the coil to the surrounding components during quench. An "approximation" of this function for 500 K is given in Fig. 5C. Almost all of the energy stored in the magnet

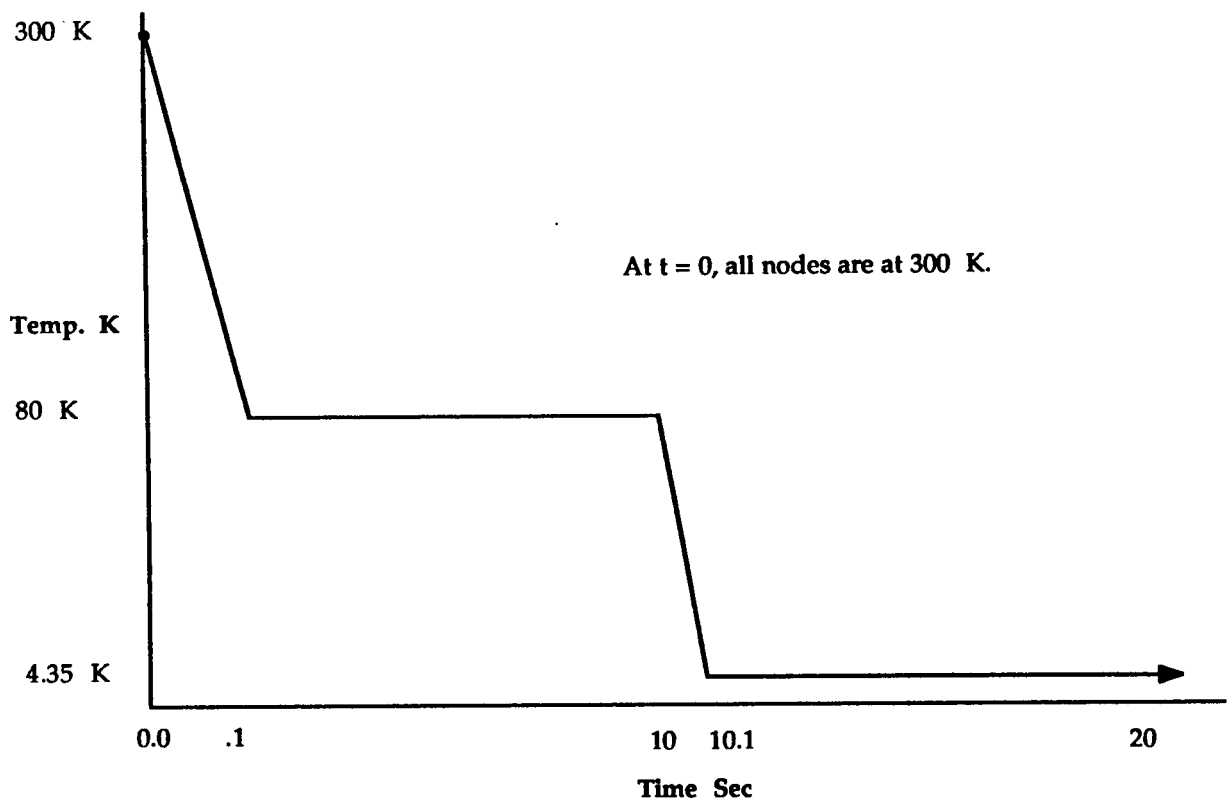


Fig. 5A. Cool down

is expended by 600 ms. After an initial quench, heaters down-line trigger additional quenches in the coil. In the analysis performed here, the nodes in the coil were programmed to read the maximum temperature specified in Fig. B.11-6 (Fig. 5B) -- and at maximum rate. TACO in-turn, calculated the consequence of such an input to the coil and a temperature distribution as a function of time was calculated for each node in the cold mass.

Using the values of energy deposition into the coil, I^2R , that were used to calculate the solid line in Fig. 5B, a heat transfer calculation was performed using TACO up to 80 seconds. The TACO calculation does not include vaporization of helium nor the helium flow, and 80 seconds was selected arbitrarily. The TACO calculation is more accurate than solid line since the

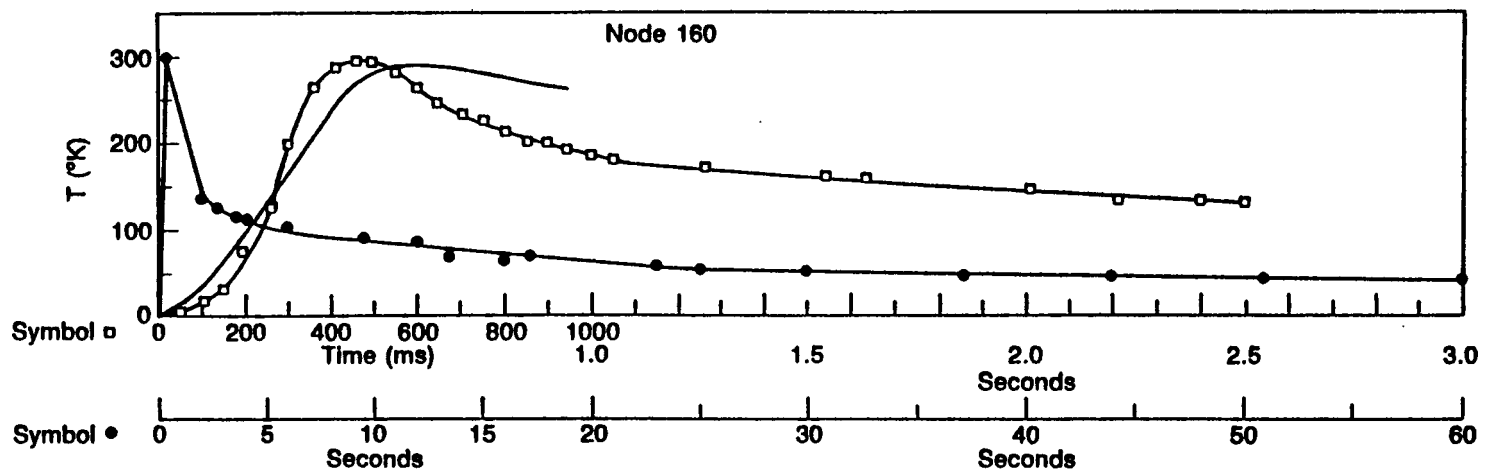


Fig. 5B.

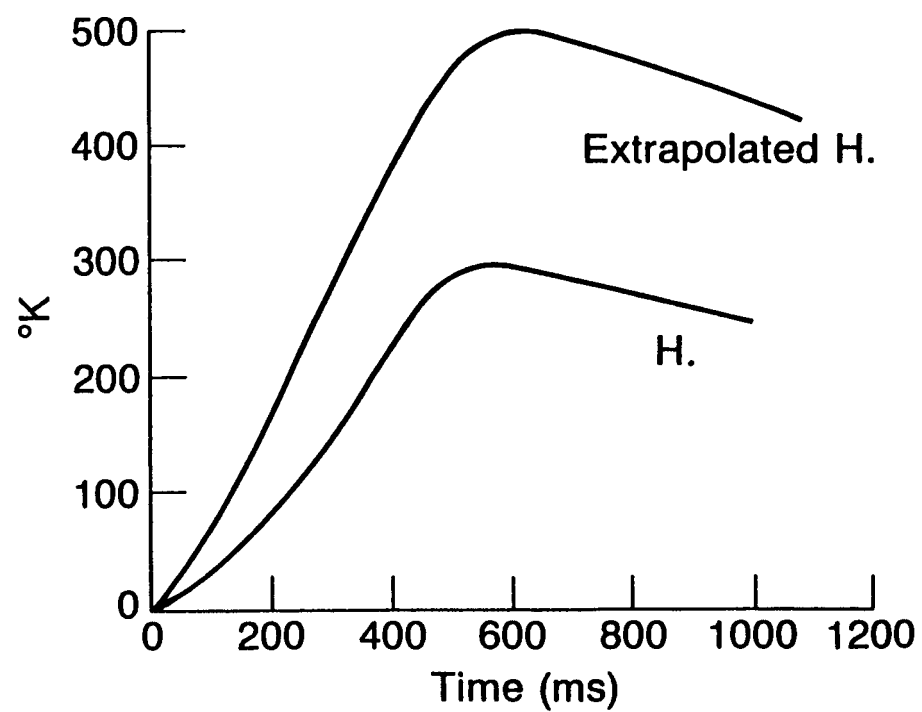


Fig. 5C.

solid line is an extrapolation after 500 m.s. The output from the TACO calculations are the temperatures throughout the cold mass as a function of time up to 80 seconds, which is then used in NIKE. The TACO calculation conserves energy and overprediction of temperature in the latter part of quench is avoided.

If allowance is made for vaporization of helium, the results using heat transfer, TACO, and Fig. 5C are in agreement. After 0.4 seconds, the new profile is more accurate and new stress calculations were required.

Prestress is the stress in the coil after cool down, necessary to prevent the coil from moving away from the collar in the circumferential direction when the coil is energized. Prestress is the resultant circumferential stress obtained as consequence of assembly. The prestress in the calculation is imposed by having a 3 mil deflection on the inner coil and a 2 mil deflection on the outer coil, along the equatorial plane, since the equatorial plane relates the model to the "world". While it is possible to apply the deflection at the pole and reduce its affect due to cool-down, the NIKE program is not set-up to do this easily. It could be incorporated in the code without much effort, but currently it is unavailable. Symmetry is obtained by allowing movement only along the equatorial axis and the polar axis except at the coils and at specific nodes to prohibit translation of the entire mass and rotation. (At $t = 0$, node deflection on coil is zero since impulsive loading creates analytical distortions). At $t = 0.05$, the deflection is 3 and 2 mils as indicated and for entire calculation, at the equatorial plane. The 3 mil deflection corresponds to a initial stress of 7500 in the circumferential direction, all along the inner coil, before cool down.

In Fig. 6A, the various components are visible; ring, coolant channel, yoke, collar, coil, wedge, G-10, annulus, beam tube and the active slide

STRUCTURAL QUENCH/STEADY STATE OPERATION - AL. COLLAR 4-2-87

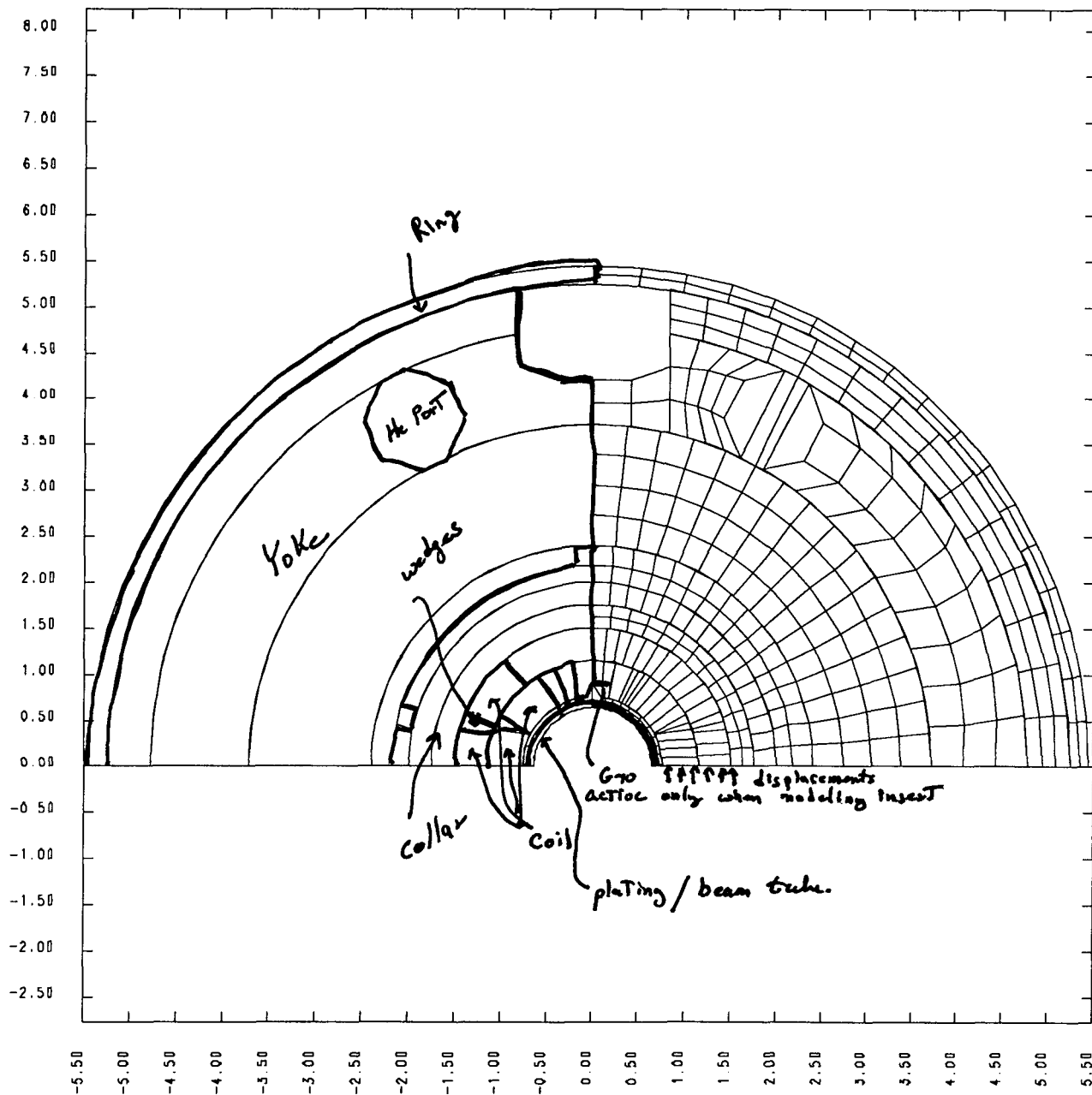


Fig. 6A. Mesh showing components.

STRUCTURAL ANALYSIS QUENCH/TRANSIENT SOL. L. He. elements, 7-10-86

dsf = 1.00000e+00

time= 6.60000e-01

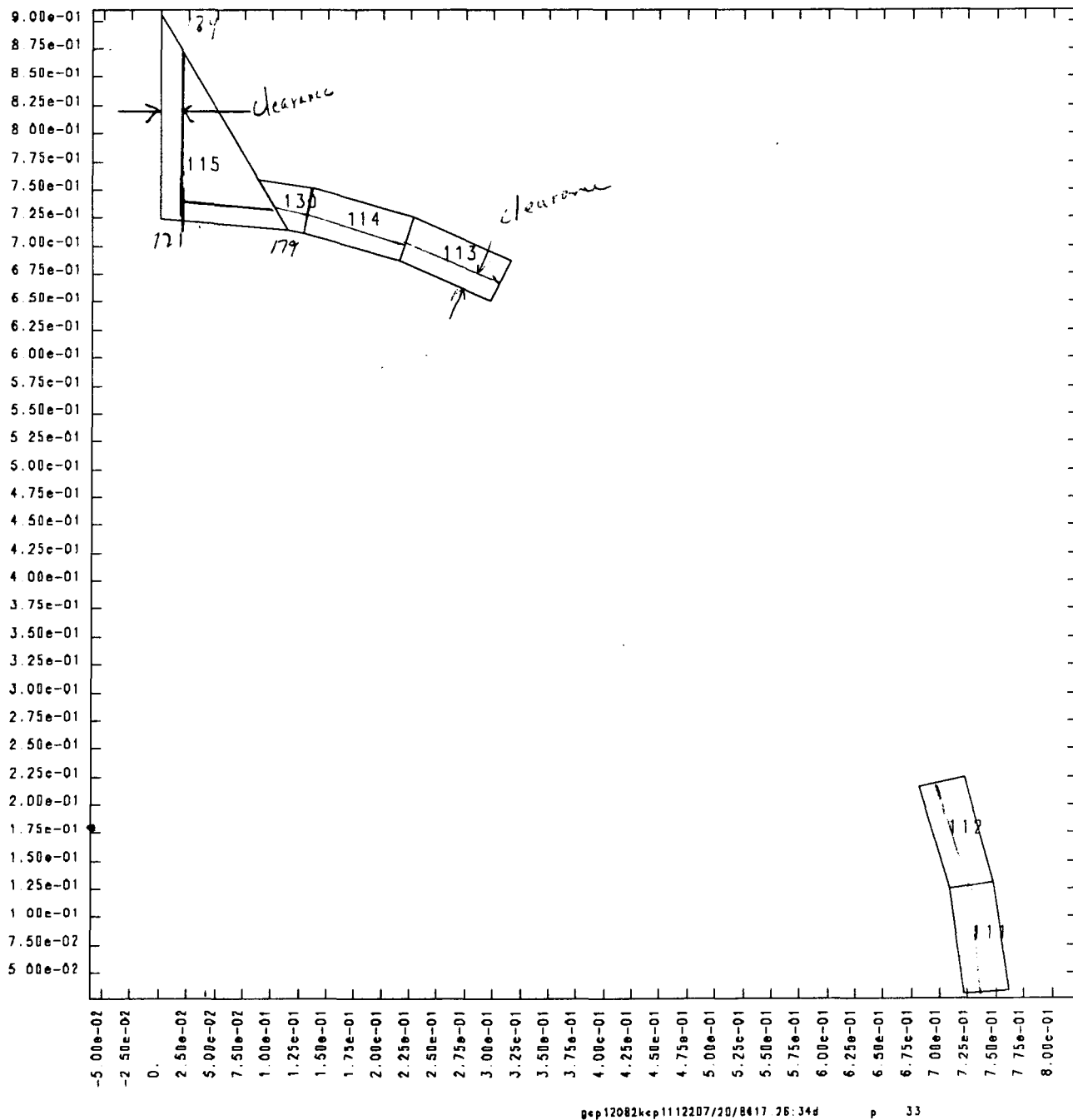


Fig. 6B. Clearance between G-10 space and beam tube.

lines. Initially a clearance was not provided between G-10 and the plastics around the beam tube. As a consequence, the stress in the beam tube were very high. When clearances were provided, Fig. 6B, these high stresses disappeared. In particular, when the G-10 spacers were modeled more accurately at the pole, i.e., a clearance provided between the pole and G-10 (element 115) in addition to a radial clearance of 5 mils, did the high stress in the beam tube and copper-plating disappear. The absence of a clearance distorted the stress in the coil. With an adequate clearance, friction is introduced on all sliding surfaces without obtaining results that are in contradiction with measurement. On cool down, without adequate clearance the coils (I.C. and O.C.) separate and lose contact. If there is insufficient clearance, then the coils will be pinned at two points and deflect in the center thus prohibiting transfer of circumferential stress, see Fig. 14. Friction will exacerbate this condition. BNL observed the high stress in the beam tube and includes a clearance. LBL inserts the beam tube after assembly and automatically allows for clearance. The calculation with the aluminum collar and no clearance resulted in a maximum stress in beam tube approximately twice that of the aluminum collar. With sufficient clearance, there is no large stresses in the effect on the beam tube. Therefore, sufficient clearance is required for collaring and is included in the model.

There is also a clearance between the collar and the yoke when a steel collar is employed but not when an aluminum collar is used.

It is these undocumented clearances which were not accounted for in our initial calculations, the consequence of which produced results that were inconsistent with observations/measurements. The ANSYS calculations did not include the beam tube, and surface contact was maintained (sliding only).

The loading conditions consist of thermal loading, displacements of the coil at the equatorial plane, the helium pressure, and the Lorentz forces on the beam tube and coil, Fig. 7. Complicating the loading requirements are the clearances and considerations of an aluminum collar over a steel collar.

The thermal loads have already been described. NIKE reads the temperature at each node as a function of time, determines the appropriate material properties, and add the thermal displacement to the structural displacement. Almost all functions used to describe pressure, load, or displacement need to be inputted as a function of time and position, lets say $g(t,x)$. Now $g(t,x)$ can be decomposed to $c_1(t) c_2(x)$ where c_1 and c_2 are functions only of time or position. $c_1(t)$ is often referred to as a multiplier. Therefore, at t_1 , where t_1 is a specific time, the computer will read the value for $c_1(t_1)$ and multiply the two functions, and that will be the force, displacement, or pressure. The Lorentz force on the coil is constant during operation and when quench begins, decreases with the current. Therefore $g(t,x) = c_1(t) c_2(x)$ where $c_1(t)$ is the current decay and $c_2(x)$ is the scalar value dependent only on location (node). This is manner by which forces, displacement, and pressures are input to NIKE. I believe it is done in this way because this follows Fourier series solutions to certain classes of differential equations. In the Appendix, the input to NIKE is given in tables which are of the form $c_1(t)$ or $c_2(x)$.

VII. Results

The primary purposes or objectives of the analysis are to perform time dependent analysis to capture interaction of components within cold mass assembly:

1. Insure the adequacy of the design.
2. Determine those specific areas were the current design does not meet requirements.
3. Consider modification of the design and evaluate the suggested modifications.
4. Evaluate the measurement techniques.
5. By performing sensitivity studies to identity those parameters which the design is particularly sensitive. This will then suggest what additional material property tests should be performed.
6. Determine where the analysis fails short of its objective, and identify the direction of future work.
7. Provide documentation to expedite analysis of other type magnets.

In order to address the above, it is necessary to decompose this chapter on results into various sections which in-turn parallel sets of computer calculations: these are pre-stress, operation, quench, warm-up, stability, and miscellaneous. Miscellaneous or secondary results include clearance, bumpers, and sensitivity studies and are found in the Appendix. In all cases, both aluminum and steel collars are evaluated. In addition to the difference in material properties between steel and aluminum, there is the clearance between the yoke and collar when using steel collars and none, when using aluminum collars. Therefore, there are always two TACO or heat transfer calculations required. The results contained herein with the exception of one set of calculations (identified), include all the appropriate clearances and none of

our initial calculations. These results in are based on the design as of 4/87 together with proposed changes (elimination of bumpers).

a) Prestress -- prestress is that stress required to prevent the circumferential displacement of coil away from the collar during energization and operation. Prestress is one of the experimental measurements which could be used to validate analysis or visa versa. The experimental verification will be discussed in the next section.

While the results in this chapter are separated by sections or sets of calculations, it is clear that they are all interrelated. If the model is adopted as discussed with sufficient clearance (≥ 5 mils), what is the prestress. For $t = 40$ mils thickness, $E_{coil} = 3 \times 10^6$, $\alpha = 1.3 \times 10^{-5}$, at $T = 4.35$ K, we have:

Table I
Effect of Input Displacement on Prestress
(ksi)

	A I=9/7 mil Steel Collar I.C. (Insert)	B I=7.3/4.5 mil Steel (Insert)	C I=5.6/3.2 mil Steel (Insert)	D I=3.2/2 mil Steel (Insert)	E I=3.2/2 mils Al Collar (No Insert)
116 (Eq.)	6.25	-4.35	-2.6	-0.567	-0.55
129 (Pole)	-5.73	-3.9	2.0	0	-0.96
O.C.					
135(Eq.)	10.77	-15.3	-12.0	-2.3	2.5
143 (Pole)	-7.07	-3.75	-1.7	-0.29	-0.7
S.G. Lee (131 & 132)	-8.8	-6.35	-3.8	-2.0	-7.85
	2				

where I.C. is inner coil, O.C. is outer coil, and 116, 129, 135, 143, 131, 132 are element numbers.

Comparing the steel to Al ($I = 3.2/2.0$ mil), columns D and E, the Al collar shows significantly higher pre-stress at the end of cool down. Numerous calculations have all shown that the pressure or absence of an insert does not effect any component except beam tube and plating and then only if the clearance is insufficient. At the pole, the stress in Al is 0.96 ksi and steel is 0 for the I.C. and 0.7 ksi in Al compared to 0.29 ksi instead. It is clear from Table XII, that 3.2 and 2 mils deflection is insufficient and that higher deflection are required; 7.3 and 4.5 mils for inner and outer coils respectively. Comparing column B to column D, we see that it takes an additional 4.1 mils deflection at equatorial plane over 3.2 mils existing to gain 3.9 ksi prestress, or in other words we lost approximately 44% of our initial stress due to cool down. This is shown in the following figure.

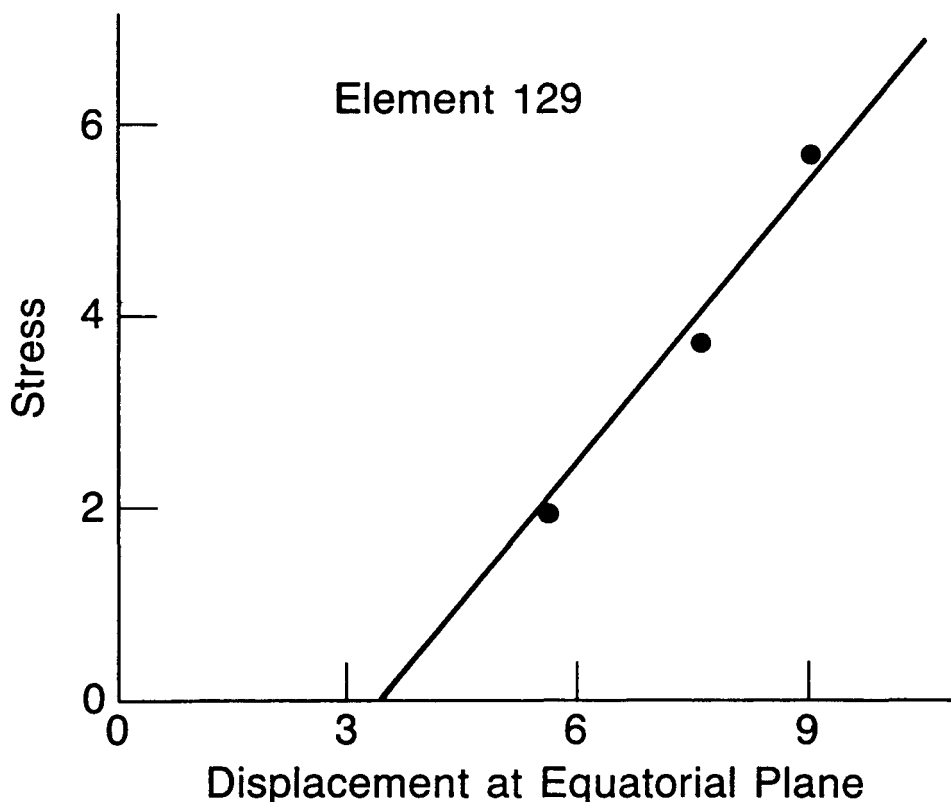


Fig. 7. Relationship between deflection at equatorial plane (I.C.) and Pre-stress

It should be noted that the calculations are the results of transient cool down phenomena. The highest stress occurs at the end of cool down. The stress state at 4.35 K as a result of transient temperature effects, presence of bumpers, 3 mil clearance, 7.3/4.5 mil input, is as follows:

Table II
Maximum Stress at End of Cool Down
(ksi)

	<u>Al Collar</u>	<u>Steel Collar</u>
Plating	70.5 ksi	60.0
Beam tube	91.0	76
Coil I.C. σ_{θ}	-4.35	-4.35
σ_{θ}	-4.9	-3.9
O.C. σ_{θ}	-15.3	-15.3
σ_{θ}	-4.1	-3.75
Collar	62.5	100
Yoke	21	27
Ring	19	20

NIKE can produce the results at steady state, 4.35 K without going through the transient phenomena. It can set $T_1 = 300$ K and $T_2 = 4.35$ or $T_1 = 300$ K, $T_2 = 80$ K, and $T_3 = 4.35$ K when the temperatures are the temperature at every node in the cold mass. However, this method of calculation (which does away for the need for the TACO calculation), produces results for pre-stress at the end of cool down that differ from a transient calculation. The transient calculation is more accurate as this is the way cool-down occurs. The difference in pre-stress can be ~20% depending on the values of α selected for the coil and the collar and how many interim values of α are selected in the transient calculation.

From Table XIII it is observed that the aluminum collar has a stress of 62.5 ksi at 4.35 K and steel has a stress of 100 ksi. This is due to the fact that E of aluminum is 1/3 that of steel.

All the stresses in Table II meet the design requirements. The Central Design Group (CDG) has proposed a set of structural and other requirements¹¹. The yield strength of nitronic 40 at 4.35 K is 180 ksi and the Al is 94.8 ksi. The design requirements for bending is \leq 90% yield and membrane + bending \leq 2/3 yield, therefore the design requirements for cool-down are satisfied. The stress in the coil can go to approximately 20 ksi at 300 K during assembly, so that values in Table I are acceptable. While 20 ksi is sort of a limit at 300 K, a definitive value is being determined based on mechanics and the properties of the composite. The coil is being analyzed separately and the stress on the coil plastics ascertained. If we know the properties of the plastics well enough, we can then determine the level of creep. Therefore, every effort must be made to evaluate the properties.

b) Operation. When the system is at steady state at 4.35 K, the magnet is energized and the Lorentz forces on the coil are activated. R. Meuser¹⁰ provided the input to the NIKE model based on 6.6 Tesla. Meuser's input is partially given in Fig. 9 (for complete input see Appendix II). Converting Meuser's force to stresses is given in Fig. 10. It should be noted that to convert force to stress, the code is simply dividing by area -- displacement has no role in this portion of the calculation. It is noted that the stress at the equatorial plane for I.C. is 7291 psi. The pre-stress in the elements adjacent to the collar are 2000 psi and 1700 psi for I.C. and O.C. respectively. Considering the potential variability in Lorentz force (6.6 Tesla to 8.5 Tesla) and a factor of safety, a minimum value of two times these stressors are required to prevent the coils from separating from the collar: 4000 psi I.C. and 3000 psi O.C. These results are in close agreement with Attachment B⁸ and undocumented data coming from BNL since Attachment B was published.

The 4000 psi I.C. is required which compares to 3600 psi in Attachment B. Now if we return to the pre-stress after cool down, for $I = 7.3/4.5$ mils, we have 3.9 ksi I.C. and 3.75 ksi for outer coil and therefore 7.5/4.5 mils will meet the pre-stress requirement.

c) Quench. The input to the quench calculations are shown in Figs. 5C and 7. The temperature from Fig. 5C are the temperatures of the coil at each node and is input to TACO. TACO then calculates the temperature at each node of the cold mass as a function of time. This is done separately for the Al collar and the steel collar. The 300 K curve in Fig. 5C is found in Ref. 8. The 500 K curve in Fig. 5C is an extrapolation. While we made the 500 calculation, it was concluded that most plastics would deteriorate at 500 K. Therefore, with the current design utilizing G-10, kapton, epoxy, Kevlar, and Teflon, 500 K as a CDG requirement is not feasible.

Quench

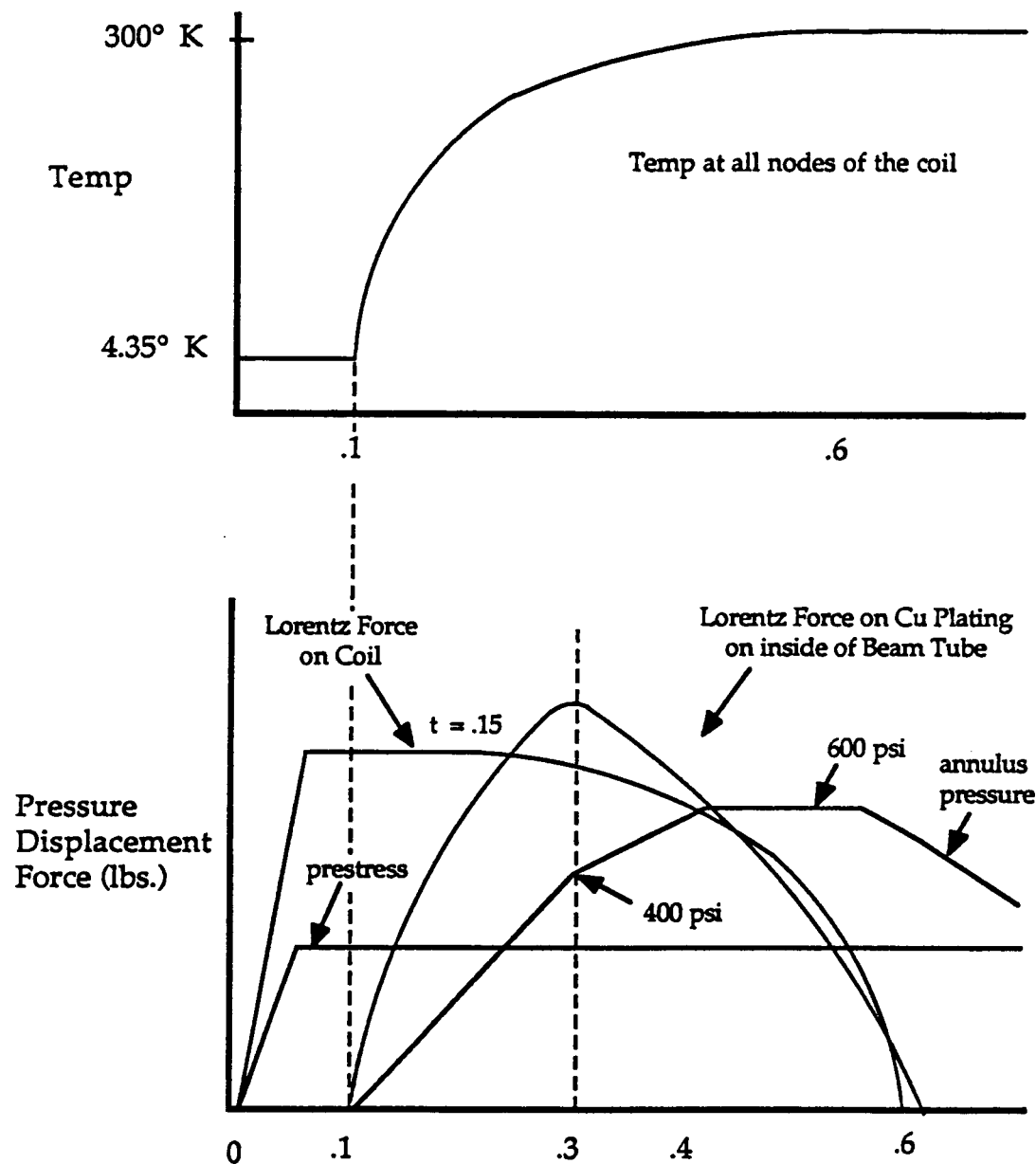


Fig. 8. Loading conditions.

STRUCTURAL ANALYSIS QUENCH/TRANSIENT SOL. L. He. elements, 7-10-86

dsf = 1.00000e+00

time= 6.60000e-01

LORENTZ FORCE - 1bs./in

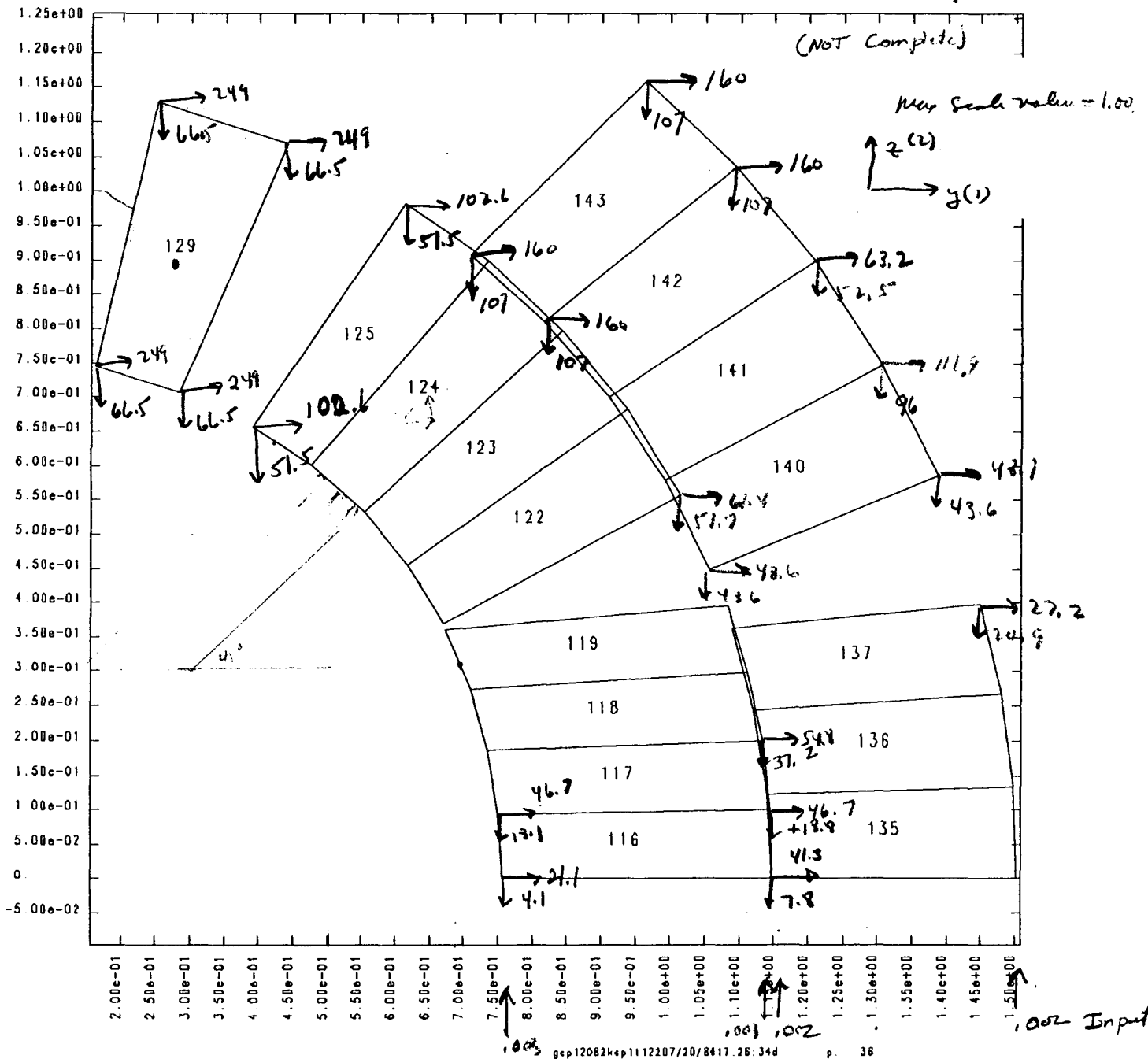


Fig. 9. Lorentz Force -- pounds/inch.

STRUCTURAL ANALYSIS QUENCH/TRANSIENT SOL. L. He. elements, 7-10-86

dsf = 1.00000e+00

time= 6.60000e-01

LORENTZ "STRESS" at 4.35°K. PSI

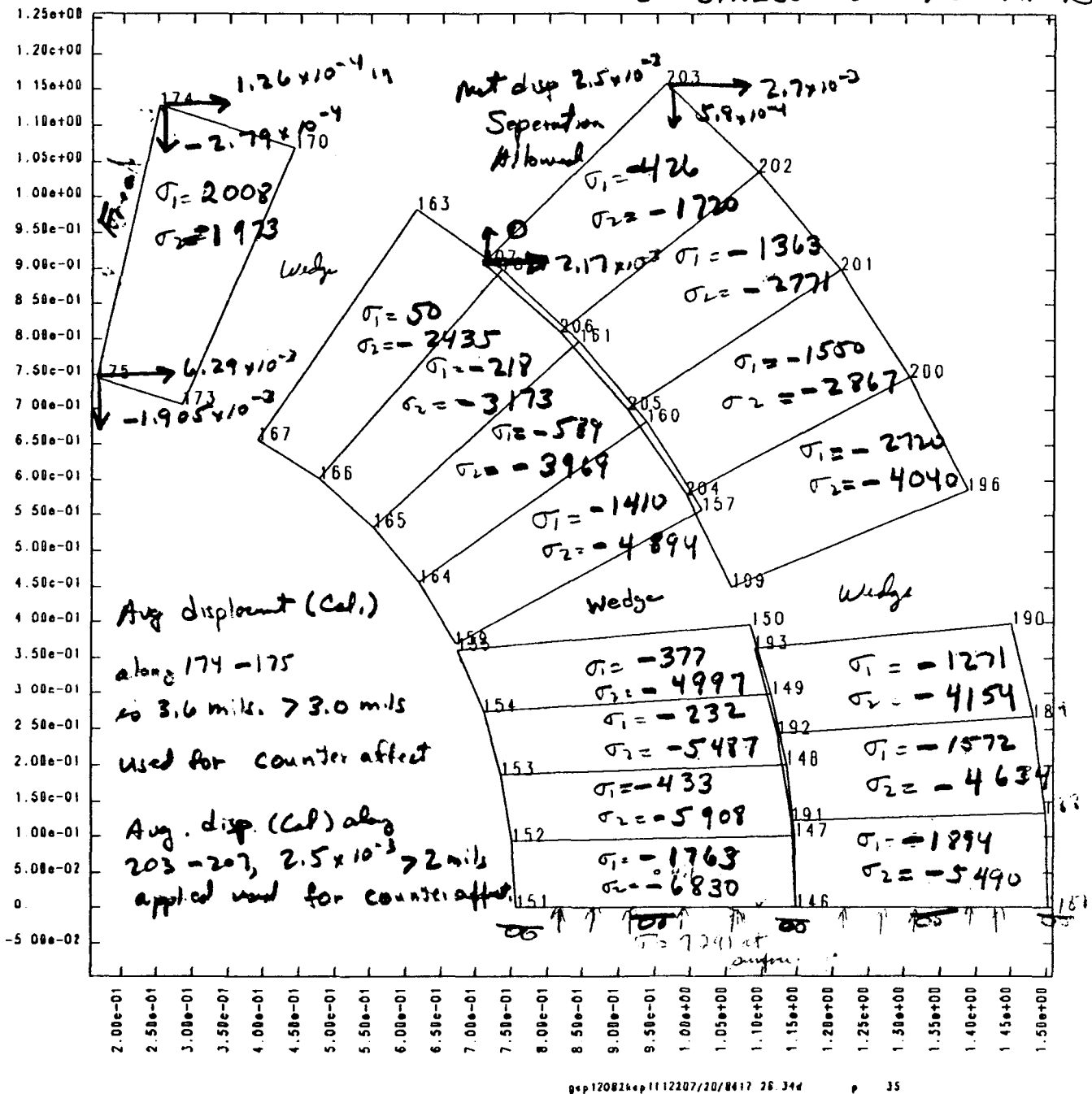


Fig. 10. Lorentz Stress

Since the curve given in Fig. 5C, 300 K, does not account for heat transfer of the coil into cold mass, and the energy is depleted at 500 m.s., a TACO calculation was performed using the energy deposited in the coil rather than the temperature distribution given in Fig. 5C. This calculation was run to 80 seconds. It does not include the effect of the vaporization of helium or flow of helium, which accounts for the difference in early time but in general is more accurate. The TACO calculation (using energy deposited) provides the nodal temperatures in the cold mass as a function of time.

The Lorentz force due to eddy currents on the inside of the beam tube was also provided by Meuser¹³. However, this value can vary by a factor of 2 depending on the degree of heat transfer that has taken place. This specific loading will be discussed further under stability when the solution to the problem of a external pressure on a elliptical tube (elliptical due to Lorentz force) is discussed.

The 600 psi annulus pressure is the best guess until measurements can be obtained and its distribution is shown in Fig. 8. The other loading condition have been discussed earlier in this report. Several sets of quench calculation were preformed;

- a. 3 mil clearance, bumpers, separation of components allowed, 500 m.s quench curve, 100 psi Lorentz pressure, Al collar - no insert,
 $I = 3/2$ mils
- b. Same as A. Al collar - insert
- c. Same as A. Steel collar - no insert

This is the design as it appears in Attachment B except that a clearance is added and is the design in the latest drawings at CDG (3/87).

Table III

Maximum Stress/Current Model Quench Calculation
(ksi)

Time (sec.)	t = .1			t = .3			t = .5		
	A	B	C	A	B	C	A	B	C
Cu Plating*	5.4	9	9	26.8	8.5	38	8.3	14	28
Beam Tube*	8.7	10	15	40.0	10	50	51.3	30	45
Coil I** σ_θ	7.5	7.5	8.2	8.5	9.2	9.2	13.8	13	9.5
Coil O** σ_θ	10.9	11	11.7	12.0	12	13.7	15.3	16	12.5
Collar*	4.2	4	5.2	26	26	40	76	78	130
Yoke*	4.2	4	5	6.2	7	10	17	17	18
Ring*	.42	.4	.5	2	1.8	1.9	5.5	6	5
S.G. Location	.7	1.1	1.2	14.5	6	9.3	42	17	26

A = Al collar no insert, B = Al collar insert, C = Steel collar no insert.

* Max stress (ksi)

**Uniform stress generally (ksi)

The coil temperature at $t = 0.1$ seconds is $T = 4.35$ K, $t = 0.3$ seconds is $T = 100$ K, and $t = 0.5$ seconds is $T = 230$ K. Stress in the coil are generally uniform in the circumferential direction. Collar, yoke, ring stresses are within CDG requirements except at $t = 0.5$ for the collar. The 3 mil clearance appears not be sufficient. Note only at $t = 0.5$ seconds are the stresses exceeded. The collar, yoke, and ring stresses are within CDG requirements¹¹ except at $t = 0.5$ for the collar. The collar stress in Al is less than that in the steel collar, but the stress in beam tube is higher for Al. The insert is the equivalent of an active slide line between pole piece and collar and behaves like an additional clearance. The reason the collar stresses are high is because of the thermal stress gradient between the coil and the collar where two of the surfaces of the coil interact with two surfaces of the collar. The pre-stress is somewhat lower than required based on previous analysis; the input used was 3/2 mils at equatorial plane.

A calculation was performed where the G-10 spacer was removed entirely and replaced with Helium. The collar was steel, separation was permitted, an insert included in model (steel), clearance between yoke and collar and 9 mil and 7 mil deflection on the coils at the equatorial plane, $t = 40$ mils thickness.

Table IV

Max Stress - Steel Collar - Quench
No G-10 Bumper - Adequate Prestress - 100 psi Lorentz Pressure
(ksi)

<u>Time (sec.)</u>	<u>$t = .1$</u>	<u>$t = .3$</u>	<u>$t = .5$</u>
Cu Plating	.150	2.1	2.0
Beam Tube	.5	3.06	2.9
Coil I σ_θ	14.8	17.3	18
Coil 0 σ_θ	22	25	21
Collar	17	23	110*
Yoke	7.4	13.5	25
Ring	1.2	2.4	5
S.G. Location	9.75	13.5	14

* See Appendix Fig. 6A on collar elements (element 170, 171) for location of high stresses. Note with the G-10 spacer eliminated, the stresses in plating and beam tube practically disappear (3 mil clearance is insufficient). The G-10 bumpers function is to act as supports to limit beam tube deflection after cool down.

The previous calculations were run with 100 psi Lorentz pressure. The nominal value is 150 psi which is used in the following quench calculation.

The thickness of the beam tube in the calculation is increased to 50 mils.

Table V

Maximum Stress in ksi, Steel Collar/No Bumpers/150 psi Lorentz Pressure
 $t = 0.05$ in., Prestress I.C. 7.3 mils/O.C. 4.5 mils

<u>Time (sec.)</u>	<u>$t = 0.1$</u>	<u>$t = 0.3$</u>	<u>$t = 0.5$</u>
Plating	2.4 ksi	4.5	8.0
Beam Tube	2.7 ksi	5.2	10.0
I.C.	13.75	17.0	17.0
	10.25	12.4	11.0
O.C.	26.75	28.75	22.0
	10.425	14.25	14.8
Collar	10.0	30.0	120.0 $\Delta T = 223 - 94$ = 129 K across the element at $t = 0.5$
Yoke	4.5	10.5	25.0
Ring	0.9	2.2	4.8

The only problem is in collar thermal stress due to the temperature gradient across collar of 129 K at $t = 0.5$ seconds.

Using the quench curve to 80 seconds, using the same model and input (except temperature), the results are given in Table VI.

It is observed that since the bumper is removed, the pole piece has no back-up support. As a consequence of the pre-stress, these four elements that make up the pole piece see stress $> 100,000$ psi. It is these four elements that go to make up the insert on other calculations.

Since it is being contemplated on removing the bumper and keeping the thickness = 40 mils, the following calculations were performed. The only area of concern is in the pole piece since it no longer has the support of the G-10 bumper. All stresses are within CDG requirements except the pole piece. The temperature of the coil are given in the 80 second plot given in Fig. 5. It is assumed that future measurements of the helium pressure will indicate that the maximum pressure is $\ll 600$ psi.

Table VI

Maximum Stress in ksi, 80 Seconds Quench Curve,
 Steel Collar, $t = 0.05$ in, 150 psi, Lorentz Force, No Bumper

<u>Time (sec.)</u>	<u>$t = 0.5$</u>	<u>$t = 0.6$</u>	<u>$t = 0.8$</u>	<u>$t = 0.10$</u>	<u>$t = 0.12$</u>
Plating	9.0	9.0	8.4	7.0	6.750
Beam Tube	12.0	12.0	11.0	9.5	8.3
I.C.	17.0	17.0	17.0	16.6	13.6
	12.3	12.5	12.5	12.5	15.8
O.C.	26.0	26.9	28.0	28.0	27.36
	14.0	14.0	14.0	13.5	15.0
Collar *	37.2	37.5	28.0	26.0	21.0
	*	*	*	*	*
Yoke	12.9	13.4	13.8	13.8	12.5
Ring	2.0	2.0	2.0	2.0	2.5

* Stress in pole protruding from collar exceeds yield > 100,000 psi.

Table VII

Maximum Principal Stress
(ksi)Steel Collar, No Bumper, $t = 0.04$, Lorentz 150 psi, $I = 7.3/4.5$ mils
(ksi)

<u>Time(sec.)</u>	<u>$t = 0.05$</u>	<u>$t = 0.25$</u>	<u>$t = 0.35$</u>	<u>$t = 0.55$</u>	<u>$t = 0.85$</u>	<u>$t = 5.85$</u>	<u>$t = 35.85$</u>	<u>$t = 60.85$</u>	<u>$t = 80.85$</u>
Plating	1.8	5.0	9.8	12.0	11.0	9.6	9.6	9.2	8.8
Beam Tube	3.0	6.0	11.0	15.0	14.0	11.0	11.0	10.0	10.0
I.C. σ_θ	13.5	14.0	16.8	17.0	16.695	10.9	10.375	10.275	2.0**
σ_θ	10.0	8.5	12.5	12.4	12.6	13.7	13.4	13.270	6.4**
O.C. σ_θ	26.256	27.0	29.0	26.350	28.3	25.2	24.7	24.5	1.0**
σ_θ	9.560	10.6	13.5	14.0	13.8	12.0	11.5	11.0	1.0**
Collar	9.0 *	9.0	17.0	38.0	29.0	12.0	12.0	11.530	2.2
Yoke	6.0	7.0	9.8	13.0	13.7	7.35	4.3	4.2	1.1
Ring	0.75	0.80	1.5	2.0	2.4	1.90	1.2	1.3	0.350

* Elements 131 - 134, pole piece > 100 ksi

** Pre-stress removed at 80 seconds

Table VIII
Maximum Stress

Al Collar, No Bumper, $t = 0.04$, Lorentz 150 psi, $I = 7.3/4.5$ mils
(ksi)

<u>Time/ Components</u>	<u>$t =$ 0.05</u>	<u>$t =$ 0.25</u>	<u>$t =$ 0.35</u>	<u>$t =$ 0.55</u>	<u>$t =$ 0.65</u>	<u>$t =$ 0.90</u>	<u>$t =$ 1.30</u>	<u>$t =$ 6.3</u>
Plating	2.4	4.4	7.5	12.0	12.0	9.675	8.7	9.0
Beam Tube	4.6	5.7	11.0	15.0	14.0	12.0	11.0	11.0
I.C. σ_θ	12.5	12.5	14.5	15.0	15.0	15.0	12.2	10.0
σ_θ	8.4	8.750	10.5	10.8	10.8	10.6	14.0	13.0
O.C. σ_θ	25.5	26.3	28.2	25.25	26.2	27.5	26.133	25.325
σ_θ	6.9	7.8	10.35	11.0	11.0	10.75	12.0	11.0
Collar	7.0	7.8 *	11.0 (75.0)*	22.0 *	20.5 *	18.0 *	14.5 *	10.0 *
Yoke	5.8	6.8	9.0	11.0	11.3	11.3	8.0	6.2
Ring	0.90	0.98	1.5	2.1	2.2	2.4	2.1	2.0

* elements 131-134 > 100 ksi, pole piece.

Table continued

Table VIII (continued)

Maximum Stress
 Al Collar, No Bumper, $t = 0.04$, Lorentz 150 psi
 (ksi)

<u>Time (sec.)</u>	<u>$t = 11.3$</u>	<u>$t = 31.3$</u>	<u>$t = 61.3$</u>	<u>$t = 76.3$ sec.</u>
Plating	7.7	7.0	7.0	7.8
Beam Tube	8.0	8.0	10.0	10.0
I.C.	9.0 12.3	8.6 11.7	8.6 11.56	8.6 11.475
O.C.	24.5 10.0	23.7 9.0	23.6 9.0	23.6 9.0
Collar	10.0	9.0	8.6	8.6
	*	*	*	*
Yoke	5.5	4.7	3.6	4.0
Ring	1.6	1.3	1.2	1.2

All the stresses are within CDG requirements as discussed.

d) Warm up. If the temperature increased to 320 K, the only loading would be the pre-stress. With 7.3/4.5 mil input displacement, the temperature uniformly was increased to 320 from 300 K. The following maximum stress were obtained.

Table IX

Maximum Stress, Steel Collar,
Bumpers, Clearance/Pre-stress
(ksi)

<u>320 K</u>	<u>Max Stress, 320 K, ksi</u>	<u>Element #</u>
Copper Plating	27.0 8.6	(30) (27)
Beam Tube	32.64	(437)
Coil I.C. O.C.	6.875 6.385 13.142 7.2	(116) (129) (135) (143)
Collar	5.16	(149)
Yoke	3.5	
Ring	1.9	

No apparent creep.

The maximum stresses are significantly below yield and considering the materials, would not creep. None of the plastics used in the cold mass would creep at 320 K under these relatively low stresses. However, if the times are long, e.g. years, then the plastics will creep even under the low stresses. But the degree of creep will be small and not affect other components or the system, except possibly the plastics (Kapton) in the coil.

e) Stability. The presence of bumpers is required if the thickness is to remain the same i.e. 40 mils, and the design pressure of helium in the annulus of 40 atms. is not decreased. The effect of the several layers of plastic on the beam tube is not considered in what follows, but would make the final result more conservative. That is the additional layers of plastic would in effect increase t/d ratio, thickness to diameter ratio, and thereby increase the critical pressure required for a long tube to go unstable.

The maximum stress due to eddy currents was shown to be 40,000 psi, from the computational analysis, (NIKE3D, NIKE). Analytically, it can be shown that

$$M_{\max.} = \frac{2\alpha R^2}{4} \quad \text{where} \quad (1)$$

$$\alpha = 48.37 \text{ psi (Ref. 10)}$$

$$R = 0.64 + \frac{t}{2} = 0.66 \text{ ignoring cu. plating thickness of } 0.05 \text{ in.}$$

$$\sigma = \frac{Mc}{I} = \frac{M(12)}{1 t^3} \left(\frac{t}{2}\right) \quad (2)$$

$$\sigma = \frac{Mc}{I} = M(12) \frac{1}{t^3} \left(\frac{t}{2}\right) = \frac{M 6}{t^2}$$

$$\sigma = \frac{3\alpha r^2}{t^2} = \frac{3(48.37)(0.66)^2}{(0.04)^2} = 40,000 \quad (3)$$

CDG requirements¹¹ are, where σ_0 is yield, $0.90\sigma_0$. For bending, $\sigma = 0.9(54,000) = 48,600 > 40,000 \text{ psi (low value)}$

The next criteria is instability.

For a long tube

$$P_{cr.} = \frac{2E}{1-\mu^2} \left(\frac{t}{d}\right)^3 \text{ where } t \text{ is thickness, } d \text{ outside diameter, (4)}$$

E modulus of elasticity, μ Poissons ratio

$$P_{cr.} = \frac{2(30 \times 10)^6}{1-(0.278)^2} \left(\frac{0.045}{1.36}\right)^3 = 2340 \text{ psi}$$

$$\frac{P_{cr.}}{4} = 585 \text{ psi} \quad (5)$$

The pressure in the annulus is 600 psi; therefore, the tube will not go unstable as a consequence of 600 psi external pressure acting alone. The maximum annulus pressure is 600 psi at $t = 0.4$ to 0.7 seconds. At $t = 0.7$ seconds, the Lorentz force on the beam tube is minimum. At $t = 0.3$ seconds, the Lorentz force on beam tube is a maximum and then is on returned pressure of 400 psi (see Fig. 8).

Beam tube shape due to Lorentz Force on inside surface.

Superimposed is a annulus pressure of 600 psi.

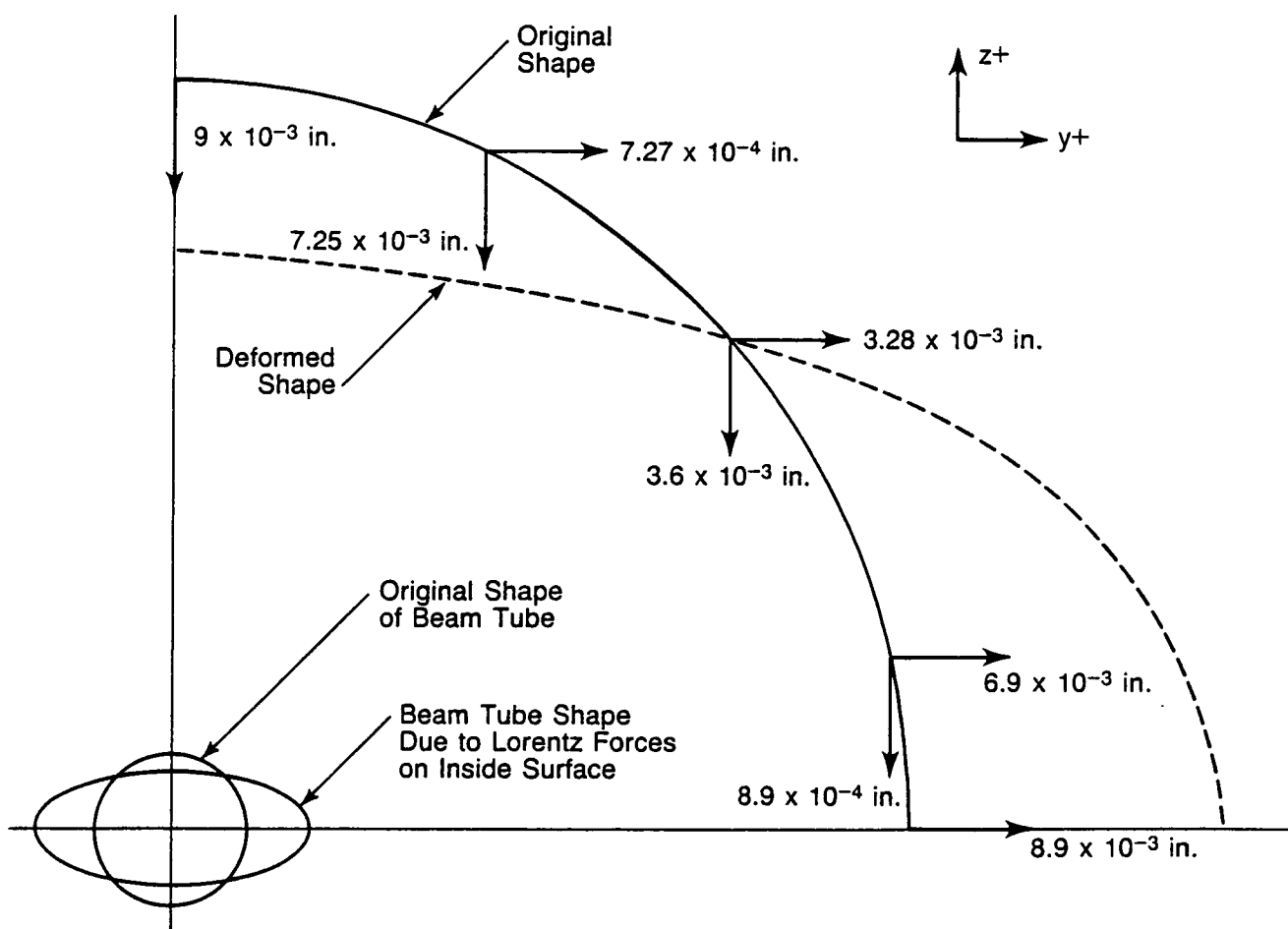


Fig. 11. Ovality condition.

The bumpers provide support to the beam tube when the clearance has been eliminated. When the bumpers have been removed, a condition of instability can occur. The maximum displacement of 8.7 mils (node 144) which is base of inner coil is obtained by NIKE as a consequence of the minimum value of Lorentz force (see Fig. 11). The displacements are elastic.

The main question regarding instability occurs when there is a Lorentz force due to eddy currents on the inside surface and an external pressure is applied. That is an external pressure is applied to a deformed tube.

Timoshenko and Gere¹² treated this problem and the analysis follows. The radial deflection can be determined by the following expression from Ref. 12.

$$w = \frac{PR^3}{4EI} (\cos\theta + \theta \sin\theta - \frac{4}{\pi}) \quad (6)$$

$$\text{At } \theta = \pi/2, \quad w = \frac{PR^3}{4EI} \left(1 - \frac{4}{\pi}\right) \quad (7)$$

The load P can be related to the moment which then can be related to Lorentz pressure, α , and $(1-\mu^2)$ inserted for the case of a long cylinder

$$w_{\max} = \frac{\alpha R^4}{4EI} \frac{(\pi-4)}{(\pi-2)} (1-\mu^2) \quad (8)$$

For $\alpha = \alpha_{\max}$, $w = .01$ in., whereas the computer calculation is $w = 9 \times 10^{-3}$.

$$P_{cr.} = \frac{E}{4(1-\mu^2)} \left(\frac{t}{R}\right)^3 \quad (9)$$

If we define $m = R/t$, $n = w_1/R$, σ_{yp} = yield stress.

Then the design formula for the maximum external pressure to be placed on an elliptical tube is given by

$$q^2 - \left[\frac{\sigma_{yp}}{m} + (1+6mn)P_{cr.} \right] q - \frac{\sigma_{yp}}{m} q P_{cr.} = 0. \quad (10)$$

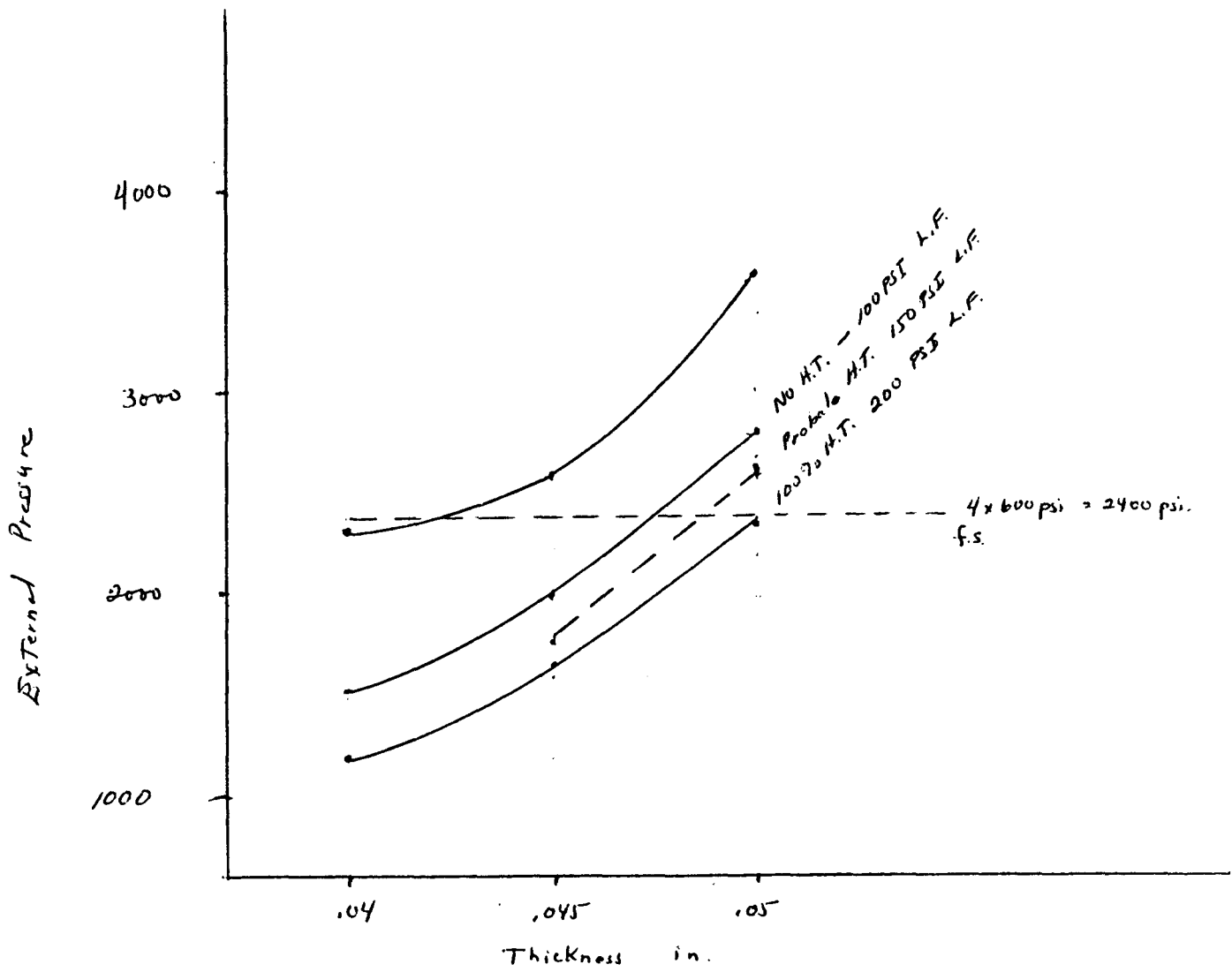


Fig. 12. Stability Criteria.

If we hold the outside radius at 0.68, change t and R respectively, then recalculate P_{cr} , w_i , m , n , then q_{up} can be determined, where q_{yp} is the design pressure (and less than P_{cr}). The yield stress, σ_{yp} is 140,000 psi for an assumed 60 K₂ temperature.

Table X
Stability Analysis

<u>Thickness t (in.)</u>	<u>$t = 0.04$</u>	<u>$t = 0.045$</u>	<u>$t = 0.05$</u>
P_{cr} (psi)	2340	2600	3600
Lorentz Force			
A No Heat Transfer (psi)	1550	2011	2831
B Probably H.T. (psi)		1783	2668
C Complete H.T. (psi)	1197	1655	2378

It is felt that the most realistic value for Lorentz pressure is case B. Per CDG Req.¹¹ the design pressure is 445 psi for $t = .045$ and 667 psi for $t = .05$ inches.

At present we are designing on the basis of 40 atm. helium pressure = 600 psi therefore $t = 0.05$ meets CDG Requirements¹¹ if there are no bumpers. If we can obtain a better value of helium pressure, say 25 atm = 376 psi, then we can safely use $t = 0.045$ inches. Therefore it is recommended to use $t = .050$ inches and remove the bumpers. The beam tube at $t = 0.05$ in. satisfies the CDG requirements¹¹ with respect to stability.

The lack of clearance in our original model, as shown in Ref. 9 created problems beyond the fact that the stresses in the beam tube exceeded CDG requirements.¹¹ One can trade off clearance versus thickness as for a stability provided clearance > 3 mils. A clearance ≥ 9 mils will not provide any support (see Fig. 11).

VIII. Comparison with Experimental Results

There have been a number of measurements performed at BNL and LBL which need to be compared to analysis. In the final analysis, this is the correlation with real coils in their real environment and it is a measure of how accurate we model the coil and other components and how well measurements are performed.

A number of measurements have been made with an insert to determine the value of the coil stress. As indicated earlier, a number of analyses were performed which model test configurations. In all cases, a bath is utilized which gives a uniform temperature -- 4.35K. In analysis, the cooling comes from the coolant channel and the annulus and is a transient calculation until steady state is achieved. Other papers, noticeably by Peters^{14,8}, describe the experimental measurement for pre-stress. To be complete, a simplified description is contained herein. A section of the collar is removed (elements 131, 132, 133 and 134) and replaced by a strain-gauged insert. At LBL, the insert is Al irrelevant of whether the collar's steel or Al. At BNL, the insert is Al for Al collars and steel for steel collars. At this time, the gauges are "calibrated" directly and via the coil. The stress measurement then is for the section in the coil adjacent to the collar. No data has been reported officially for the insert itself.

Craig Peters has compiled all data to date on cool down loss and prestress^{14,15}. The stress that has been measured is the stress at the insert and not in the coil adjacent to the insert. The stress in the coil is inferred from calibration of load cell prior to assembly. It is the m.v. output from a gage in the insert as "calibrated" by a pressure at the equatorial plane. It is assumed by those calibrating the insert that there is no friction, no separation, and the circumferential stress is uniform

throughout the coil. It should be noted that there are two wedges in the inner coil (in order to obtain a uniform field) and the properties of the coil and wedges are different. The LBL compilation of prestress in coil^{14,15} depend greatly on model and assembly load.

LBL last measurement yielded a coil prestress of 4.0 ksi I.C. and 4.3 ksi O.C. If we compare the prestress in the coil in the elements adjacent to the collar, our basic plane of reference is the same.

NIKE prestress in I.C. is 3.9 ksi and 3.75 ksi for O.C. (7.3/4.5 mil displacement or input).

Another correlation was obtained by comparison of displacement of the collar. On page 82 of Attachment B, reported LBL measurement for 4 K with energized coil

Table XI
Comparison of Measured and Calculated Displacements

	<u>LBL Measured mils (p. 82)</u>	<u>LBL Measured mils (2/2/87)</u>	<u>NIKE Calculation mils</u>
Vertical	1.1-2.1	3.0-2	2.1 (node 446, 4.35k)
Horizontal	1.6	2.25-3.5	1.54 (node 331, 4.35K)

It is assumed that the pre-stress at 4 K is ~ 3000 psi I.C. and ~ 2000 psi O.C. from page 83 of Attachment B. We are using 3.9 ksi and 3.75 respectively. The Lorentz forces for 6.6 Tesla are approximately the same. The comparable calculation for 4 K energized looking at the displacement of the nodes at the ends of the collar are as given above, which indicates that the analysis is consistent with measurement. The comparison with the deflection measurement is critical since prestress values are dependent on assembly load and model. For the deflection measurement with the same values of prestress in the coil, a comparison of the collar deflection is more meaningful.

Craig Peters in a presentation at LBL stated that it was his observation that the stress at the Strain Gage (S.G.) location, i.e., stress measured directly, was 35% higher than the coil stress. Calculations verify this value directly i.e., 35%.

Table XII

Cool down - Effect of Insert
(Steel Insert in Steel Collar)

<u>Element</u>	<u>$I = 9 \text{ mil}/7\text{mil}$ Bumper/Insert</u>	<u>$I = 5.6/3.2$ Bumper/Insert</u>	<u>$I = 7.3/4.5$ Bumper/Insert</u>
I.C. 116* 129 (Pole)	-6.25 -5.73	-2.6 -1.95	-4.35 -3.9
O.C. 135 143 (Pole)	-10.77 -7.07	-12 -1.7	-15.3 -3.75
S.G. Loc.(131 & 132/2)	-8.8	-3.8	-6.35
R =	35%	48.6%	38%
(S.G. Loc - 129)/S.G. Loc			

* element numbers

In the above table, three calculations were performed where the variable was the displacement at equatorial plane. Separation was permitted and the insert was included by activating the slide plane. The purpose of this calculation was to select appropriate displacement, since the displacement and stress in coil at the pole (I.C.) is non-linear. For the range of initial displacement corresponding to Peters, that value was 35% and 38%. For a somewhat lower value of required displacement, the value was 48.6%. This can be interpreted in two ways; further verification of the calculation or verification of the S.G. reading and their interpretation.

In the case of an Al insert in Al collar and an Al insert in a steel collar, in a specific calculation where the surfaces were in contact (code 1 - pure sliding), we have

Table XIII

	Maximum Stress (ksi)	
	<u>Al Collar</u>	<u>Steel Collar</u>
I.C. 116	6.36	5.95
129 (pole)	2.28	2.17
S.G. Loc.(131 & 132/2)	3.33	2.00
R	32%	

For the case of Al collars with Al inserts, the stress in the insert is about 30% higher than coil, which confirms Peters measurements. The Al insert in a steel collar is lower, 2.00, and closer to the coil value of stress.

Additional data from LBL and BNL for pre-stress is given in Table XIV.

Table XIV
LBL and BNL Pre-stress
(ksi)

	Initial Stress	Stress at Cool Down		Stress of Cool Down Calculated NIKE
		Measured	Calculated	
LBL Al Insert in SS collar C-4	I	0	I	0
		7.9	2.9	2.75 (Proportional to 7.9)
BNL cal.	6.87	5.9	3.65	2.94
BNL D002	7.0	3.8	2.675	2.54

$$\begin{aligned}
 \text{Basis } \sigma = \epsilon E = & \frac{7.3 \text{ mils } (2 \times 10^6)}{1.30} = 11.2 \text{ ksi} & \text{when } l_{\text{coil}} \text{ and } l_{\text{wedge}} \\
 & & = 1.30 \text{ in. and pre-stress at} \\
 & & 4.35 \text{ K is } 3.9 \text{ ksi (correspond} \\
 & & \text{to a } 7.3 \text{ mil displacement.)} \\
 \frac{7}{11.2} (3.9) & = 2.54 \\
 \frac{7.9}{11.2} (3.9) & = 2.75
 \end{aligned}$$

It was shown that 7.3 mil input yields 3.9 ksi prestress. To compare to D002 or C-4, we divide the displacement by circumferential length of coil and wedge (1.30 in.) and multiply by E (modulus of coil and wedge per BNL) which gives stress 11.2 ksi. Then the ratio input stress 7 to 11.2 is the modifying factor to NIKE output 3.9. This gives you 2.54 compared to BNL 2.67 and 2.75 compared to LBL's 2.9 ksi. Therefore, when the controlling parameters are adjusted to match, the output between measured values and calculations are very close. LBL's C-S with an initial stress of 5 ksi gives a stress at cool down of 1 ksi is reasonable in view of the relationship between input and prestress at low values of input as noted from the calculations.

At the recent IEEE Particle Accelerator Conference (March 1987, Washington D.C.), BNL published the following curve, Fig. 13. What it indicates, is that pre-stress is lost at 5250 amps. Working backwards, using 7291.0 ksi at the equatorial plane for the Lorentz stress (B^2/Bo^2) where 5.25 Tesla refers to 5.250 amps, we get 4613 psi. Therefore, the average stress is 2307 psi. Therefore, it would appear that pre-stress is about 2000-2300, independent of the strain gage reading. Since the stress gage reading gives 2450, we conclude that this is a fairly accurate number.

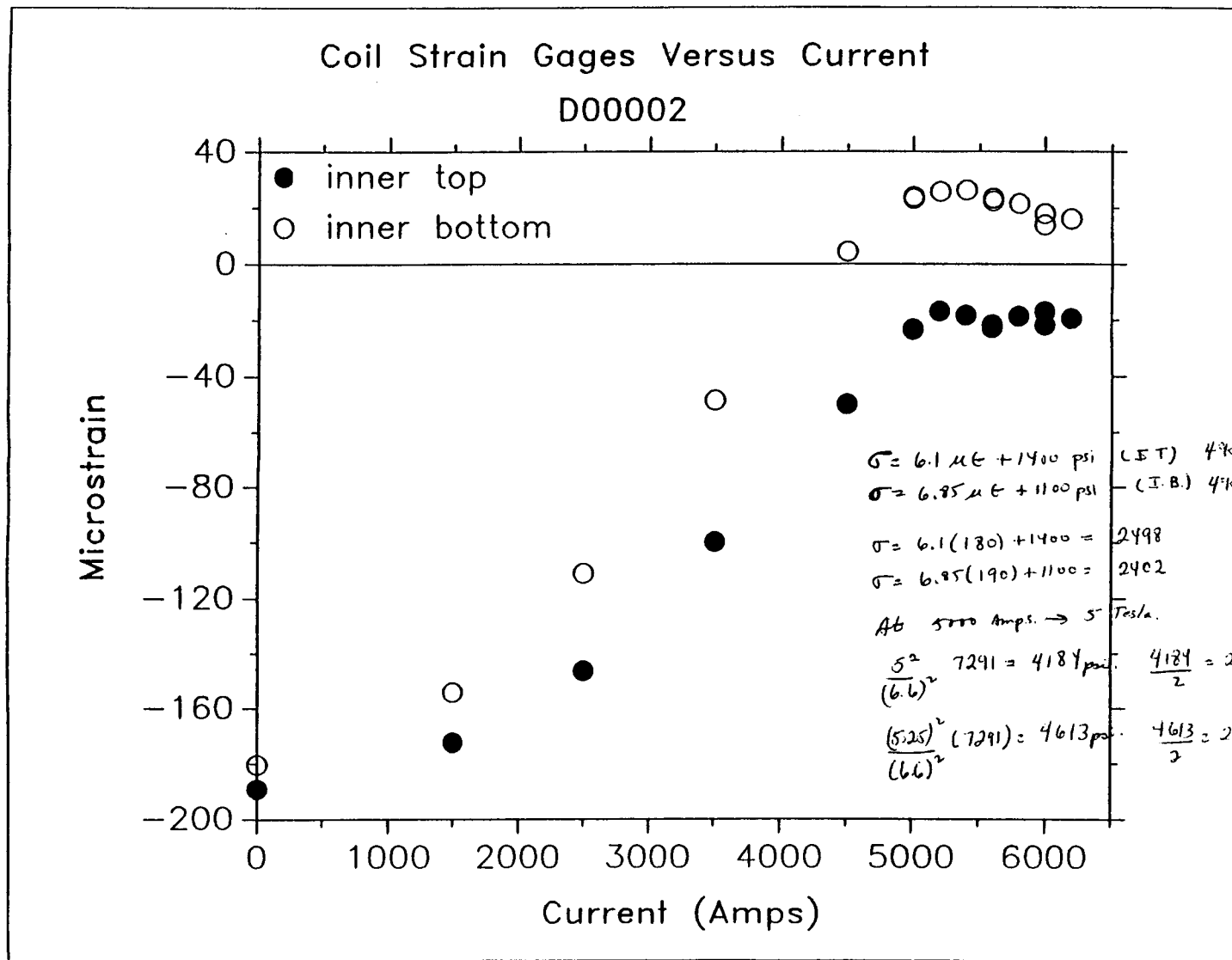


Fig. 13. Coil Strain Gages Versus Current D00002

IX. Future Work

Six items were identified under objectives of the analysis. Each of the items were addressed in detail.

In general, the design appears adequate. The collar stress adjacent to the coil exceeds CDG requirements because of the rapid rise of the coil temperature. An independent heat transfer calculation was performed on the basis of energy deposited, I_2R , and with the exception of the vaporization of helium and helium flow, similar results were obtained for the $0 \leq t \leq 500$ ms. However, this calculation needs further refinement and efforts are being made to determine more accurately the temperatures. The assembly pressure needs to be increased to insure stress in coil after cool down -- to 7.3 mils on inner coil from 3 mils which is like 2 on collaring due to the variabilities anticipated. The clearance with bumpers should be at a 5 mils $\pm 1/2$ mil, if thickness remains at 40 mils.

Results indicate that the G-10 bumper is the vehicle by which thermal and other stresses are transmitted to the beam tube and copper plating. When clearances are provided, these stresses disappear. Analysis of computer calculations is 5 mils clearance is sufficient and the thickness is adequate based on CDG requirements¹¹ to prevent collapse. However, the presence of bumpers is required if the thickness (0.40") is to remain the same and the design pressure of 40 atms is not decreased.

Thermal Stress - The thermal stress due to temperature gradient occur only on quench between the collar and the coil at times $t \sim 0.5$ seconds, $\Delta T = 129K$. This is due to constraint on the collar and timing. Efforts are being made to evaluate more accurately the temperature rise of the coil in this time regime.

As the calculations indicate, α and E are the most sensitive properties. Unless grossly wrong, the results are acceptable. However, effort should be made to obtain more accurate properties of coil and plastic materials and design criteria (allowable maximum stress) can be determined. What is stress on the Kapton in the coil and is it subject to creep. The maximum stress in O.C. at 320 K is 13 ksi; at 4.35 K creep is retarded. Hence, the coil needs to be further evaluated. While an orthotropic model for modeling the coil is more appropriate, its affect is not that noticeable since the material is modeled properly in the plane of interest. That is, if the E in the cross sectional plane is modeled properly, the stress r, Θ will be fairly reliable and constant but stress in longitudinal direction will depend on the value of E in the longitudinal direction.

If one is interested in the longitudinal effect, the model which is a plane strain model, is still not accurate even if orthotropic properties are used, since we do not capture the temperature in the longitudinal direction which requires a 3D calculation and an improved NIKE 3D orthotropic model.

Calculated results indicate that the measurements to-date, are valid. Or conversely, the measurement confirm analysis.

Aluminum appears to have several advantages over steel collars: lower stress, higher pre-stress.

The helium pressure in the annulus need to be measured. Further measurements are required of the quench temperature.

The maximum pressure due to eddy currents with no heat transfer is 100 psi and with complete heat transfer 200 psi. A probable realistic value is 150 psi. However, a factor of 1.5/2 on the stress in the beam tube would not bring the stress outside CDG requirements. Either bumpers or increase in thickness is required for stability. The failure criteria of the combined

helium pressure and eddy current forces has been viewed from the most conservative approach as the maximum effects were considered since this calculation was performed by closed form technique.

Transient effects -- The computer program addresses the simultaneous loading of displacement, forces, pressures, etc. It is the computer program that has the capability to address the transient loading.

It is the opinion of the author that the results using these codes are accurate. Should they not agree with what is observed through measurements, then either we are not interpreting the computer results correctly or there is a flaw in the model -- i.e., the model is not as described or the material properties are not sufficiently accurate.

TACO calculations need to be further improved to account for vaporization of helium and flow of helium. Quench calculations with the new distribution will need to be re-run.

The coefficient of thermal expansion/contraction for the coil and other components as a function of temperature is required. For the plane strain model, it was assumed for the coil $\alpha = 1.3 \times 10^{-5}$ in/in/K in r, θ plane for all temperatures. Even at 4.35 K this value is subject to debate. To perform a transient analysis, α , from 300 K to 4.35 K is required.

The main deficiency in the plane strain model is that it is a two dimensional model. The temperature in the longitudinal direction obviously cannot be captured with this model. Similarly, the thermal stresses in the longitudinal direction are not calculated. To adequately model this, coupled with the other inputs, requires a 3D model. The interaction of the system with the support posts is more accurately described by a 3D model. Because of the personal interest of the code developers, the 3D codes contain a higher level of sophistication than in 2D codes. The choice of element types is

extensive in 3D codes compared to the quadrilateral elements in 2D codes. Beam elements and shell elements are found in NIKE3D and are not found in NIKE2D (NIKE). As a consequence, instead of 300 quadrilateral elements to model the beam tube in 2D, only 30 are required. The 30 beam elements are more accurate than the 300 quadrilateral elements. The quadrature and print-out options are greatly expanded in the 3D codes. Therefore, it is anticipated that the number of elements in 2D and 3D problem will remain the same, and similarly the running time on the Cray computers.

As in the 2D calculations, the heat transfer calculations require the same identical model. One has the choice of using TAC03D which was developed by Mason an LLNL who is now at Sandia or TOPAZ3D which is Shapiro's code, who is at LLNL. Both codes are equivalent and are on the MFE NET library. We will use TAC03D because it is certified and has been in existence longer and is more widely accepted than TOPAZ.

The primary problem to be addressed in the 3D problem is the quench propagation and the thermal stresses. In the two dimensional case, for quench, a peak temperature in the coil of 300 K is obtained in about 550 m.s. Cool down will also be evaluated from a 3D analysis. The length of the model to be considered is 1740.6 cm. With this length, interaction affects can be evaluated and the same model can be used for cool-down as well as quenches. Since we will consider all the plastics together, and use shell and beam elements, the total number of element will not vary significantly between the 2D model and 3D model. A description of the longitudinal model is given in B.13-2.⁹ The crux of the problem is the quench propagation. Let us assume that a quench starts in the inner coil and an element whose boundary on two sides is the collar. The quench will propagate circumferentially, radially, and axially until the heaters are trigger additional quenches. The rate of propagation will depend on the rate energy is being deposited in the system.

The work of General Dynamics, where the temperature every-where is provided as a function time, will be incorporated in the structural analysis to obtain the thermal stress. TAC03D will augment the work of being performed by General Dynamics. The material properties in the three directions will be required. The metals can be assumed isotropic. The plastics will have to be evaluated.

Some of the requirements remain the same. A quarter section will be retained as symmetry is still applicable. The difficulty will be keeping track of the sequence of events longitudinally. It is anticipated that this activity will go faster than the 2D effort. The result, will be a verified model of the entire system. If one notes the temperature and stresses on the cold mass and the materials used, the phenomena of creep needs to be evaluated. Considering a life at 20 years minimum, creep at room temperature is important even for metals. NIKE has the capability to model thermo-elastic creep. Here, the shear modulus, bulk modulus, coefficient of thermal expansion, and constant describing creep rate

$$\epsilon = a_0 \sigma^{b_0}$$

are specified by temperature. TAC0 will obtain the temperatures as a function of time. NIKE will model each material as a function of temperature and thereby time. NIKE, as before, calculates the displacement at each node and using this model, includes displacement due to creep. In particular, the coil, which is a composite needs to be characterized, and some of the other plastics. We can assume that the Al, steel, and iron do not creep in this temperature range.

Another area that is important is evaluating the steel and Al used in the design from a fracture mechanics viewpoint -- susceptibility to crack propagation at cryogenic temperatures at low stresses. Steel is very sensitive, especially if welded which is not the case here. Cracks can propagate in metals due to inherent flaws at stresses below design stress in certain materials. The cold mass requires such an evaluation to insure that only fracture safe materials are utilized.

As different design magnets are considered, 2D and 3D calculations will be required. The results presented in this report is for only one type of magnet, the dipole magnet.

Summary

In summary, a plane strain model has been developed and in conjunction with two computer codes, TACO and NIKE, and can be used to determine the stresses, displacements and temperatures, for several operating conditions -- cool down, operation and quench. Over 50 different cases were evaluated using the final model and certified codes. The print-outs which contain the stress state, principal stress, temperature, deflections and are functions of time are in the Magnet Division Office and in special directories in the Cray Computer in MFE Computer Center in Livermore.

Calculations on the collar have been performed with the ANSYS codes both by BNL and LBL. To the extent that NIKE and ANSYS have treated the same problem, they are in agreement. ANSYS has many more elements for the collar than NIKE. NIKE was used to evaluate the system and NIKE calculations went on to evaluate transient conditions, slip conditions, component interaction, and friction.

References

1. W.E. Mason, Jr., TACO - A Finite Element Heat Transfer Code, UCID 1790 Rev. 1. (1980).
2. J. Hallquist, A Vectorized, Implicit, Finite Deformation, Finite Element Code for Analyzing the Static and Dynamic Response of 2-D Solids, NIKE - NIKE2D - UCID - 19677,2/83
3. John Hallquist, MAZE - An Input Generator for DYNAZD and NIKE, MAZE, UCID 19029, Rev 2, June 1983.
4. DOE Order 5700.6A, QA.; ANSI/ASME-NQA-1-1979.
5. J. Hallquist and JoAnne Levatin, ORION: An Interactive Color Post-Processor for 2D Finite Element Codes, Aug. 1985, UCID 19310 Rev. 2.
6. NIKE3D - J.O. Hallquist, An Implicit, finite-deformation, finite element code for analyzing the static and dynamic response of 3 dimensional solids, July 1984, USID, 18822 Rev. 1.
7. TOPAZ - A Finite Element Heat Conduction Code for Analyzing 2D-Solids, Arthur B. Shapiro, UCDD 20045, March 1984.
8. SSC Conceptual Design, Attachment B, Magnet Design Details, March 1986, SSC-SR-2020B.
9. Ibid, p. 72.
10. SSC Dipoles: Eddy Current Focus Generated During a A-Quench, R.B. Meuser, August 5, 1986.
11. Requirements CDG - SSC Magnet System Requirements, 10/23/86 SSC-100.
12. Timoshenko and Gere, McGraw-Hill, 1961.
13. R. Meuser, Nov. 1979, Conductor Position Errors Due to Friction, M5432, Eng. Note, LBL.
14. C. Peters, SSC-Mag-121, SSC-N-295, Coil Prestress Measurement for Nineteen 1-M Collared Dipole Models Constructed at LBL, 2-3-87.
15. SSC-Mar-122, SSC-N-296, LBD-1265, 2/3/87.
16. C. Peters, Springback, Creep, and Cool down Prestress Losses in Nineteen Collared 1-M Dipole Models Constructed at LBL.
17. Seely and Smith, Advanced Mechanics of Material, p. 183, 2nd edition.

APPENDIX

Appendix I Material Description

Table I
Material Properties/TACO Input

<u>TACO Material</u>	<u>lbs/in³ Density</u>	<u>K Temperature</u>	<u>BTU/lb. K Specific Heat</u>	<u>BTU/sec, in, K Conductivity</u>
Copper	.324	0.0	2.09×10^{-6}	
		18	2.09×10^{-3}	
		50	2.09×10^{-2}	
		300	0.0815	
		0		102.3×10^{-4}
		4		144.4×10^{-4}
		20		409.2×10^{-4}
		140		96.3×10^{-4}
		300		96.3×10^{-4}
Nitronic 40	0.283	0	2.089×10^{-4}	
		50	2.089×10^{-2}	
		300	9.94×10^{-2}	
		1		1.00×10^{-5}
		100		2.166×10^{-4}
		175		3.129×10^{-4}
		300		3.492×10^{-4}
Kapton	0.05130	ALL temp	0.22770	0.0373×10^{-4}
<hr/>				
Kapton/				
Teflon	0.05130	ALL temp	0.22770	0.0373×10^{-4}
<hr/>				
Epoxy Comp.	0.05130	0	0.2089×10^{-4}	
		10	52.23×10^{-4}	
		50	104.45×10^{-4}	
		300	2.09×10^{-4}	
		0		0.0193×10^{-4}
		35		0.0241×10^{-4}
		200		0.0481×10^{-4}
		300		0.0482×10^{-4}

<u>TACO Material</u>	<u>lbs/in³ Density</u>	<u>K Temperature</u>	<u>BTU/lb. K Specific Heat</u>	<u>BTU/sec, in, K Conductivity</u>
Kevlar/ teflon	0.05200	0	096×10^{-4}	same as epoxy
		93	0.241×10^{-4}	
		300	0.481×10^{-4}	
G-10	0.05200	0	8.36×10^{-4}	
		12.5	125.3×10^{-4}	
		58	125.3×10^{-3}	
		275	4178×10^{-4}	
		300	4805×10^{-4}	
		0		0.0825×10^{-5}
		300		0.1685×10^{-4}
Coil	0.25291	0	3.725×10^{-8}	
		10	4.111×10^{-8}	
		20	1.25×10^{-7}	
		25	2.27×10^{-7}	
		40	8.76×10^{-7}	
		50	13.3×10^{-7}	
		100	0.028×10^{-4}	
		160	0.0325×10^{-4}	
		200	0.0347×10^{-4}	
		300	0.0393×10^{-4}	
		4		433.3×10^{-4}
		5		505.5×10^{-4}
		8		409.2×10^{-4}
		10		962.8×10^{-4}
		15		1107×10^{-4}
		20		866.5×10^{-4}
		300		10.35×10^{-4}
Wedge	0.32400	same as Cu	same as Cu	same as Cu
Collar steel	0.28300	-----	-----same as Nitronic 40-----	-----

<u>TACO Material</u>	<u>lbs/in³ Density</u>	<u>K Temperature</u>	<u>BTU/lb. K Specific Heat</u>	<u>BTU/sec, in, K Conductivity</u>	
Yoke - Fe	0.28400	2	0.23×10^{-6}		
		4	0.079×10^{-6}		
		10	0.30×10^{-6}		
		65	25×10^{-6}		
		300	25×10^{-6}		
		2		0.12×10^{-2}	
		4		0.12×10^{-2}	
		10		0.27×10^{-2}	
		30		0.6×10^{-2}	
		150		0.22×10^{-2}	
		300		0.19×10^{-2}	
<hr/>					
Liq. He	0.0051	2.5	0.8994		
		4	1.62		
		5	2.698		
		400	2.698		
		4		532×10^{-9}	
		50		1160×10^{-9}	
		80		1600×10^{-9}	
		100		1800×10^{-9}	
		200		1800×10^{-9}	
		320		4164×10^{-9}	
<hr/>					
Aluminum					
7075-T6	0.101	ALL	0.127	9.77×10^{-4}	

Table II
Material Properties/NIKE Input

NIKE requires an additional set of material properties as stated earlier. The most sensitive is α , the coefficient of thermal contraction/expansion. The model was thermo-elastic plastic. Small change in α produce large changes in stress.

<u>Material</u>	<u>Density</u>	<u>K Temperature</u>	<u>lbs/in² Modulus</u>	<u>μ Poisons Ratio</u>	<u>in/in/K α Coef. of Thermal Expan./ Contraction</u>
copper	0.3240	0	15.6×10^{-6}	0.355	1.08×10^{-5}
		80	15.6×10^{-6}		1.4×10^{-5}
		200	15.6×10^{-6}		1.63×10^{-5}
		300	15.6×10^{-6}		1.64×10^{-5}
Nitronic 40	0.2830	0	30×10^{-6}	0.278	1.0×10^{-5}
		80	30×10^{-6}		1.3×10^{-5}
		200	30×10^{-6}		15×10^{-6}
		300	30×10^{-6}		17.28×10^{-6}
Kapton	0.0513	0	530×10^3	0.34	4.6×10^{-5}
Kapton/Teflon		80	510×10^3	0.34	9.1×10^{-5}
		200	470×10^3		1.3×10^{-4}
		300	430×10^3		2.0×10^{-5}
Epoxy	0.0513	0	1.09×10^6	0.37	4.0×10^{-5}
		80	1.31×10^6		4.7×10^{-5}
		200	1.12×10^6		5.9×10^{-5}
		300	0.652×10^6		0
Kevlar/Teflon	0.520	0	1.31×10^6	0.35	-2.0×10^{-6}
		80	0.974×10^6		-2×10^{-6}
		200	0.64×10^6		-2×10^{-6}
		300	0.29×10^6		0
(type of plastic)	0.0520	0	5.2×10^6	0.211 0.1896 0.17 0.1495	2.4×10^{-5}
		80	4.9×10^6		3.0×10^{-5}
		200	4.5×10^6		3.7×10^{-5}
		300	4.1×10^6		0

<u>Material</u>	<u>Density</u>	<u>K Temperature</u>	<u>lbs/in² Modulus</u>	<u>μ Poisons Ratio</u>	<u>in/in/K α Coef. of Thermal Expan./ Contraction</u>
Coil	0.2529	0	3.0×10^6	0.3	1.3×10^{-5}
		80	3×10^6		1.3×10^{-5}
		300	1.5×10^6		1.3×10^{-5}
Orthotropic Model					
		4.35	3×10^6 r, Θ	0.3	1.3×10^{-5}
			14.2×10^6 L	0.3	1.5×10^{-5}
(NIKE does not have the same orthotropic model is not time (temp) dependent)		300 K	9.22×10^6 L		
					Both E and α were varied on several runs based on different sources (LBL, BNL, and parties within).

Wedge (same as copper)

Collar (steel) same as Nitronic 40

Collar (Al.)	0.1011	0	1.02×10^7	0.33	1.4×10^{-5}
(same as Al insert)		30	1.02×10^7	0.33	1.8×10^{-5}
		200	1.02×10^7	0.33	2.15×10^{-5}
		300	1.02×10^7	0.33	2.3×10^{-5}

Yoke	0.2830	0	30×10^6	0.285	1×10^{-6}
(Fe)		80	28×10^6	0.285	3.8×10^{-6}
		200	28×10^6	0.285	10×10^{-6}
		300	28×10^6	0.285	12×10^{-6}

He	0.0051	0	156	0.45	1.5×10^{-4}
(He port)		5	100	0.45	1.5×10^{-4}
Annulus		300	100	0.45	1.5×10^{-4}

As a consequence of the mesh being in inches, and the units of material properties as given, the output will consist of stress in psi, deflection in inches, and temperature in K. A detailed drawing of the model is given in Fig. 2. However, the detail of the plastics around the beam tube cannot be discriminated. Therefore, the following table describes the various layers which was used in developing the computer model (Ref. letter to Dave Jackson from BNL, 4-24-86).

0.718	~4.5 mils	"F" film of 0.0001" thick Kapton + 0.0005" thick Teflon, 1.0" wide. The Teflon faces in. 30% overlap, ~ 1-2 lbs tension.
9		
0.713	~ 10-12 mils	Kevlar cord (1000 denier Dupont 29 Kevlar) impregnated with Teflon, wrapped continuously (~30 turns/inch) under ~12 lbs tension: one layer clockwise, and one layer counterclockwise. The Kevlar has an infrared sensitive adhesive, and the layers are bonded by I.R.
0.701	~2 mils	"F" film, 0.001" thick Kapton + 0.001" thick Teflon sheet (Teflon facing out); the sheet is ~1/2" wide, or just sufficiently wide to cover wire pattern.
0.699		
~8 mils		<u>Coil Pattern</u> : Coil pattern* is ultrasonically embedded in epoxy composite by the multiwire process while the substrate is flat. The finished coil pattern is wrapped around and lightly secured to bore tube (slots in substrate ensures accurate registry).
0.691	~8-9 mils	<u>Substrate</u> : "F" film of 0.003" thick kapton + 0.001" thick Teflon (facing down. On top of this comes 0.002" of proprietary epoxy composite, pressed and bonded the Kapton. Next, a glass wick, ~0.002" thick, followed by 0.0045" of the same epoxy composite.
0.682	~2 mils	<u>Electrical Insulation</u> : 0.001" Kapton + 0.0001" Teflon (with infra-red sensitive adhesive); 50% overlap
0.68		
0.64		Stainless steel bore tube

Effective overall thickness ~40 mils approximately 1 mm

* The Superconducting wires are coated with 500 volt insulation - 0.0005" in radial thickness, followed by a very thin layer of proprietary adhesive. It is thus adhesive which is the crux of the multiwire process.

Fig. 1A. Details of the Multiwire SSC.

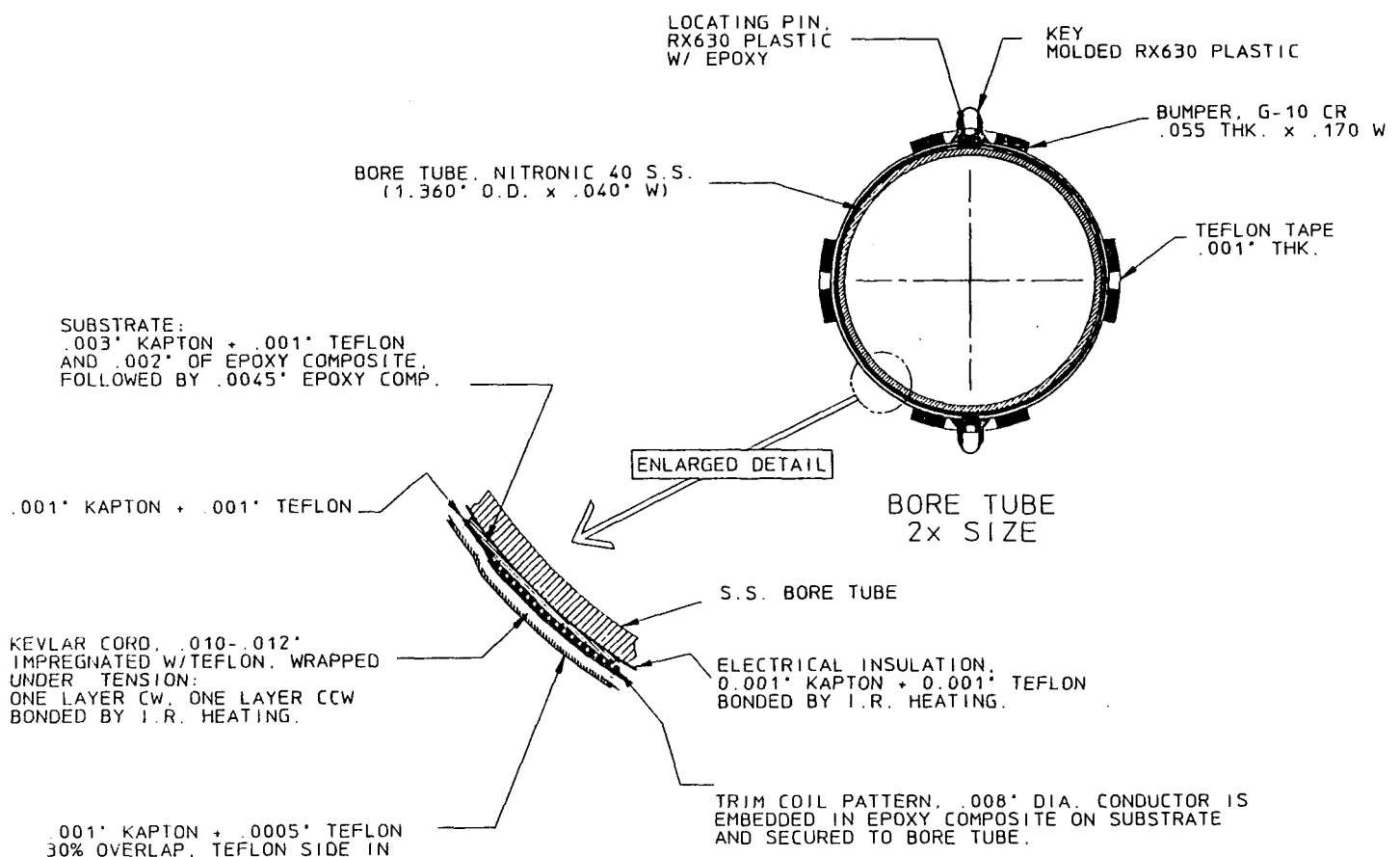


Fig. 2A. Detail of beam tube and adjacent areas.

Appendix II Loading Conditions -- Input to NIKE.

We have discussed earlier the function $g(t,x) = c_1(t)c_2(x)$ by which input is handled by NIKE. Tables III through XI are the specific input.

The Lorentz force on the coil is operational at $t < 0.1$ second, and we let the quench begin at $t = 0.1$ second. Table III is $c_1(t)$ for the Lorentz force on the coil. Table IV is $c_1(t)$ for the Lorentz force on the beam tube. Table V is $c_1(t)$ for the helium pressure, and Table VI is $c_1(t)$ for the deflection on coil. $c_2(x)$ is the spatial function. Table VII is the value of $c_2(x)$ for the Lorentz force on the coil. The set of forces P_x $= -2\alpha \cos \theta$, $P_y = 0$ is equivalent to $P_r = -\alpha(\cos 2\theta + 1)$ and $P_t = \alpha \sin 2\theta$ where $\alpha = c_1(t)$, $-(\cos 2\theta + 1) = c_2(x)$, $\sin 2\theta = c_2(x)$. $0 \leq \theta \leq 90^\circ$ as shown in Fig. 3A.

Both pressure and shear will be linearly distributed between the nodes. The source of the Lorentz force on the coil as well as the beam tube is given in Ref. 10 and is based on the operating field on the magnet. The Lorentz force is a $\cos \theta$ force. The $\cos \theta$ force can be replaced by a normal force and a shearing force and is in this case a pressure.

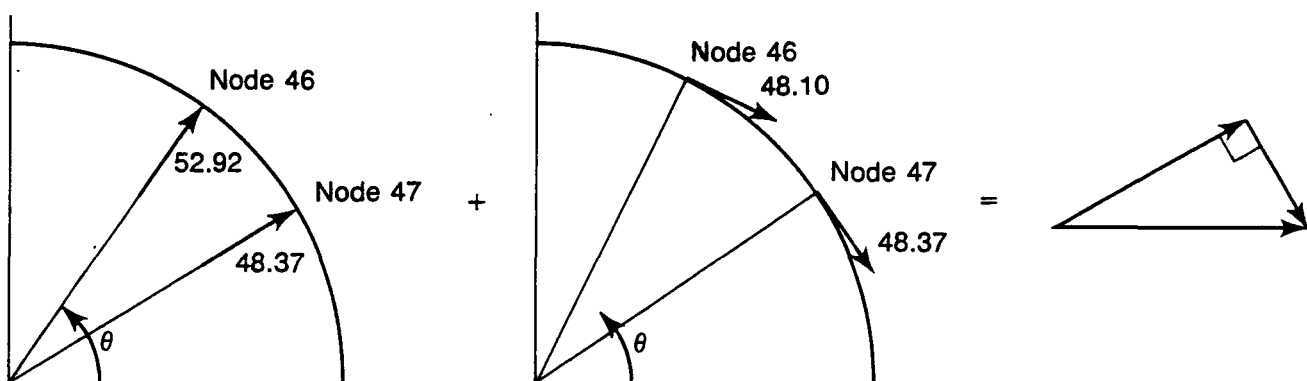


Fig. 8.

Table VIII is $c_2(x)$ for helium pressure and Tables X and IX are $c_2(x)$ for the Lorentz Force on Beam Tube. Table XI is $c_2(x)$ representing the deflection of the coil, inner and outer. Figs. 4A-9A describe the mesh in more detail in terms of $c_2(x)$.

Table III

Time Function <u>t</u>	Lorentz Force (curve 1) Coil <u>Value (scale multiplier, no units)</u>
0.0	0.0
0.05	1.0
0.1	1.0
0.15	1.0
0.2	0.969
0.25	0.9098
0.30	0.7555
0.35	0.5228
0.40	0.2736
0.45	0.1363
0.50	0.0684
0.55	0.0286
0.6	0.00852

Table IV

Time Function Lorentz Force (curve 2) Beam Tube

<u>t</u>	<u>Value (psi)</u>
0.0	0.0
0.1	0.0
0.15	-1.087
0.2	-10.69
0.25	-28.76
0.30	-48.37
0.35	-45.68
0.40	-30.6
0.45	-15.23
0.50	-7.31
0.55	-2.9
0.6	-1.291

$p_x = -2\alpha \cos\theta$
 $p_y = 0$
 $p_x = -2(-48.37) = +96.74 \text{ psi}$
 $\theta = 0 \text{ degrees}$

Table V

Annulus Pressure (He) Curve 3

<u>time</u>	<u>Pressure - Multiplier-psi</u>
0.0	0.0
0.1	0.0
0.3	400.0
0.4	600.0
0.7	600.0
1.05	450.0

Table VI

Curve 4 Deflection on Coil

<u>time</u>	<u>Value (no units)</u>
0.0	0.0
0.05	1.0
1000.0	1.0

Table VII
Forces on Coil

<u>Node</u>	<u>Direction</u>	<u>Curve#</u>	<u>lbs. Value</u>
146	1	1	4.132e+01
146	2	1	-7.815e+00
147	1	1	4.668e+01
147	2	1	-1.814e+01
148	1	1	5.484e+01
148	2	1	-3.717e+01
149	1	1	6.421e+01
149	2	1	-5.426e+01
150	1	1	3.501e+01
150	2	1	-3.118e+01
151	1	1	2.105e+01
151	2	1	-4.052e+00
152	1	1	4.669e+01
152	2	1	-1.814e+01
153	1	1	5.484e+01
153	2	1	-3.717e+01
154	1	1	6.421e+01
154	2	1	-5.426e+01
155	1	1	3.501e+01
156	2	1	-3.118e+01
157	1	1	6.141e+01
157	2	1	-5.173e+01
159	1	1	6.141e+01
159	2	1	-5.173e+01
160	1	1	1.380e+02
160	2	1	-1.085e+02
161	1	1	1.747e+02
161	2	1	-1.178e+02
162	1	1	2.008e+02
162	2	1	-1.125e+02
163	1	1	1.026e+02
163	2	1	-5.151e+01
164	1	1	1.379e+02
164	2	1	-1.085e+02
165	1	1	1.747e+02
165	2	1	-1.178e+02
166	1	1	2.008e+02
166	2	1	-1.125e+02
167	1	1	1.026e+02
167	2	1	-5.151e+01
170	1	1	2.492e+02
170	2	1	-6.657e+01
173	1	1	2.492e+02
173	2	1	-6.657e+01
174	1	1	2.492e+02
174	2	1	-6.657e+01
175	1	1	2.492e+02
175	2	1	-6.657e+01

Inner Coil



Forces on Coil

<u>Node</u>	<u>Direction</u>	<u>Curve#</u>	<u>Value</u>
187	1	1	2.027e+01
187	2	1	-3.763e+00
188	1	1	4.408e+01
188	2	1	-1.635e+01
189	1	1	5.102e+01
189	2	1	-3.351e+01
190	1	1	2.721e+01
190	2	1	-2.093e+01
191	1	1	4.408e+01
191	2	1	-1.635e+01
192	1	1	5.102e+01
192	2	1	-3.351e+01
193	1	1	2.721e+01
193	2	1	-2.093e+01
196	1	1	4.871e+01
196	2	1	-4.360e+01
199	1	1	4.860e+01
199	2	1	-4.360e+01
200	1	1	1.119e+02
200	2	1	-9.612e+01
201	1	1	6.323e+01
201	2	1	-5.252e+01
202	1	1	1.601e+02
202	2	1	-1.074e+02
203	1	1	1.601e+02
203	2	1	-1.074e+02
204	1	1	1.119e+02
204	2	1	-9.612e+01
205	1	1	6.327e+01
205	2	1	-5.252e+01
206	1	1	1.601e+02
206	2	1	-1.074e+02
207	1	1	1.601e+02
207	2	1	-1.074e+02

Table VIII
Helium Pressure

<u>Curve #3</u>	<u>Node A</u>	<u>Node B</u>	<u>Factor A</u>	<u>Factor B (no units)</u>
3	135	144	-1.	-1.
3	144	145	-1.	-1.
3	145	558	-1.	-1.
3	558	563	-1.	-1.
3	563	139	-1.	-1.
3	142	507	-1.	-1.
3	507	510	-1.	-1.
3	510	573	-1.	-1.
3	573	568	-1.	-1.
3	568	138	-1.	-1.
3	172	167	1.	1.
3	167	165	1.	1.
3	165	164	1.	1.
3	164	159	1.	1.
3	159	155	1.	1.
3	155	154	1.	1.
3	154	153	1.	1.

This is modified when the bumpers are removed and replaced with Helium elements.

3	177	176	1.	1.
3	176	140	1.	1.
3	140	139	1.	1.
3	139	563	1.	1.
3	563	558	1.	1.
3	558	145	1.	1.
3	145	144	1.	1.
3	135	134	1.	1.
3	134	133	1.	1.
3	136	137	1.	1.
3	137	138	1.	1.
3	138	568	1.	1.
3	568	573	1.	1.
3	573	510	1.	1.
3	510	517	1.	1.
3	507	142	1.	1.
3	142	143	1.	1.
3	143	144	1.	1.
3	144	179	1.	1.
3	179	121	1.	1.

Table IX

Lorentz Force on Beam (Cosθ Force)

<u>Curve #2</u>	<u>Surface Segment</u>	<u>Multiplier at B</u>	<u>Multiplier at A</u>	<u>Loading Type</u>
	<u>Node B</u>	<u>Node A</u>	<u>no units</u>	<u>no units</u>
2	639	638	0.	-.0054800
2	638	637	-.0054800	-.0218500
2	637	636	-.021850	-.048940
2	636	635	-.048940	-.086450
2	635	634	-.086450	-.133970
2	634	633	-.133970	-.190980
2	633	55	-.190980	-.256855
2	55	54	-.256855	-.330869
2	54	53	-.330869	-.412200
2	53	52	-.412200	-.500000
2	52	51	-.500000	-.593260
2	51	50	-.593260	-.690983
2	50	49	-.690983	-.792088
2	49	48	-.792088	-.895500
2	48	47	-.895500	-.100000
2	47	46	-.100000	-.110450
2	46	45	-.110450	-.120790
2	45	44	-.120790	-.130900
2	44	43	-.130900	-.140670
2	43	42	-.140670	-.150000
2	42	41	-.150000	-.158800
2	41	40	-.158800	-.166900
2	40	39	-.166900	-.174300
2	39	38	-.174300	-.180900
2	38	37	-.180900	-.186600
2	37	36	-.186600	-.191400
2	36	35	-.191400	-.195100
2	35	34	-.195100	-.197800
2	34	33	-.197800	-.199000
2	33	32	-.199000	-.100000

Table X

<u>Curve #</u>	<u>Node B</u>	<u>Node A</u>	<u>Multiplier at B</u>	<u>Multiplier at A</u>	
2	639	638	0.	+.104500	1 (shear)
2	638	637	+.1045000	+.207900	1
2	637	636	+.207900	+.309016	1
2	636	635	+.309016	+.406740	1
2	635	634	+.406740	+.500000	1
2	634	633	+.500000	+.587785	1
2	633	55	+.587785	+.669130	1
2	55	54	+.669130	+.743100	1
2	54	53	+.743100	+.809000	1
2	53	52	+.809000	+.866025	1
2	52	51	+.866025	+.913545	1
2	51	50	+.913545	+.951056	1
2	50	49	+.951056	+.978100	1
2	49	48	+.978100	+.994500	1
2	48	47	+.994500	+1.00000	1
2	47	46	+1.00000	+.994500	1
2	46	45	+.994500	+.978100	1
2	45	44	+.978100	+.951060	1
2	44	43	+.951060	+.913500	1
2	43	42	+.913500	+.866000	1
2	42	41	+.866000	+.809000	1
2	41	40	+.809000	+.743000	1
2	40	39	+.743000	+.669000	1
2	39	38	+.669000	+.587800	1
2	38	37	+.587800	+.500000	1
2	37	36	+.500000	+.406700	1
2	36	35	+.406700	+.309000	1
2	35	34	+.309000	+.207900	1
2	34	33	+.207900	+.104500	1
2	33	32	+.104500	0.	1

Table XI
Deflection at Coil

<u>Node#</u>	<u>Direction</u>	<u>Curve#</u>	<u>Value (in.)</u>
151	2	4	+30.0e-04
146	2	4	+30.0e-04
191	2	4	+20.0e-04
187	2	4	+2.00e-03

STRUCTURAL ANALYSIS QUENCH/TRANSIENT SOL. L. He. elements, 7-10-86

dsf = 1.00000e+00

time = 6.60000e-01

YOKÉ

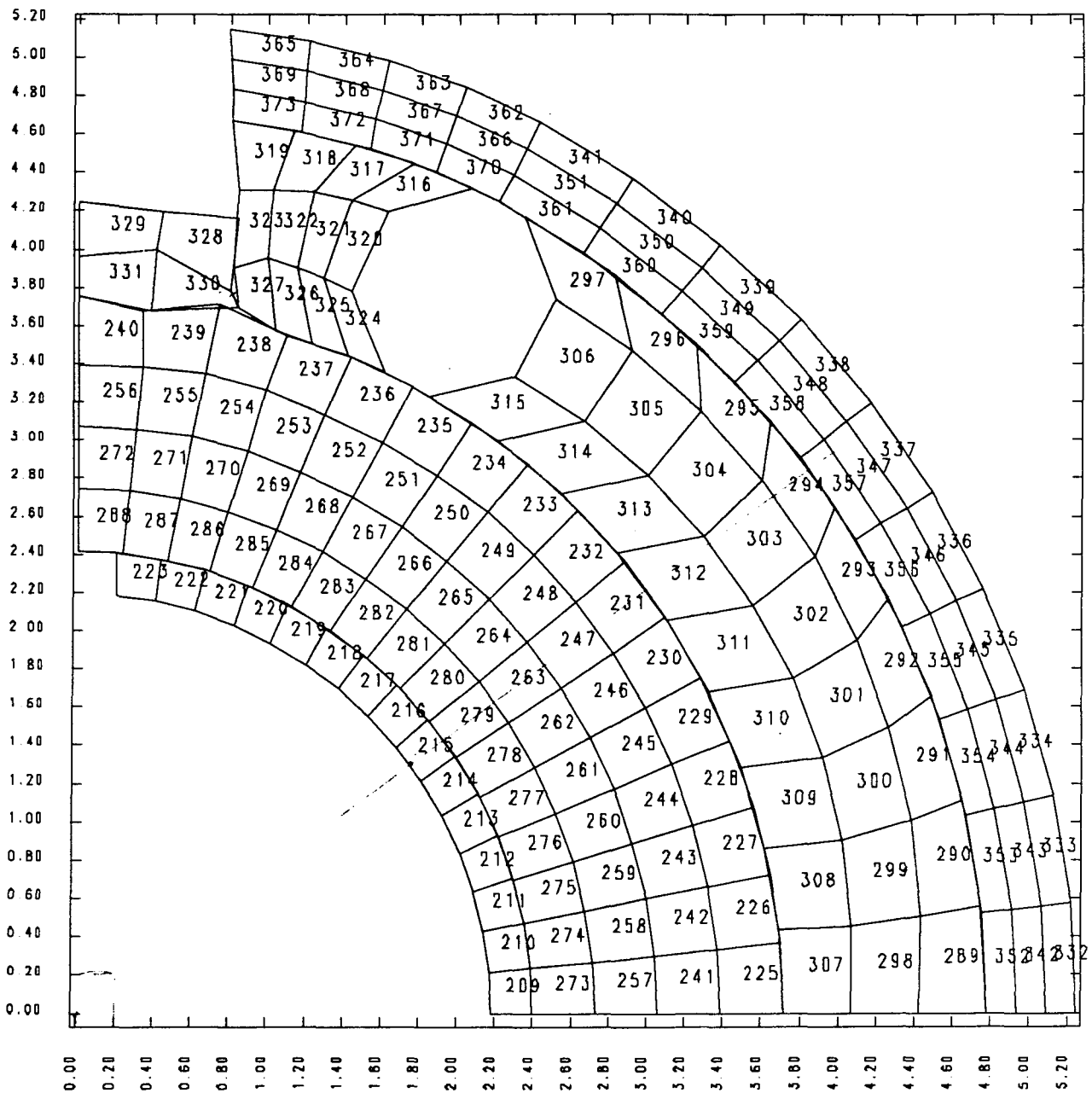


Fig. 4A. Yoke Elements

STRUCTURAL COOL DOWN OPERATION - 2 STAGES - AL COLLAR - 9-9-86

dsf = 1.00000e+00

time= 1.90000e+01

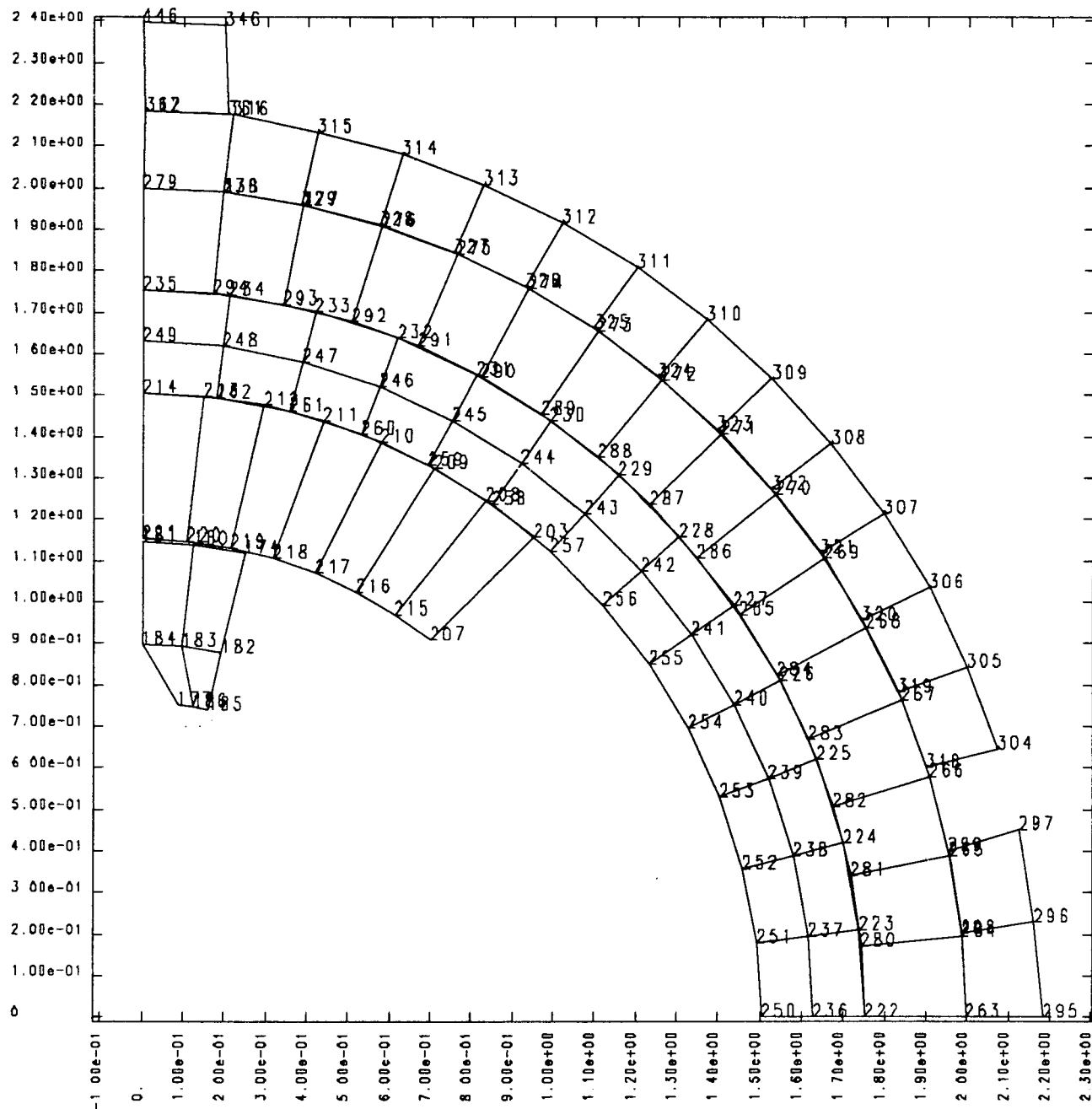


Fig. 5A. Collar/nodes.

STRUCTURAL COOL DOWN OPERATION - 2 STAGES - AL COLLAR - 9-9-86

dsf = 1.00000e+00

time= 1.90000e+01

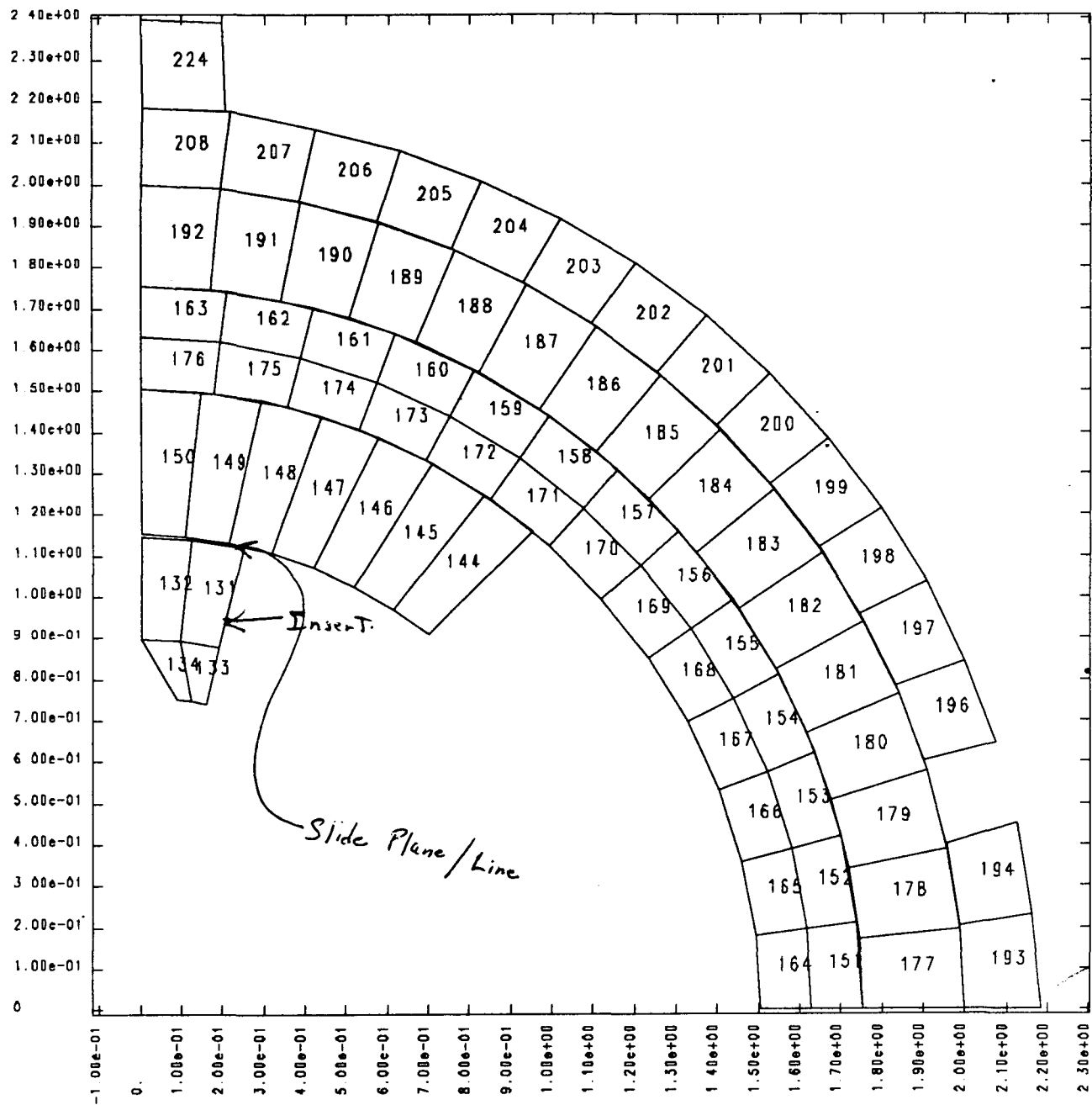


Fig. 6A. Collar/elements.

STRUCTURAL ANALYSIS QUENCH/TRANSIENT SOL. L. He. elements, 7-10-86

ds1 = 1.00000e+00

time= 6.60000e-01

Yoke

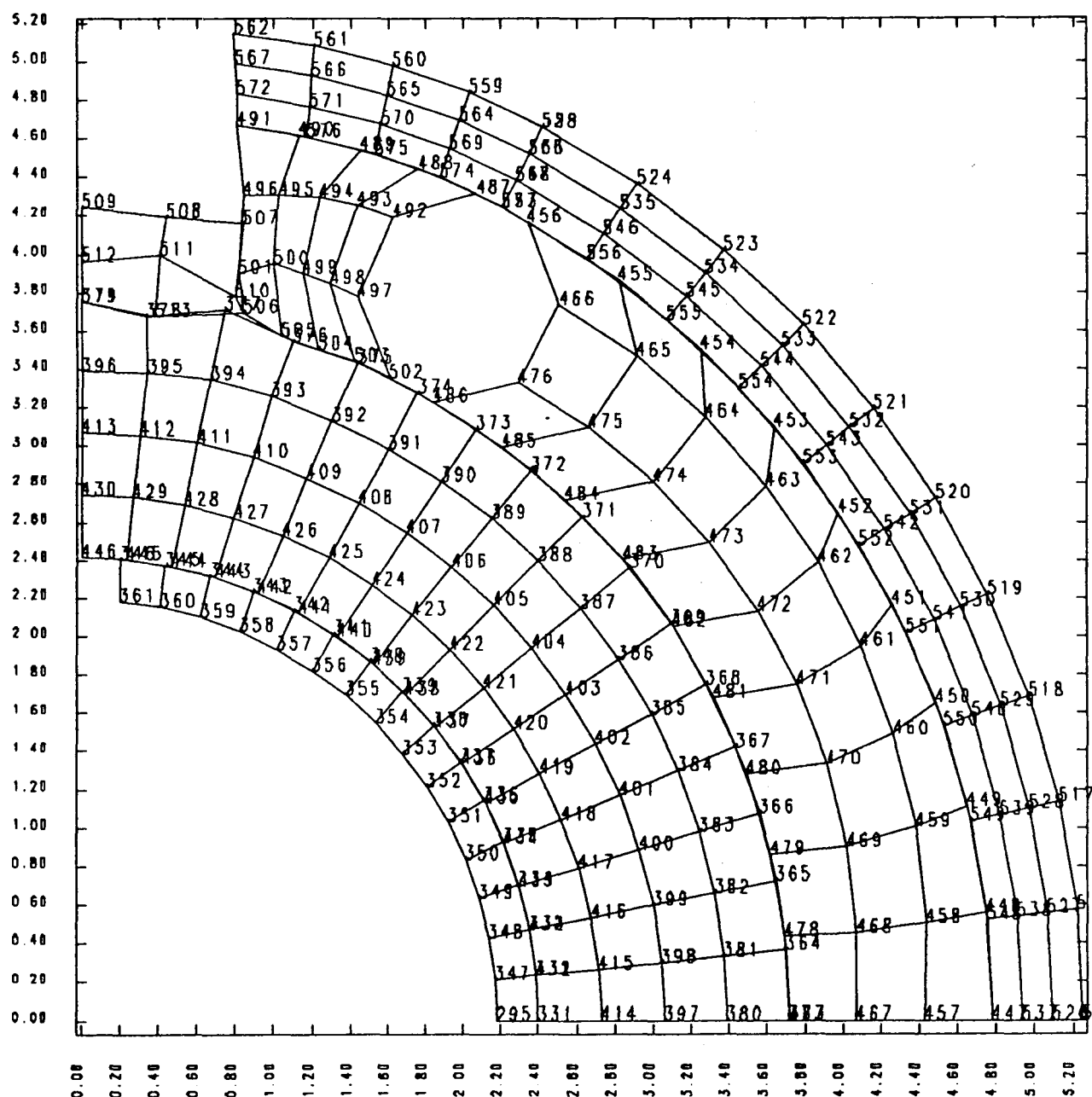


Fig. 7A. Yoke/nodes.

STRUCTURAL ANALYSIS QUENCH/TRANSIENT SOL. L. He. elements, 7-10-86

dsf = 1.00000e+00

time= 6.60000e-01

COIL

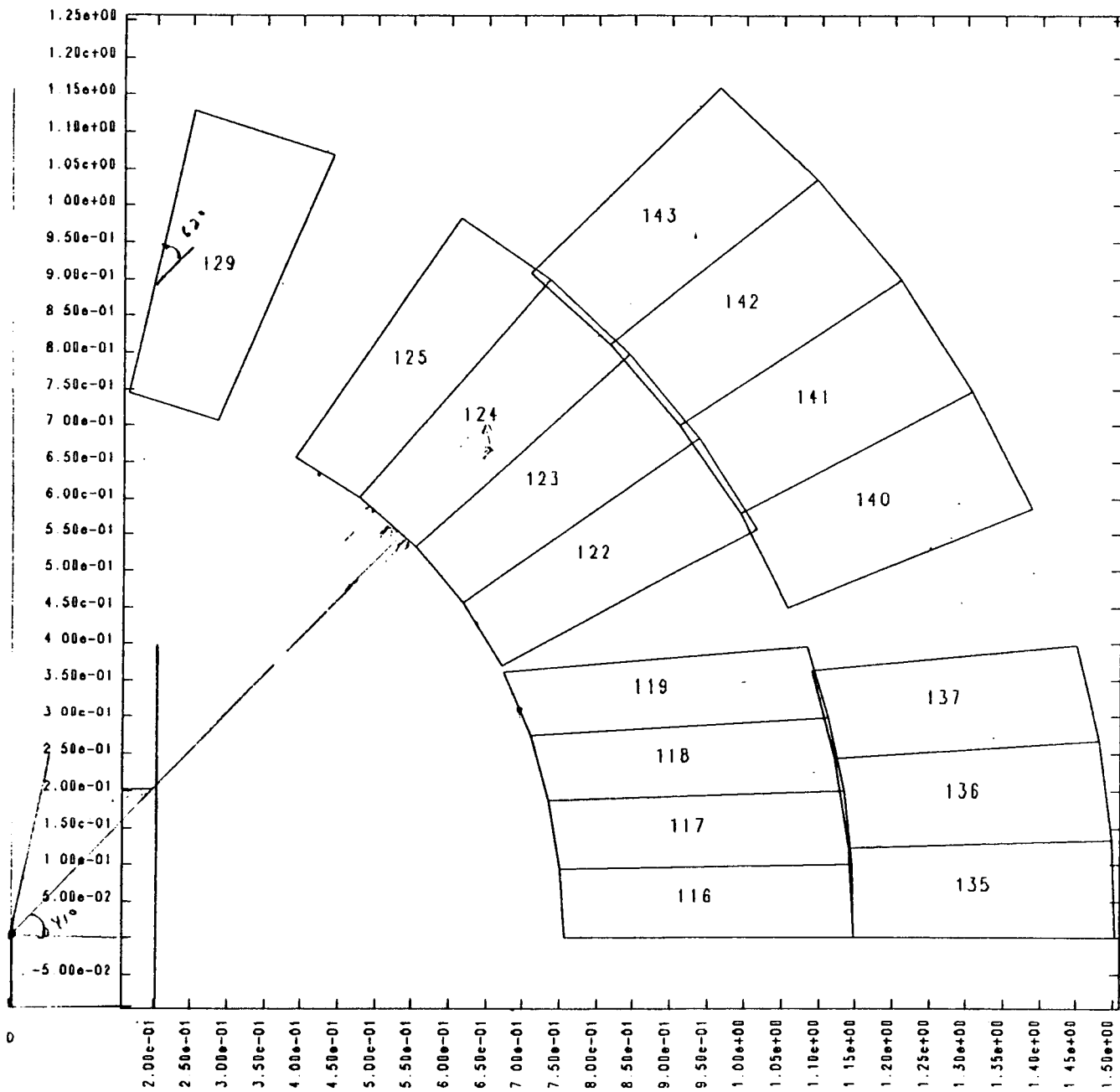


Fig. 8A. Coil/elements.

Appendix III Secondary Results

Clearances and Bumpers

The maximum stress in the copper plating and beam tube occurs under the G-10 bumpers as a consequence of thermal contraction at the end of cool down $t \geq 20$ seconds. However, when a clearance is allowed between the bumper and the plastics and the bumper is more accurately modeled at the pole -- a clearance is allowed between the bumper and z axis, the high stresses disappear in beam tube and copper plating. Clearances of a minimum of 5 mils are required. Having a permanent clearance of a few mils. reduces the stress level below the maximum value specified by the CDG.¹¹

For the results when there are no clearances between the bumper and the plastics, at the end of cool down $t \geq 20$ sec, one obtains a maximum stress in beam tube. A comparison of the stresses in the beam tube due to different conditions is as follows:

Table XII

Maximum Stress in Beam Tube
(ksi)

	<u>σ_{max} in beam tube</u>
Steel Collar - No insert	210.0
Al Insert in Al collar	59.0
St. Insert in St. collar	80.0
Al Insert in St. collar	74.8

Note: these are circumferential stresses

The insert acts as a clearance, boundary conditions are different, stress reduced significantly, because it decouples the collar from G-10 bumper.

Sensitivity Analysis

a) Variation in E of Coil

BNL has proposed somewhat different properties of the coil. Our model had $\alpha = 1.3 \times 10^{-5}$ in/in/K and $E = 3.0 \times 10^6$ at 4.35 K, 80 K and 1.5×10^6 at 300 K where α is the coefficient of thermal expansion/contraction and E the modulus of elasticity. The wedge is modeled separately where $\alpha = 0.1 \times 10^{-4}$ to 1.64×10^{-5} in/in/K. BNL's recommendation for modulus of the coil (wedge included) is 1.9 to 2.4×10^6 psi and $\alpha = 1.57 \times 10^{-5}$ in/in/K. A comparison of the results of the different models is shown below for a steel collar, no insert:

Table XIII

Maximum Stress
Comparison with Different Properties
(ksi)

	<u>Max Stress</u>	<u>With Clearance</u>	<u>Max Stress (BNL Properties)</u>
Plating	72.1	60.78	76.0
Beam Tube	122.0	76.25	131.0
Inner Coil	6.8 to 23	4.35 3.9	3.5 to 0.9
Outer Coil	13.4 to 4.2	15.3 3.75	11.4 to 2.3

Therefore, BNL's recommendation for coil properties effects essentially only the coil stress.

b) Change in Coil Material Model

The coil model is generally assumed isotropic. As the coil is a complex composite, it is anisotropic. An orthotropic model is probably a significant improvement. LBL was able to obtain orthotropic data, where

$$E_r = E_\theta, \alpha_r = \alpha_\theta, E_L, \alpha_L$$

Comparing the results for a steel collar with no insert, no significant differences were noted in r , θ plane. $E_r = E_\theta = 3.0 \times 10^6$ psi, $E_L = 14.2 \times 10^6$ psi. The reason no significant differences exist is because the model is a plane stress model and the cross sectional properties did not change. The stress in the longitudinal direction in the coil was very different, as one would anticipate. An orthotropic model is extremely important in evaluating the 3d case or longitudinal stresses. NIKE (NIKE3D) permits the use of an orthotropic model but it does not contain a temperature (or time) dependency. TACO (TACO3D) does allow for the orthotropic properties to vary with temperature.

c) Variation in α of Coil

Table XIV

Effect Pre-stress (ksi) Due to Variation in α , $T = 4.35$ K

$\alpha \times 10^{-5}$ in/in/k	<u>Collar</u>	ksi	ksi
<u>I.C.</u>	<u>O.C.</u>		
0.9	steel unconstrained	-11.3 \rightarrow -.88	-3.5 \rightarrow -2.
1.1	" "	-.65 \rightarrow -.53	-1.8 \rightarrow -.85
\rightarrow	1.3 " "	-.6 \rightarrow -.6	-2.3 \rightarrow -.23
	1.5 " "	-.56 \rightarrow -.54	-1.9 \rightarrow 0
\rightarrow	1.3 Al unconstrained	-.55 \rightarrow -.96	-2.5 \rightarrow -.7
	1.3 constrained steel elements #	2 \rightarrow 4.5, (116)(129) (135)	3.1 \rightarrow 1.57, (143)
1.3	constrained Al	2.7 \rightarrow 3.9,	-2. \rightarrow -1.46,

Al collar has a higher pre-stress at end of cool down than steel collar where we do not artificially force the parts to remain in contact (slide line 4). We do not get significant differences between $\alpha = 1.1 \times 10^{-5}$ in/in/K and 1.5×10^{-5} in/in/K. When the coils are constrained, the stresses are significantly higher but the sign of stress on positive rather than negative. The relationship between α of the coil and collars (steel or Al) are extremely important. While we know the values of steel and Al we do not have adequate

values of coil. Therefore, some of our results are masked by inappropriate material properties. The values of α of coil as a function of temperature needs to be re-evaluated. The following table points to this problem. Clearly, we should be able to do better than having $\alpha = 1.3 \times 10^{-5}$ for an extreme temperature range.

Table XV
Value of α at Different Temperature, in/in/K

<u>Material/ Temperature</u>	<u>4.35 K</u>	<u>80 K</u>	<u>300 K</u>
Al	1.4×10^{-5}	1.8×10^{-5}	2.3×10^{-5}
Steel	1.0×10^{-5}	1.3×10^{-5}	1.7×10^{-5}
Coil	1.3×10^{-5}	1.3×10^{-5}	1.3×10^{-5}

d) Variation in E

Using $\alpha = 1.3 \times 10^{-5}$, steel collar, unconstrained, clearance under bumpers, and varying E.

Table XVI
Effect of Varying E of the Coil

<u>E coil at 4.35 °K</u>	<u>input</u>	<u>ksi I.C.</u>	<u>ksi O.C.</u>	<u>ksi S.G. Loc</u>
3.0×10^6	3 mils/2 mils	$-.6 \rightarrow -.6$	$-2.3 \rightarrow -.23$	-12.9
$*3.0 \times 10^6$	9 mils/7 mils	$-5.75 \rightarrow -5.06$	$-5.05 \rightarrow -9.4$	-15.6
6.0×10^6	3 mils/2 mils	$-.76 \rightarrow -.7$	$-4.8 \rightarrow -0.4$	-12.9

* These numbers would indicate that 9 mils/7 mils are too high, and would exceed necessary requirements. It is also observed that there is a dependence on modulus. In the I.C. the stress increases about 25% and the outer coil 100%, with input constant. Note the uniformity in I.C. with a clearance under the bumpers.

If one divides the input by effective length, one gets ϵ , strain the stress $\alpha = E\epsilon$. However, note the non-linearity.

e) Variation in Displacement of Equatorial Plane

To obtain a more appropriate value of input, the input was varied, and to evaluate what a strain gaged load cell would be reading, an active slide line was inserted in the collar.

Table XVII
Variation in Displacement at Equatorial Plane

Element	A I=3/2mil No Bumper/ No Insert	B I=3/2mil Bumper Insert	C I=9/7mil Bumper Insert	D I=3/2mil No Bumper Insert	E I=9/7mil No Bumper Insert	F I=5.6/ 3.2mil Bumper Insert	G I=7.3/ 4.5mil Bumper Insert
I.C.							
116(Eq.)	-0.466	-0.567	-6.25	-0.56	-5.19	-2.6	-4.35
129(Pole)	-0.796	0	-5.73	0	-4.58	-1.95	-3.9
O.C.							
135(Eq.)	-2.3	=2.3	-10.77	-2.3	-10.6	-12.0	-15.3
143(Pole)	-.210	-0.29	-7.07	-0.29	-7.0	-1.7	-3.75
S.G.Loc							
<u>131+132</u>	0	-2.0	-8.8	0	-6.4	-3.8	-6.35
	2						

It is noted that calculation G meets our requirements with $E \text{ coil} = 3 \times 10^6$, $\alpha = 1.3 \times 10^{-5}$.

From the above table, we note $I = 3$ mils, 5.6 mils, 7.3 mils, 9 mils produce stresses in I.C. in the element adjacent to pole of 0, -2., -3.9, -5.7 ksi respectively.

Other Concerns/Bumpers

Computer calculations showed that with no clearance, the coil was restrained along the bumpers. When, the system cooled down, the coil

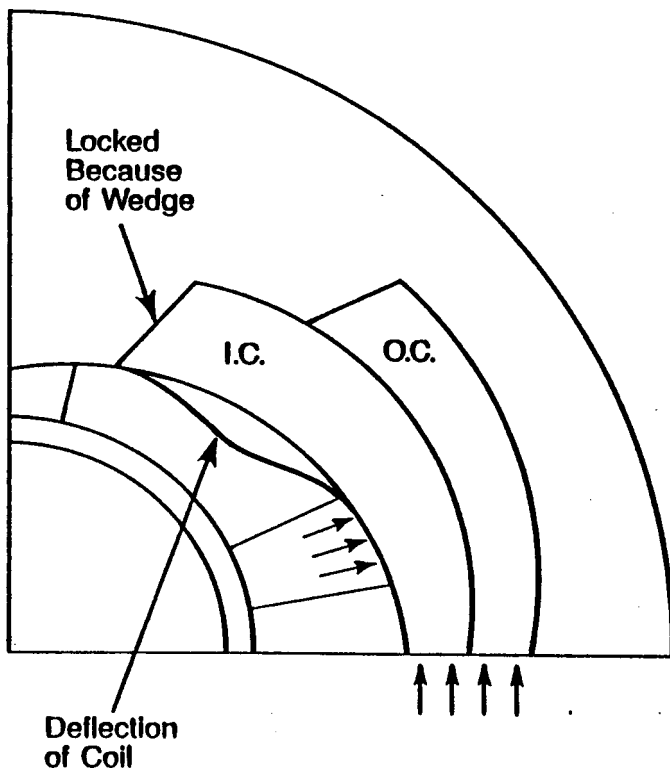


Fig. 9A. Effect of cool down when no clearance

deformed as shown. The consequence of such a deflection was that circumferential prestress was eliminated in virtually the entire coil and the prestress loaded the tube and coil where the bumpers were located. When the coil was forced to maintain contact with the collar, than the deflection shown in the diagram could not occur and the prestress remained circumferential. However, as a consequence at forcing the coils to adhere to each other and the collar, the circumferential stress was not uniform as anticipated but varied by more than a factor of two. The circumferential stress was higher in the vicinity of the equatorial plane near the lower bumper and decreased as one left the bumper toward the pole.

When adequate clearance was provided under the bumpers and at the pole, separation of parts was then permitted, a more uniform circumferential stress was obtained in both the lower and upper coil. The circumferential stress will vary due to friction, slide planes, wedges and other boundary conditions. An adequate pre-stress of 4000 I.C. was obtainable after cool down with a minimum clearance of 3 mil.

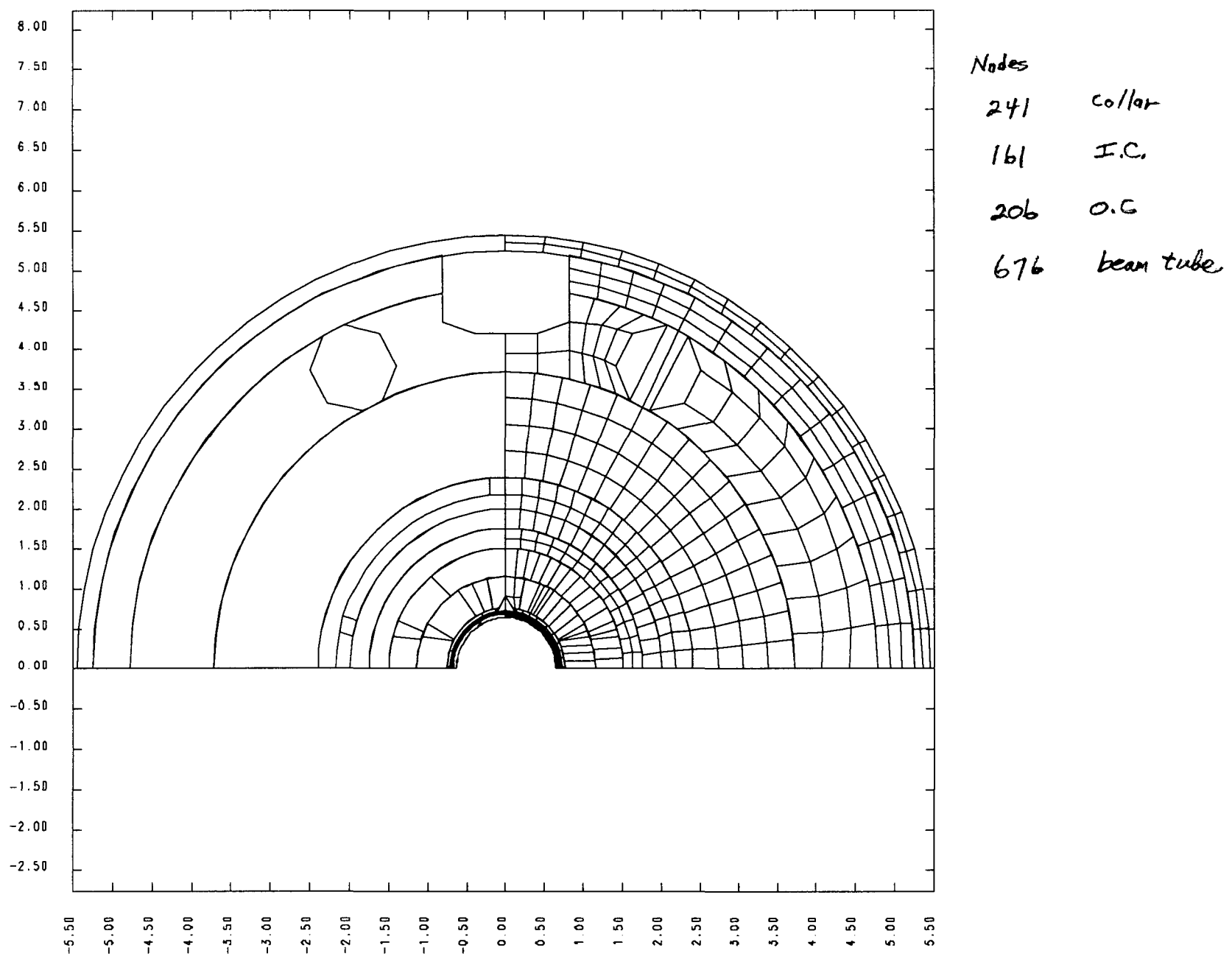
Appendix IV Orion

It is obvious that an infinite number of plots can be obtained from each calculation. As an example and to complete the process, the output from the quench calculation (80 seconds) Al collar, no bumpers, $t = 0.04$ in, 150 psi Lorentz force, was input into Orion. However, only the first second of data was used used as this is the area of primary interest. It is the plot file from NIKE that is input to Orion together with a command file. The curves are developed in Livermore on the Cray but printed on the IMOGEN at LBL.

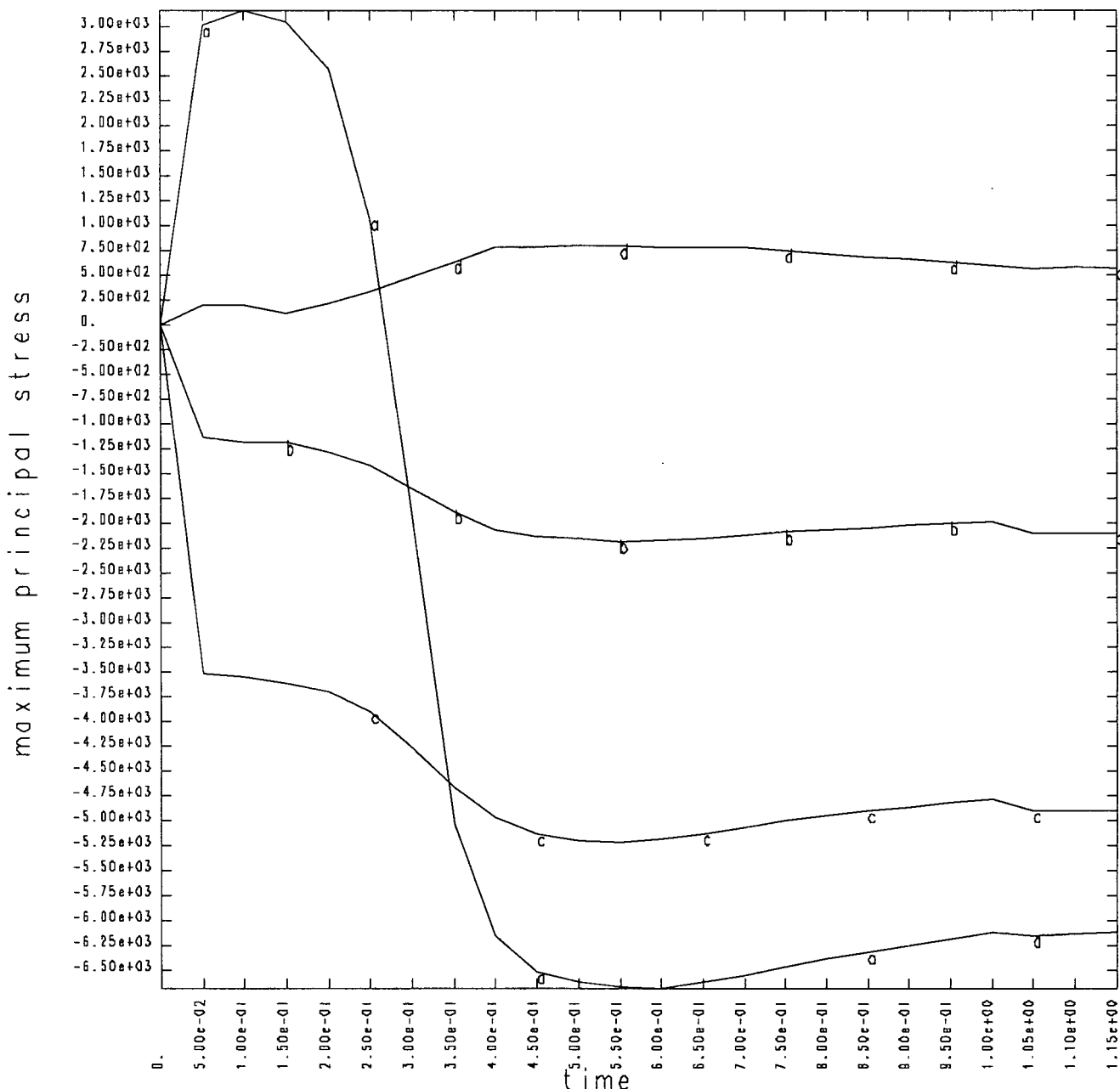
STRUCTURAL QUENCH/STEADY STATE OPERATION - AL. COLLAR 4-2-87

dsf = 1.00000e+00

time= 0.



STRUCTURAL QUENCH/STEADY STATE OPERATION - AL. COLLAR 4-2-87

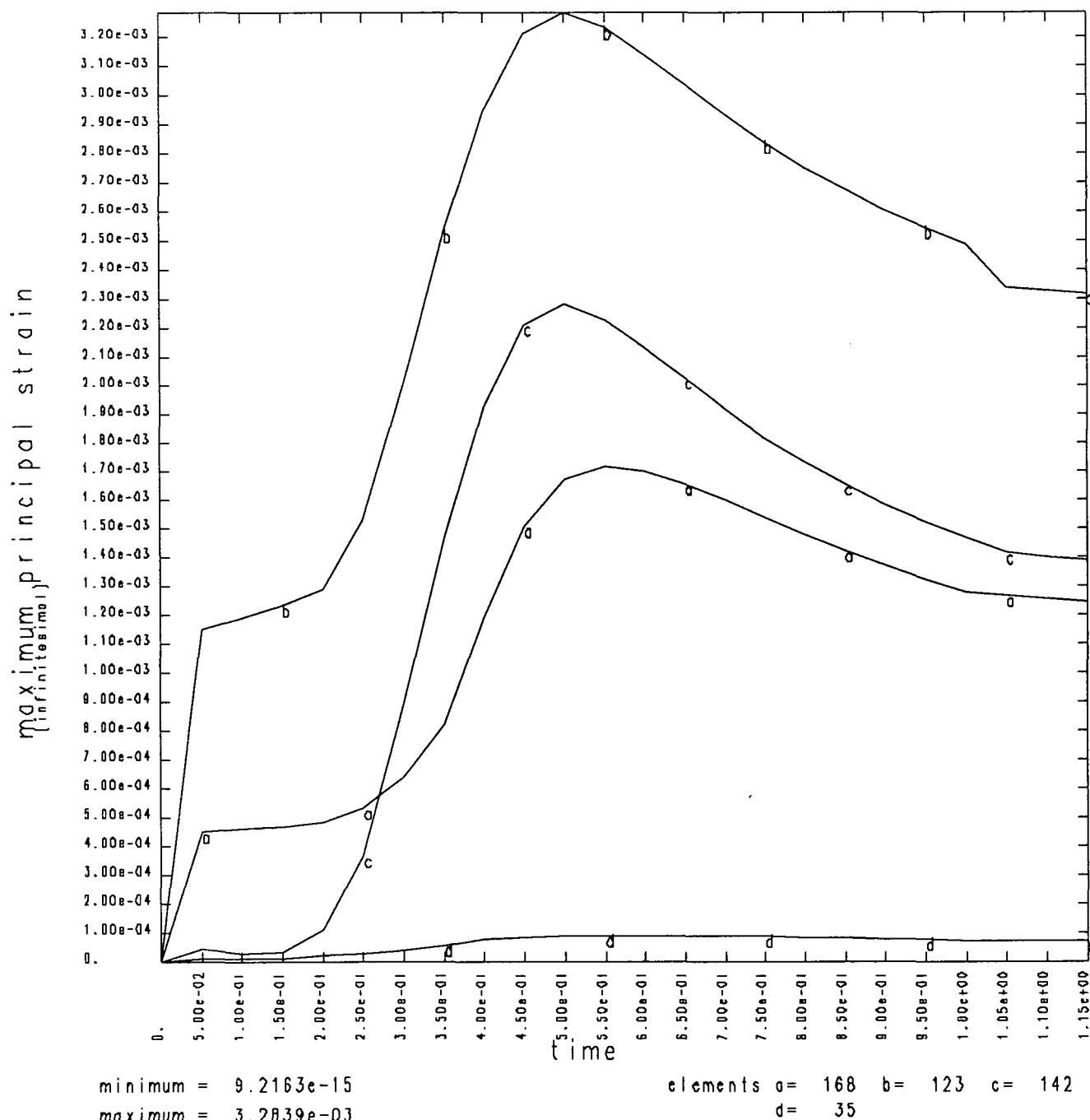


a = collar
b = coil (xc)

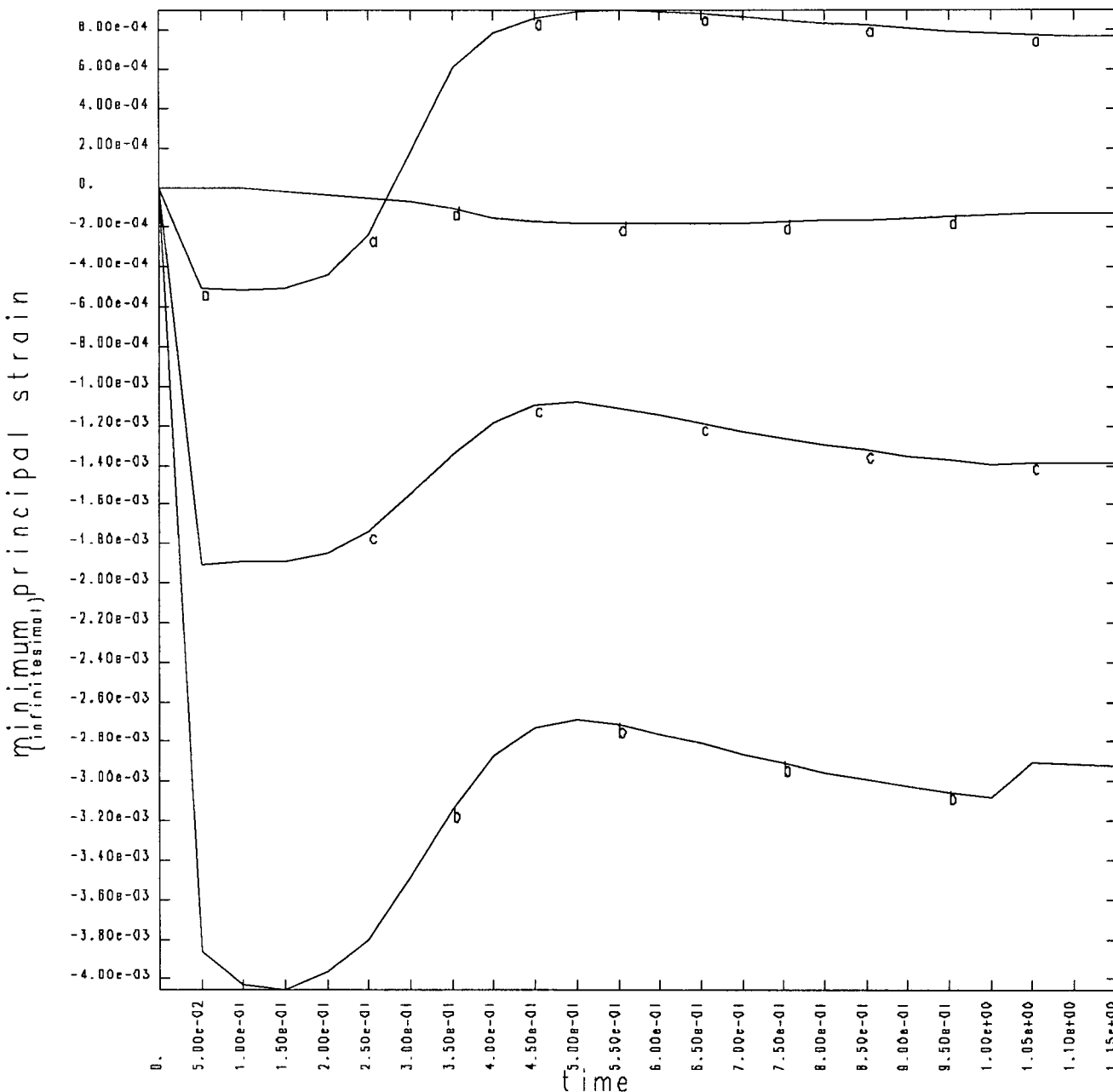
c = coil (oc)
d = beam tube

gcp12081kcp1112204/08/8715:12:35d

STRUCTURAL QUENCH/STEADY STATE OPERATION - AL. COLLAR 4-2-87



STRUCTURAL QUENCH/STEADY STATE OPERATION - AL. COLLAR 4-2-87



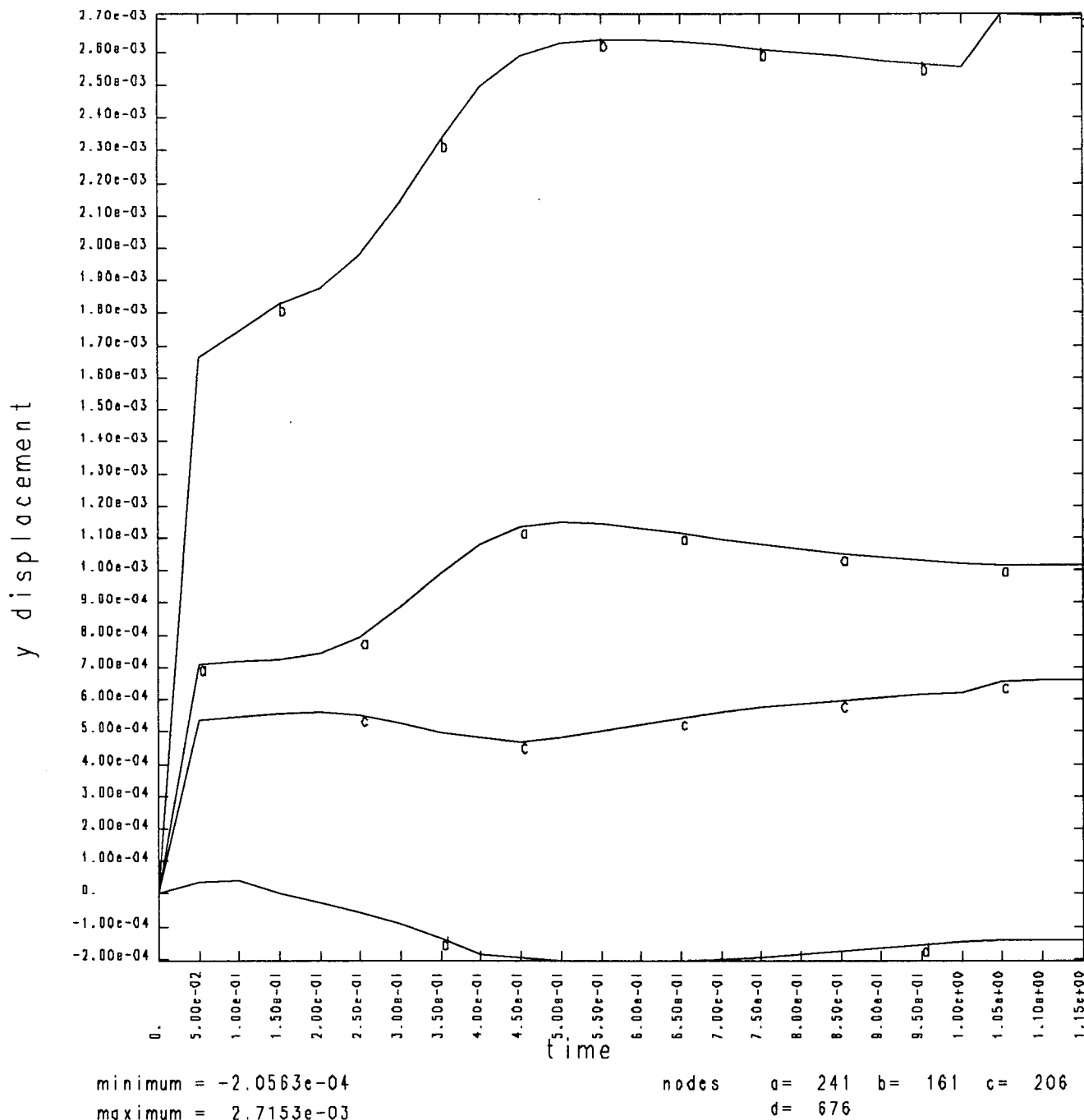
minimum = $-4.0548e-03$

maximum = $9.0010e-04$

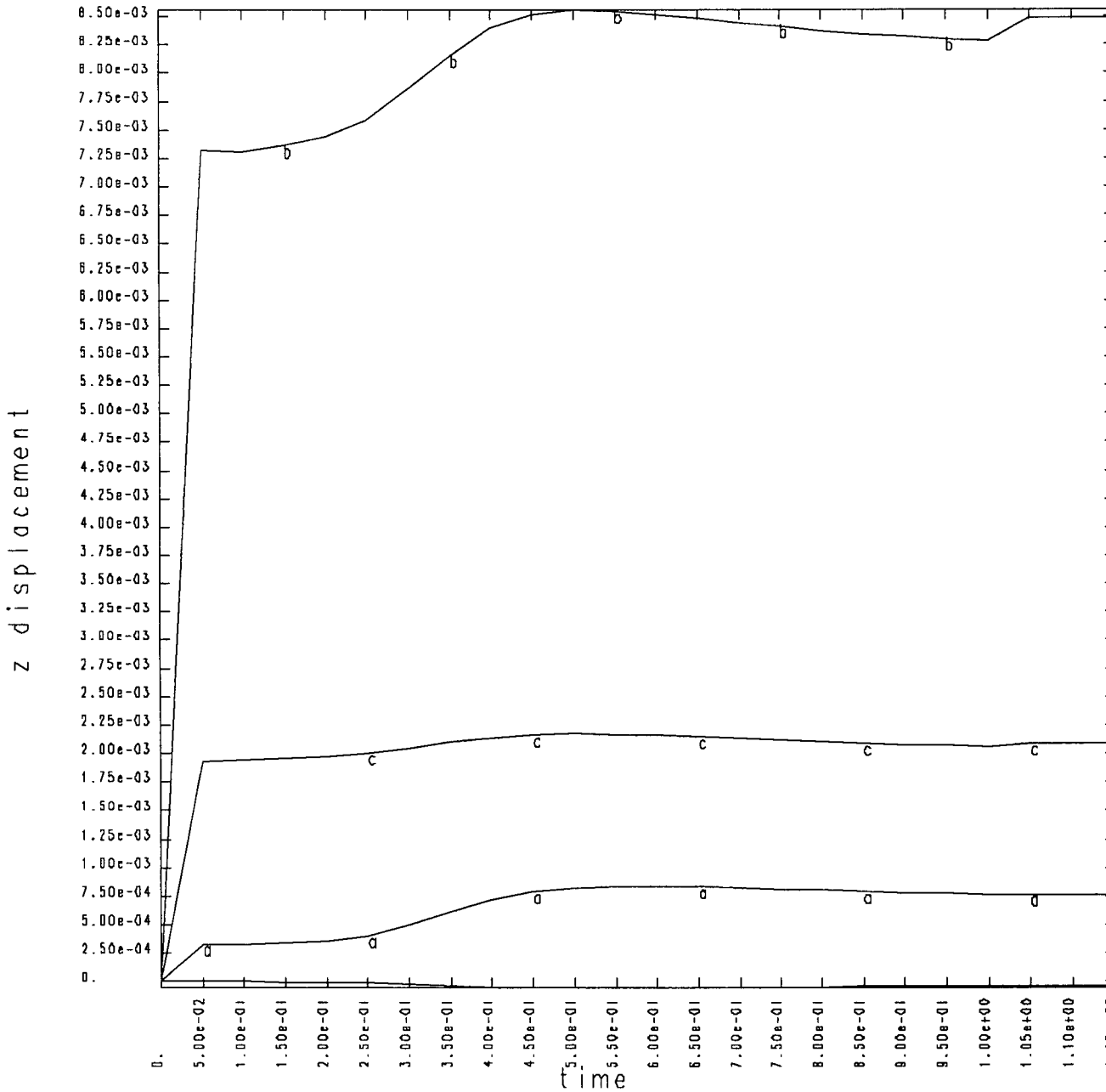
elements a = 168 b = 123 c = 142

d = 35

STRUCTURAL QUENCH/STEADY STATE OPERATION - AL. COLLAR 4-2-87



STRUCTURAL QUENCH/STEADY STATE OPERATION - AL. COLLAR 4-2-87



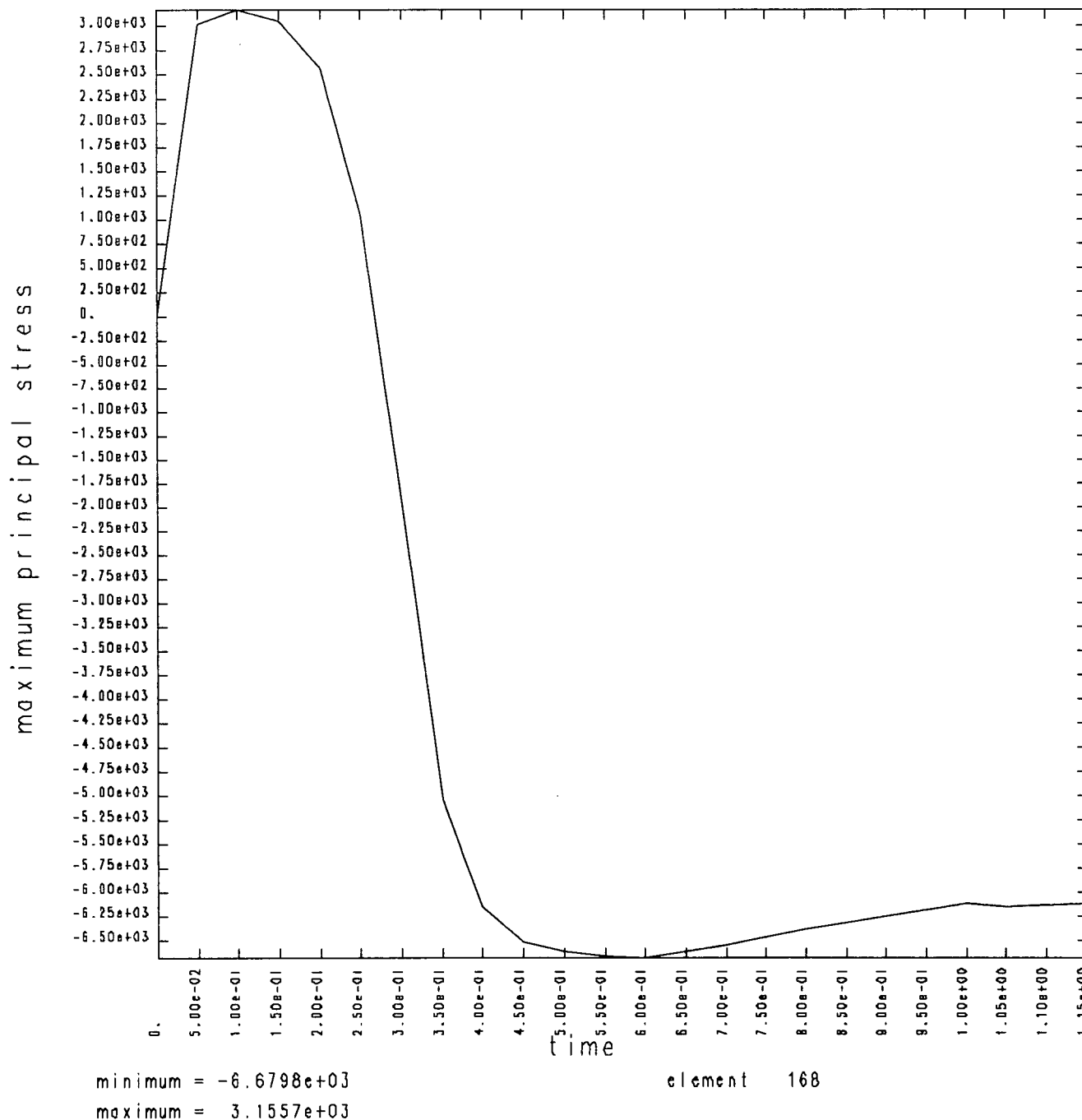
minimum = -5.3002e-05

maximum = 8.5550e-03

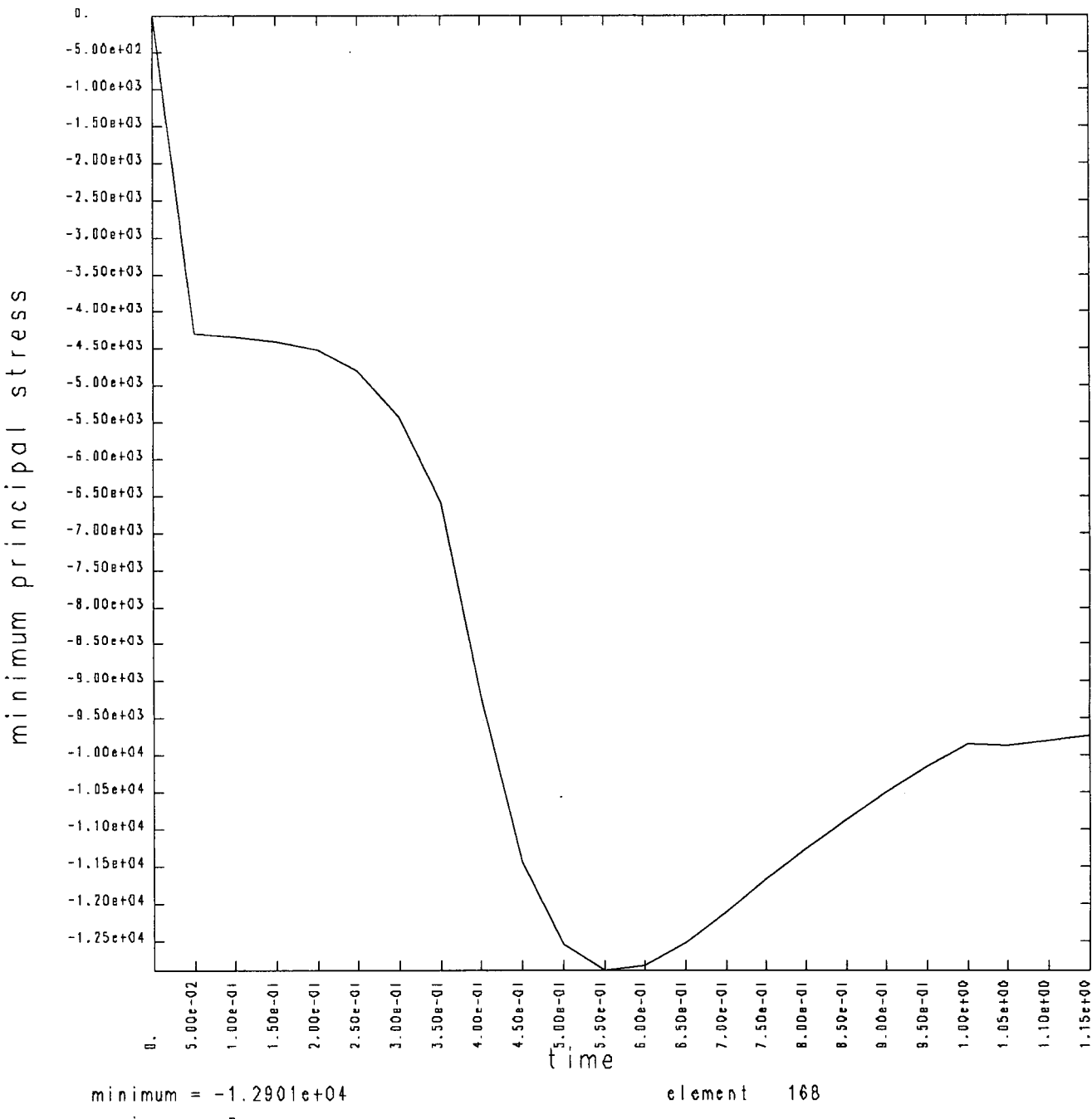
nodes a = 241 b = 161 c = 206

d = 676

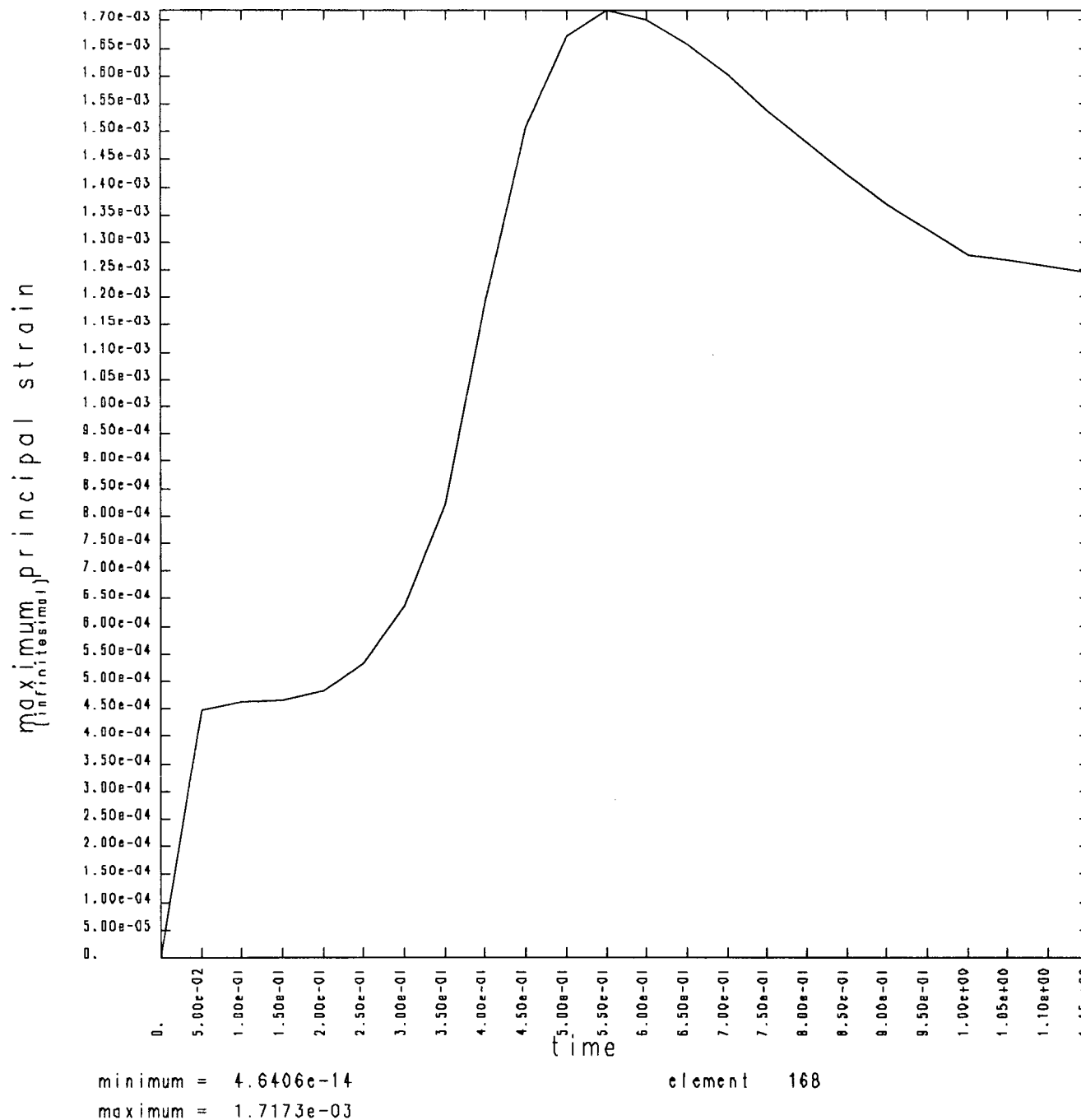
STRUCTURAL QUENCH/STEADY STATE OPERATION - AL. COLLAR 4-2-87



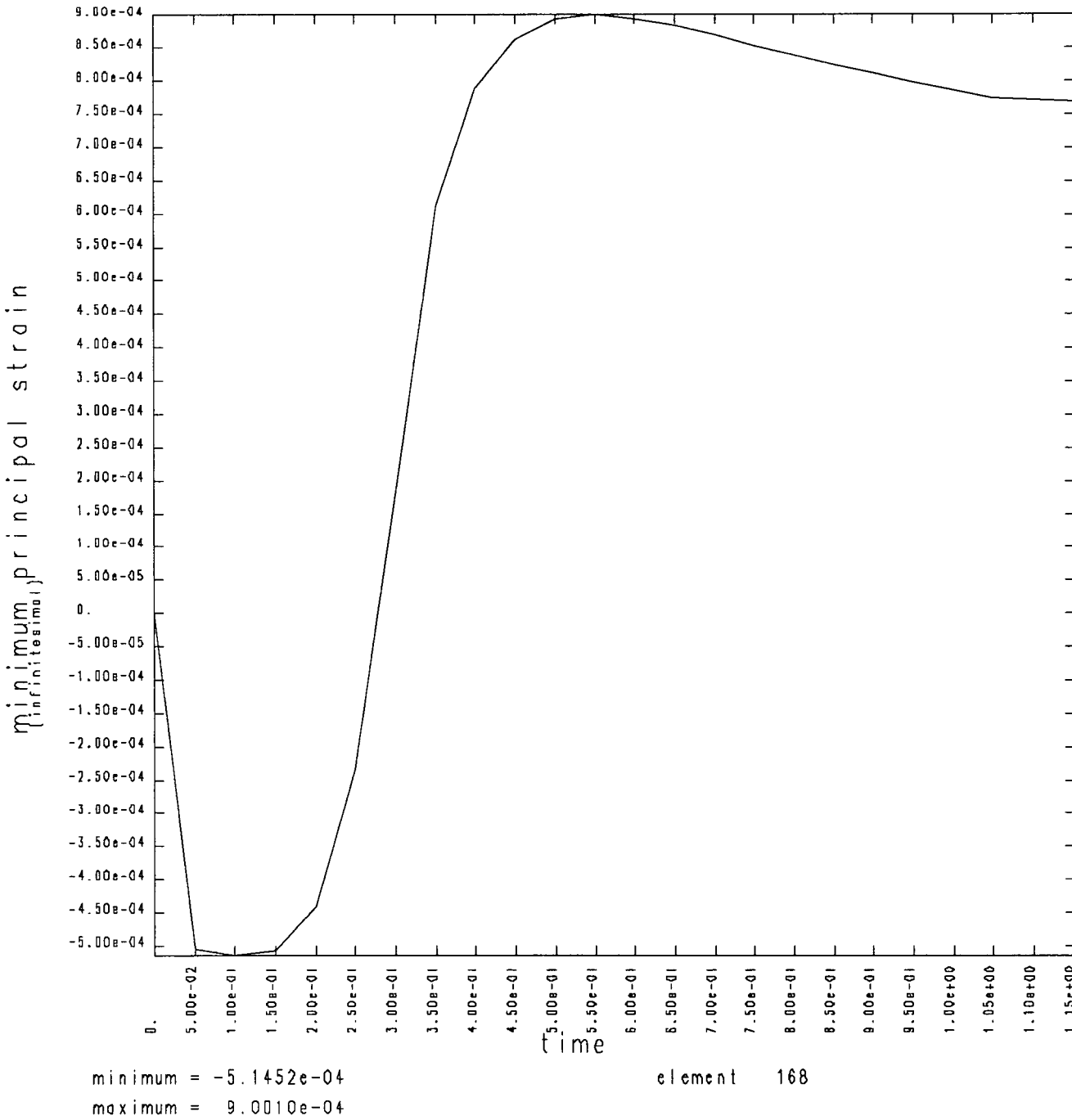
STRUCTURAL QUENCH/STEADY STATE OPERATION - AL. COLLAR 4-2-87



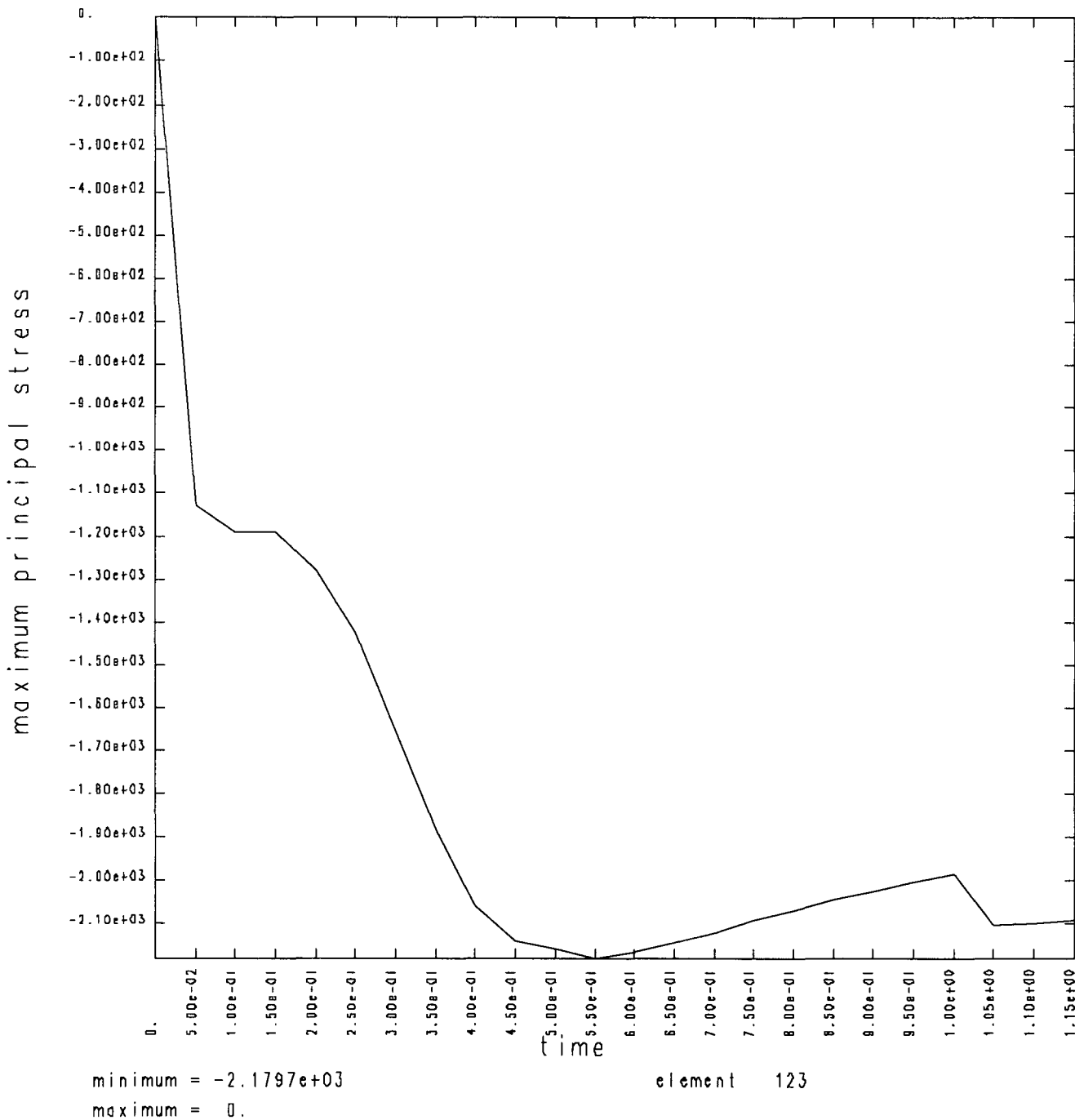
STRUCTURAL QUENCH/STEADY STATE OPERATION - AL. COLLAR 4-2-87



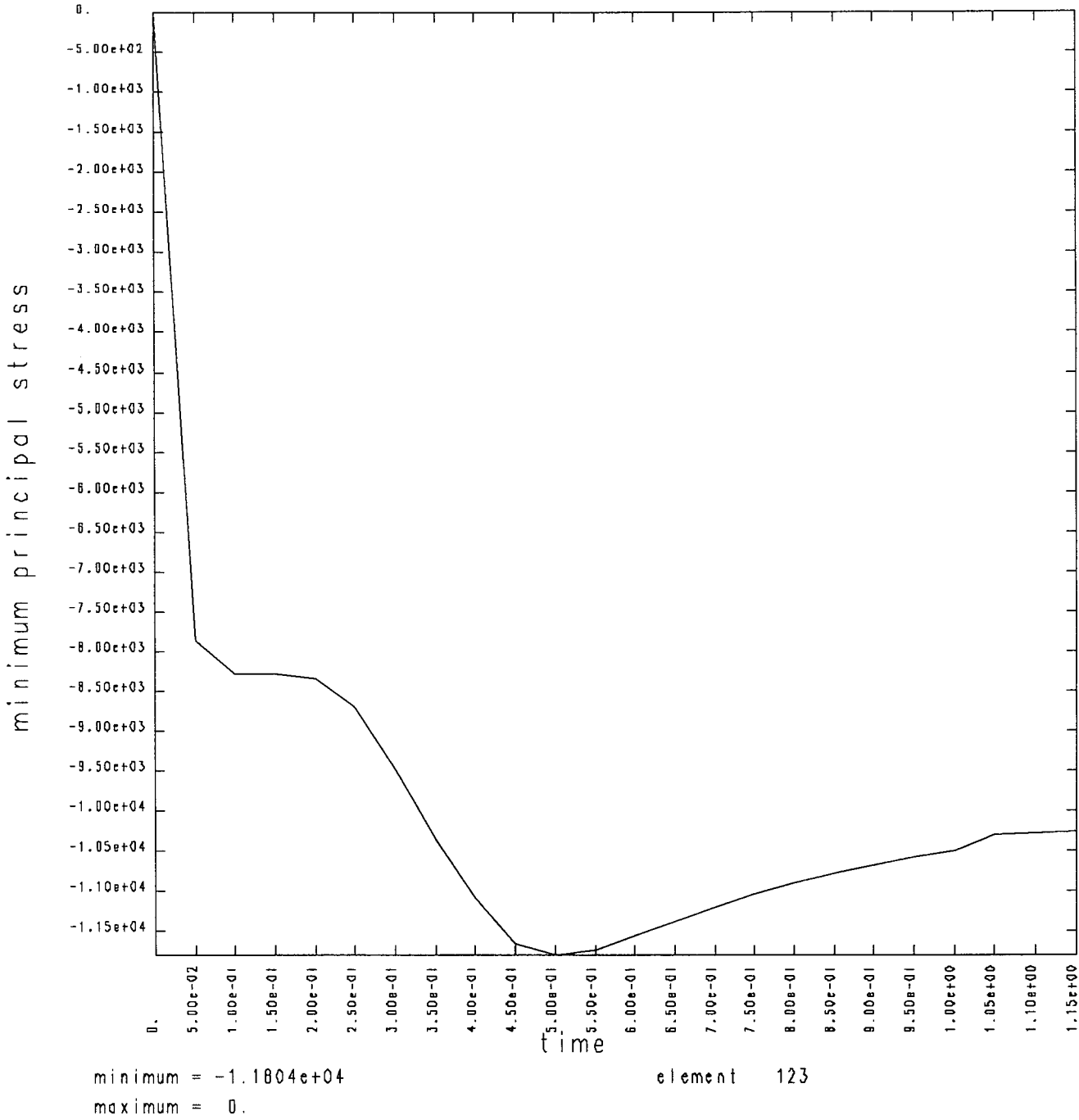
STRUCTURAL QUENCH/STEADY STATE OPERATION - AL. COLLAR 4-2-87



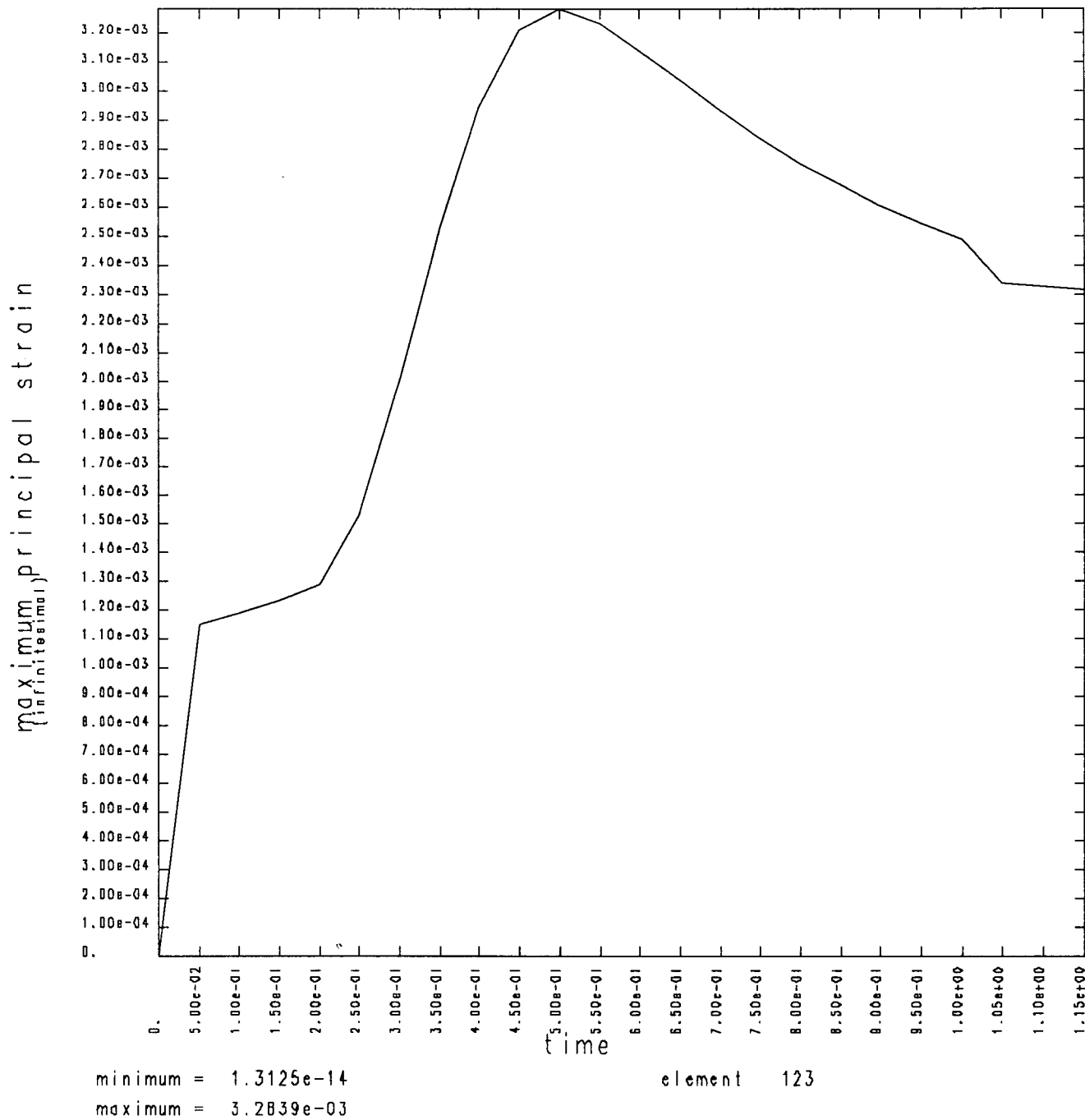
STRUCTURAL QUENCH/STEADY STATE OPERATION - AL. COLLAR 4-2-87



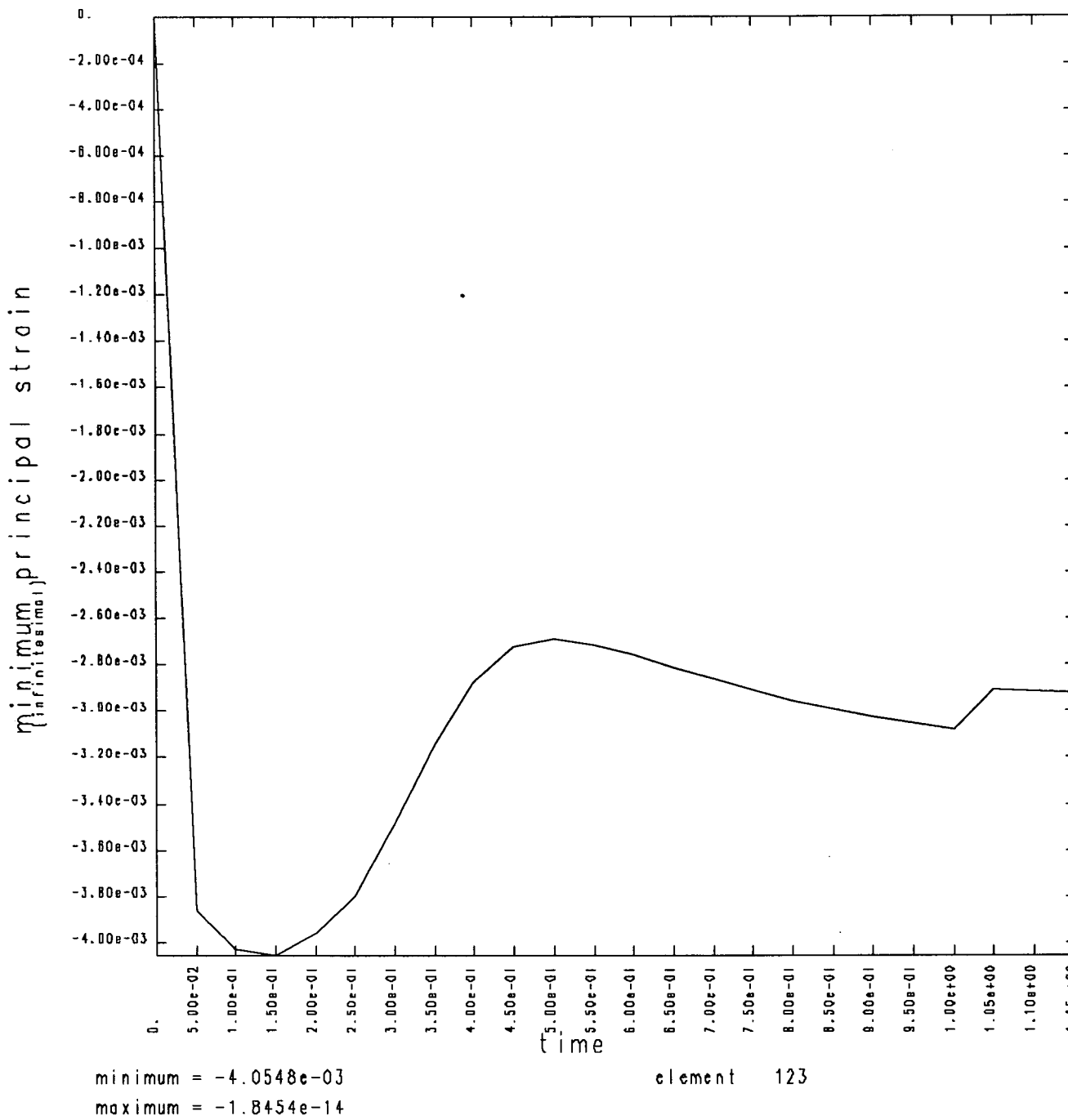
STRUCTURAL QUENCH/STEADY STATE OPERATION - AL. COLLAR 4-2-87



STRUCTURAL QUENCH/STEADY STATE OPERATION - AL. COLLAR 4-2-87

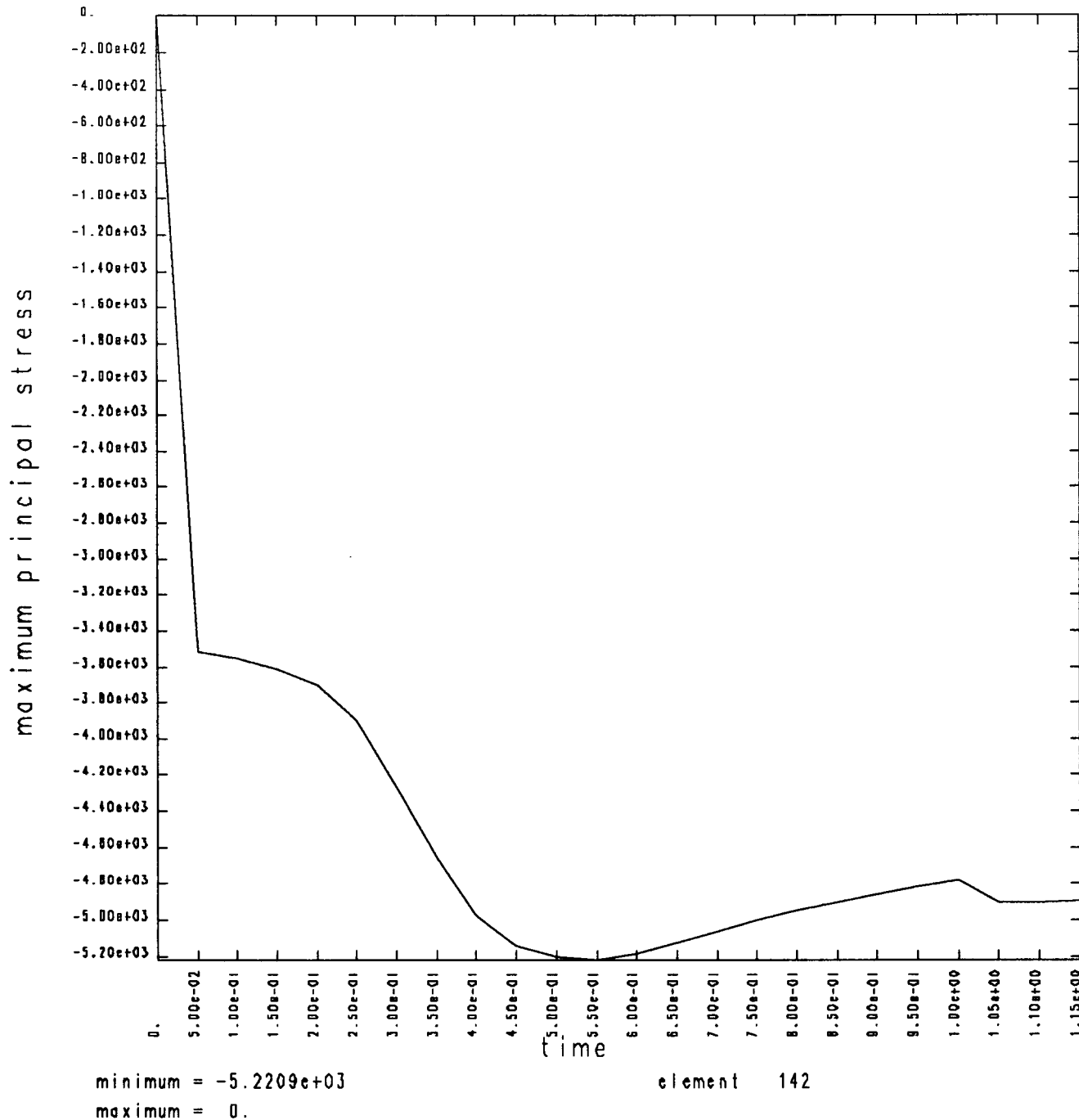


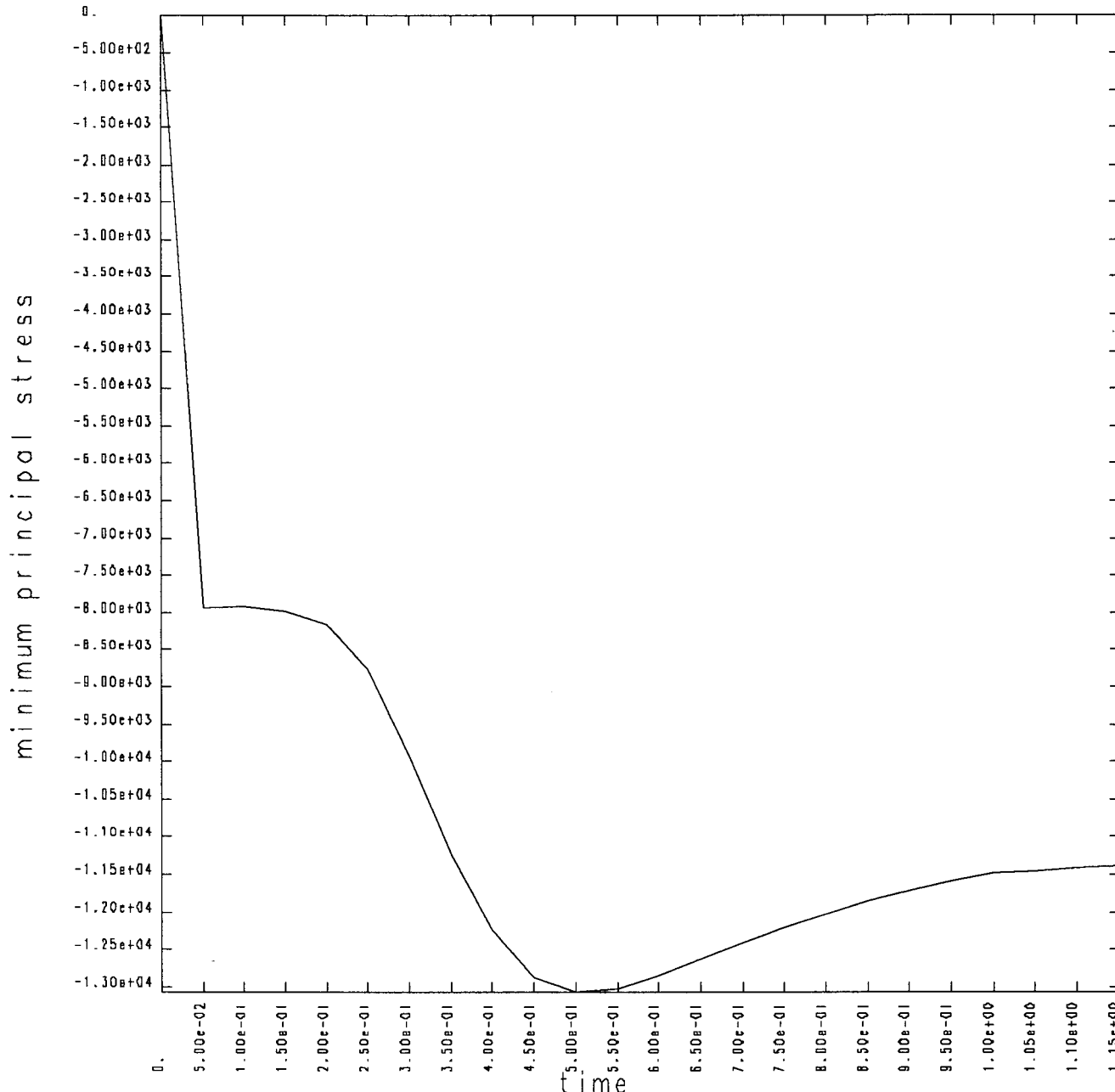
STRUCTURAL QUENCH/STEADY STATE OPERATION - AL. COLLAR 4-2-87



STRUCTURAL QUENCH/STEADY STATE OPERATION - AL. COLLAR 4-2-87

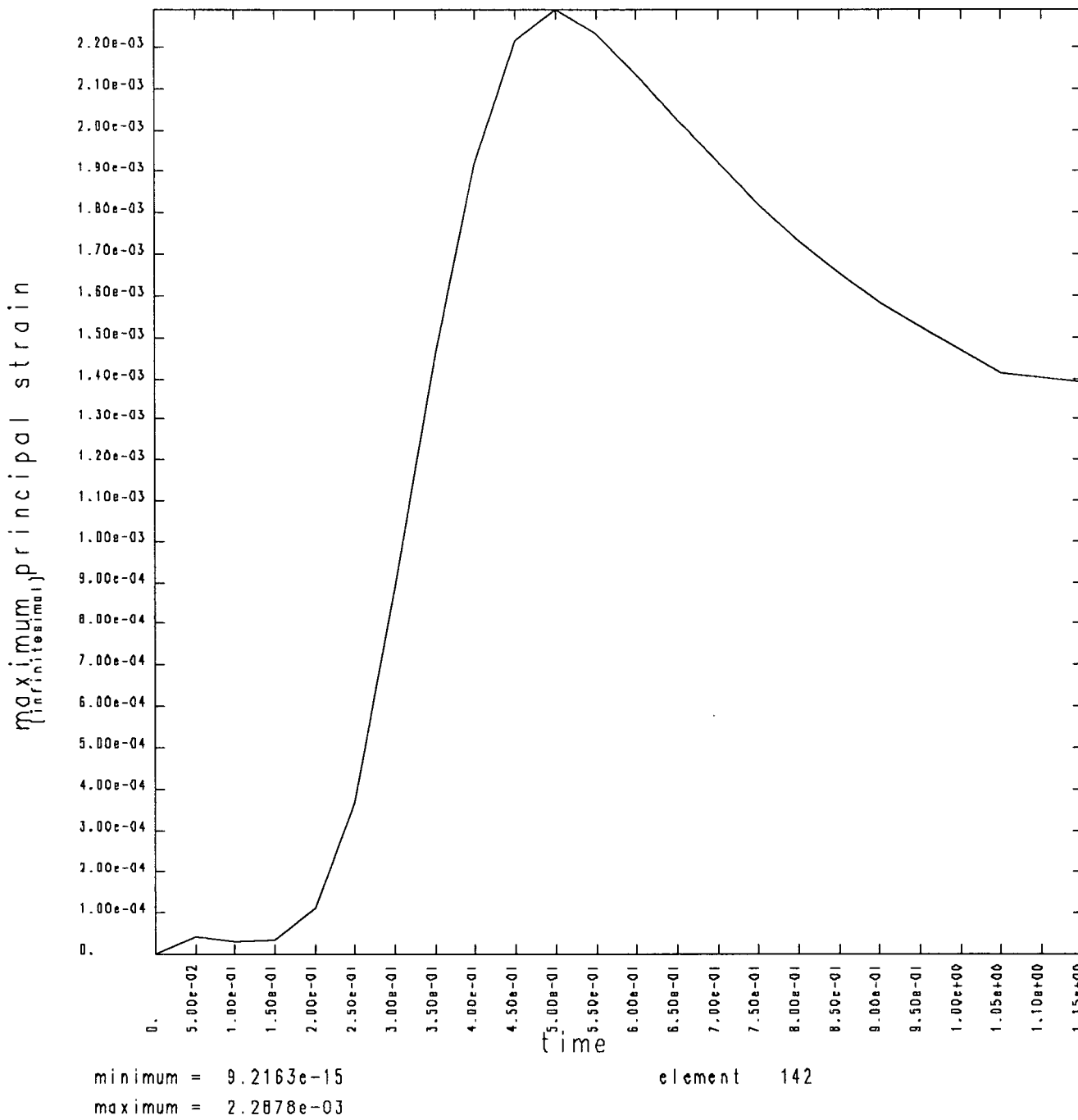
A-46





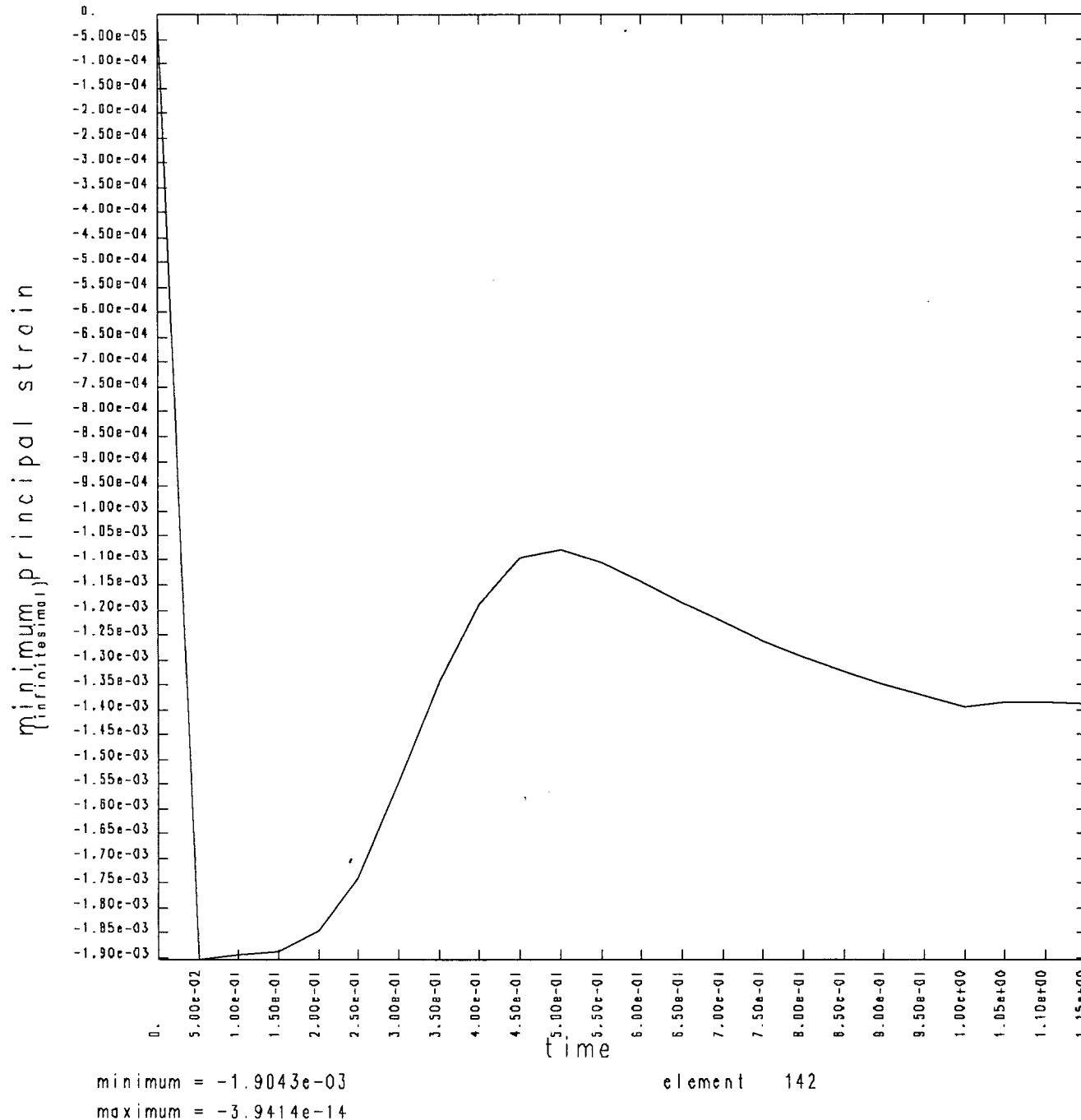
element 142

STRUCTURAL QUENCH/STEADY STATE OPERATION - AL. COLLAR 4-2-87

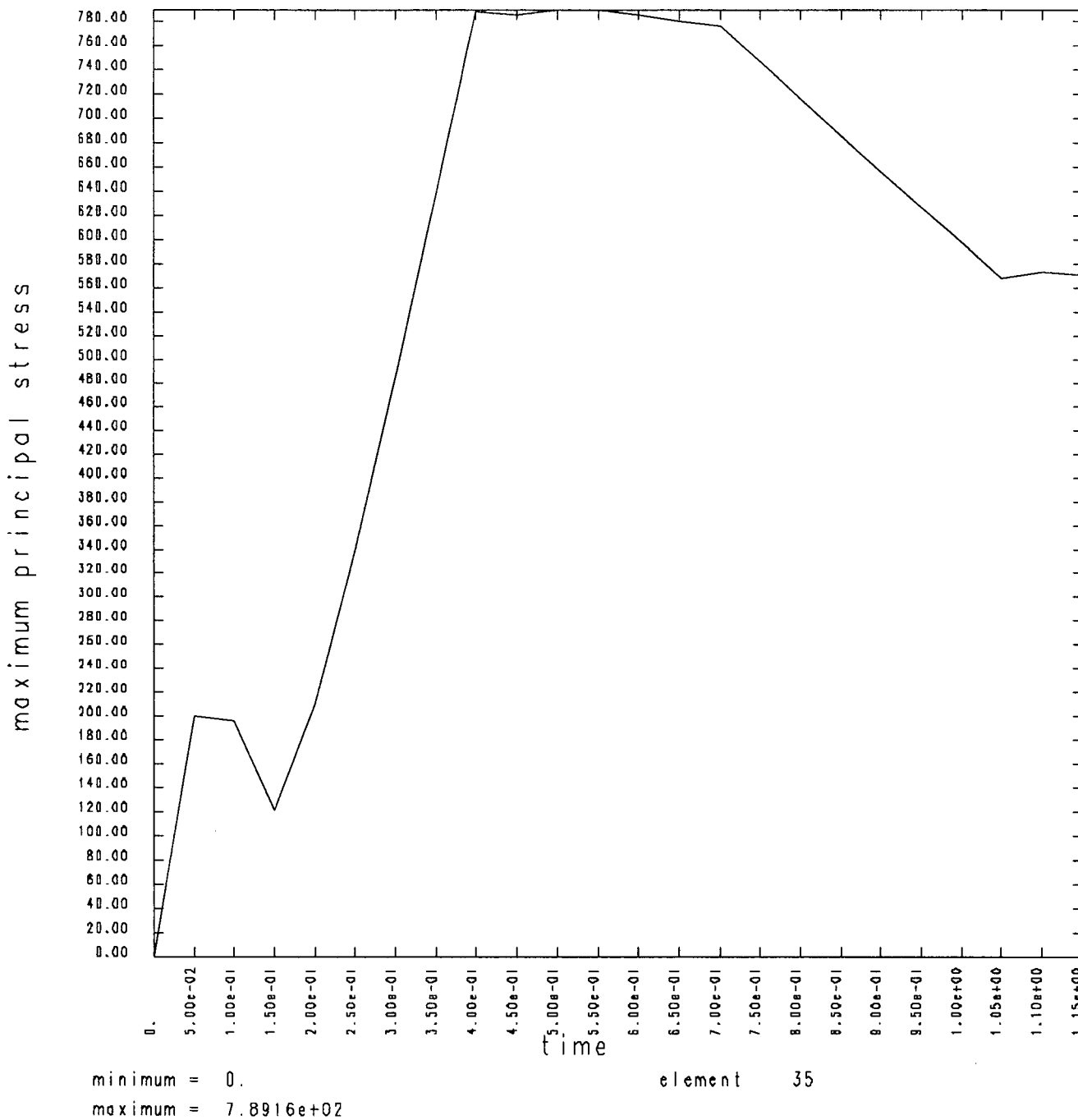


STRUCTURAL QUENCH/STEADY STATE OPERATION - AL. COLLAR 4-2-87

A-49



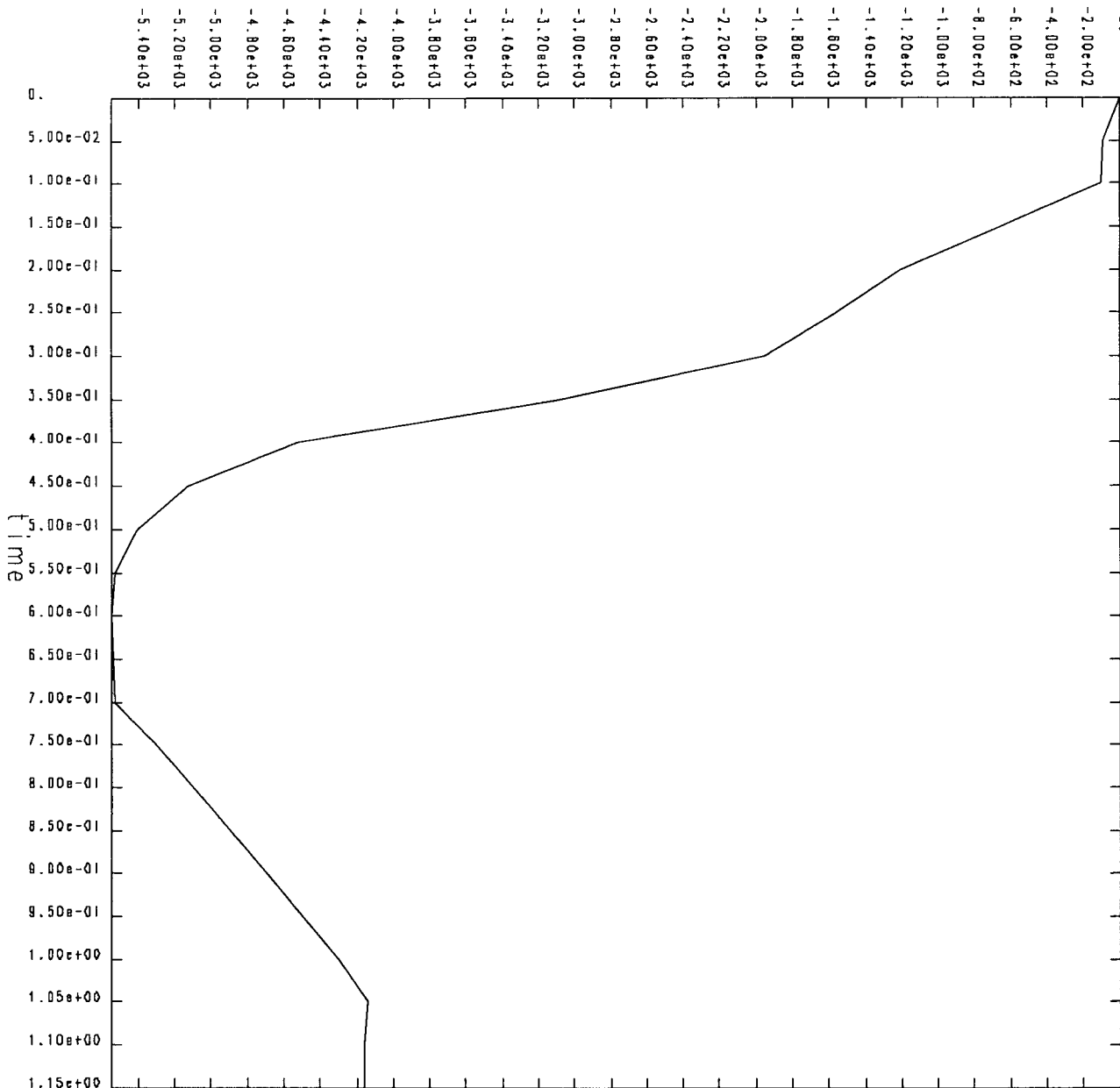
STRUCTURAL QUENCH/STEADY STATE OPERATION - AL. COLLAR 4-2-87



STRUCTURAL QUENCH/STEADY STATE OPERATION - AL. COLLAR 4-2-87

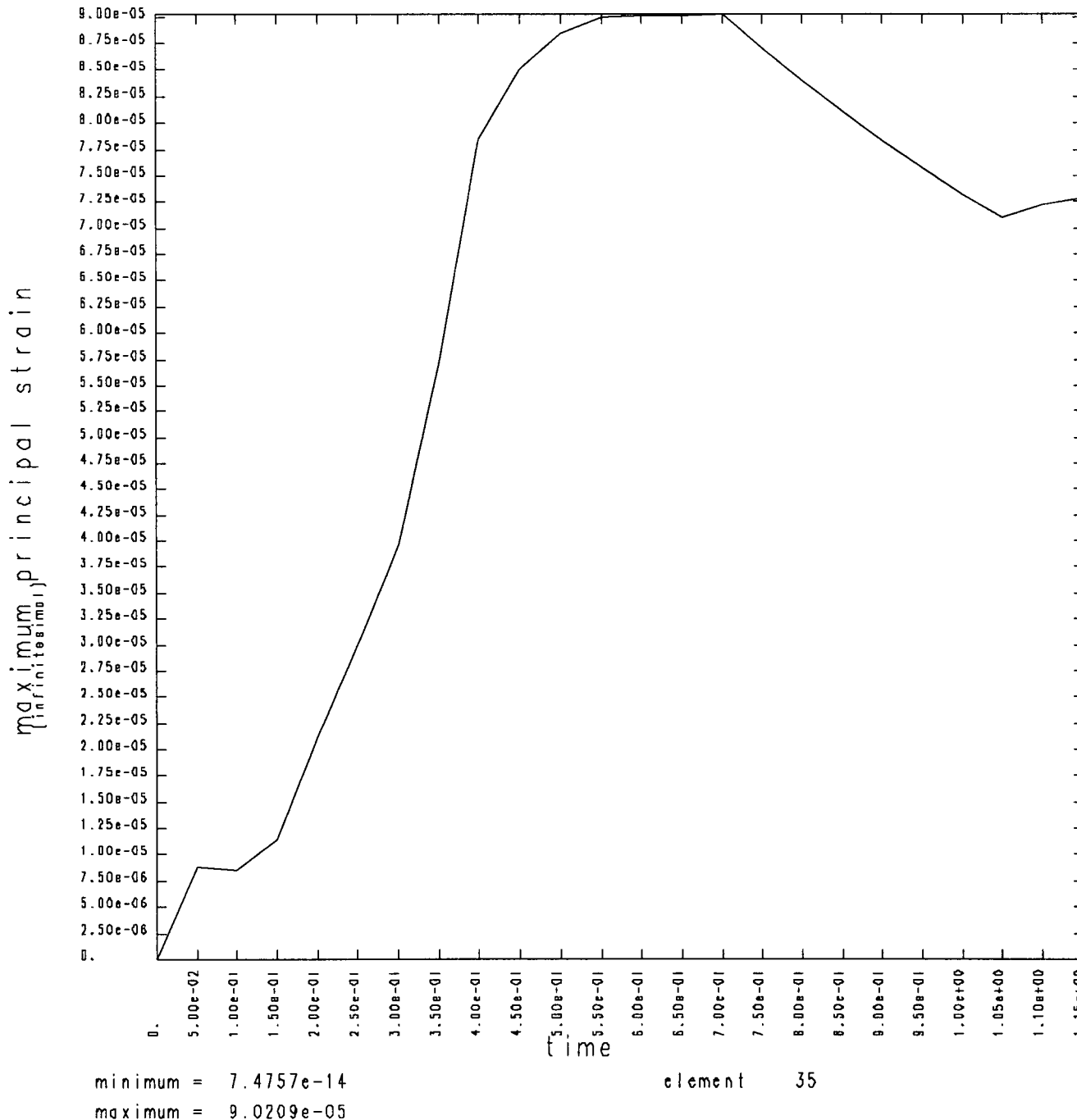
A-51

minimum principal stress

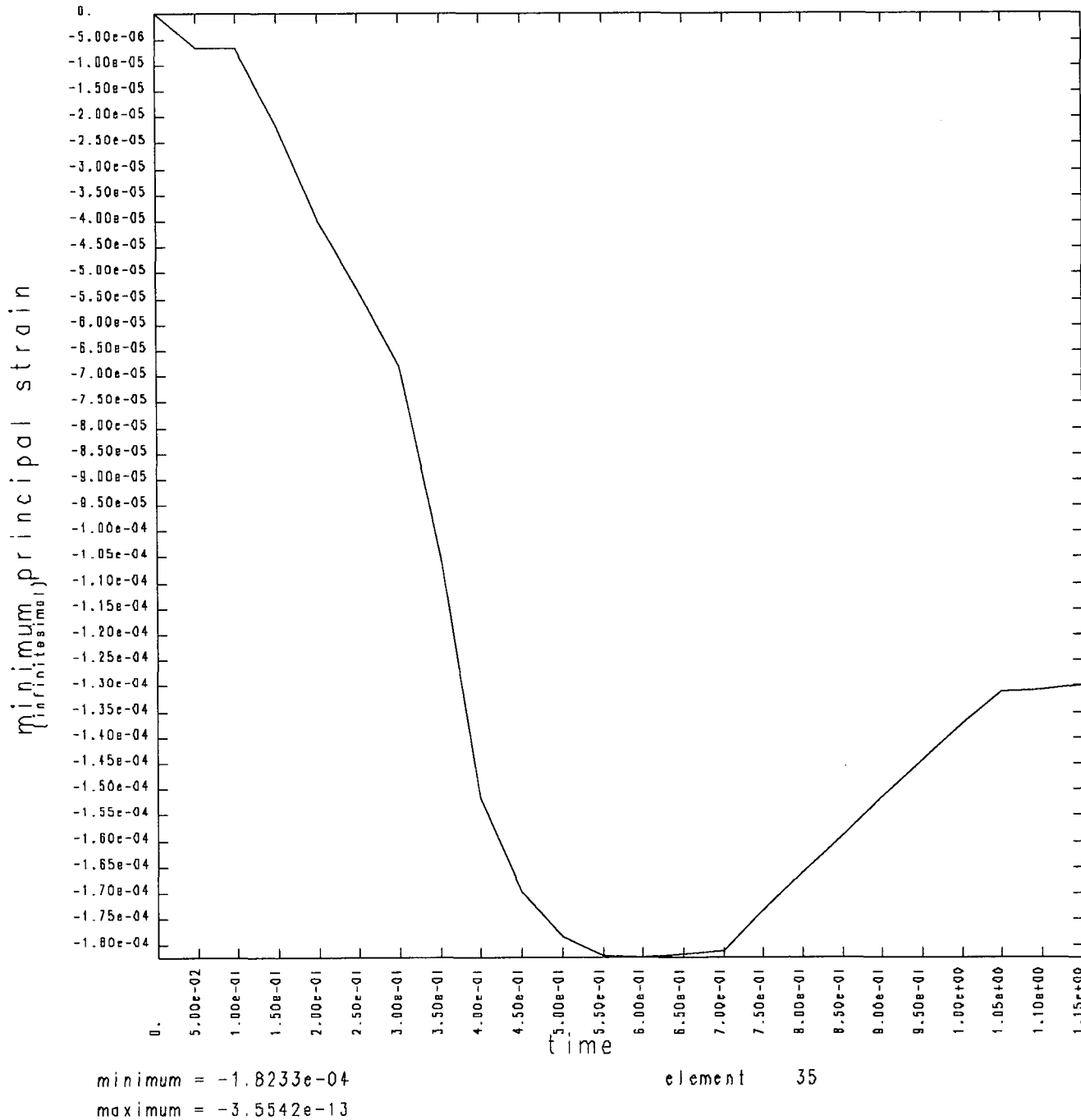


minimum = -5.5484e+03
maximum = 0.

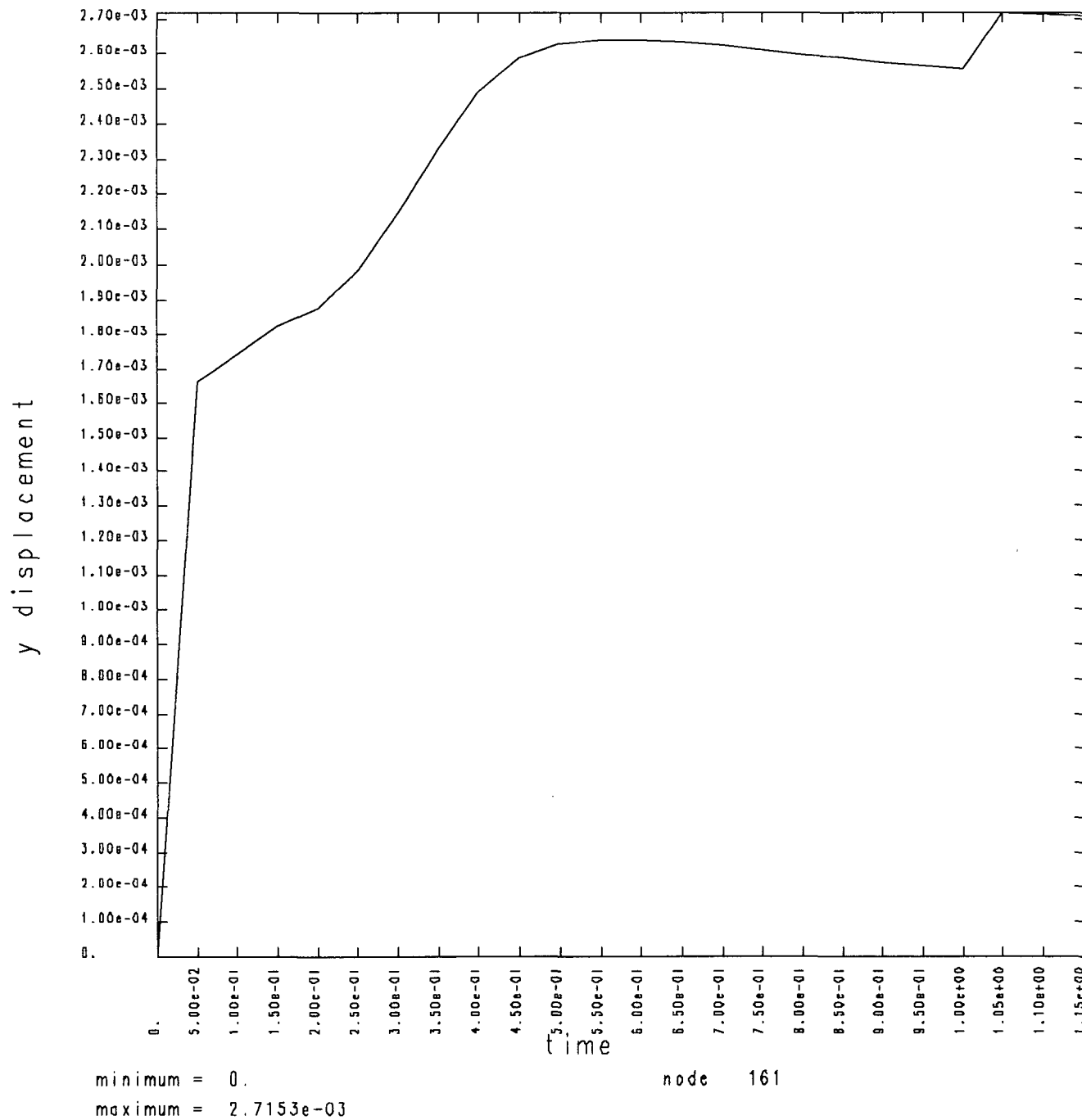
STRUCTURAL QUENCH/STEADY STATE OPERATION - AL. COLLAR 4-2-87



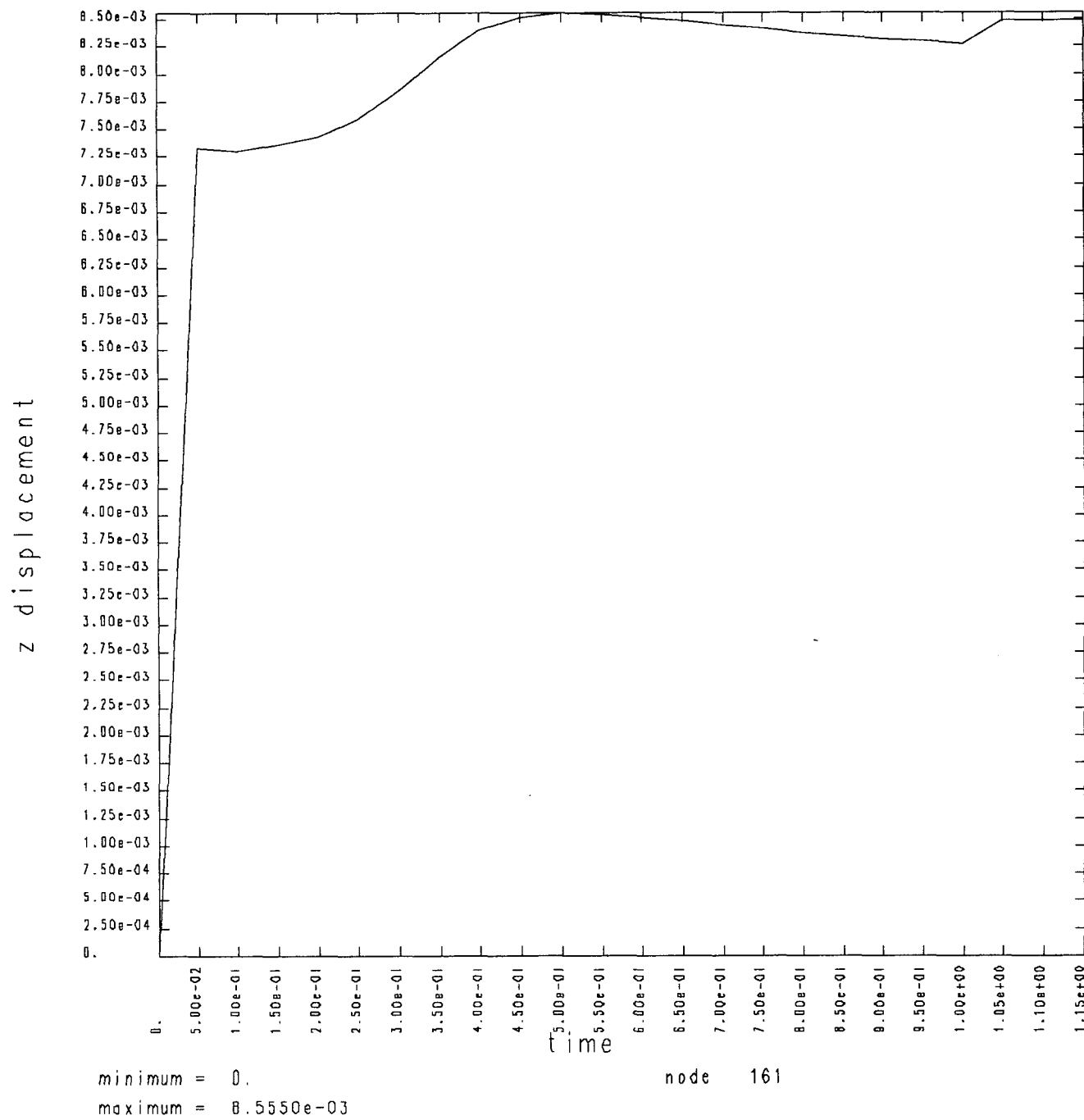
STRUCTURAL QUENCH/STEADY STATE OPERATION - AL. COLLAR 4-2-87



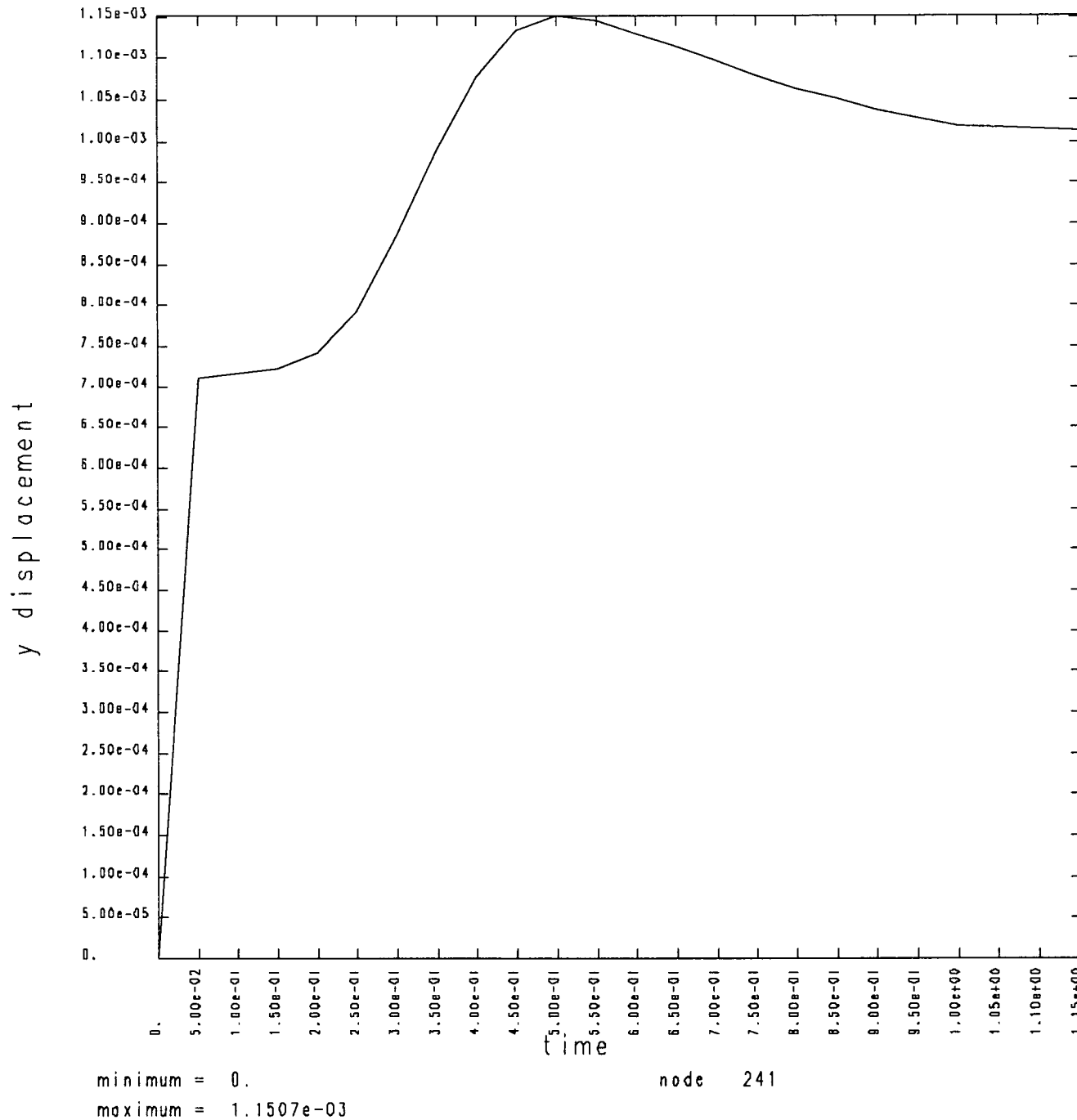
STRUCTURAL QUENCH/STEADY STATE OPERATION - AL. COLLAR 4-2-87



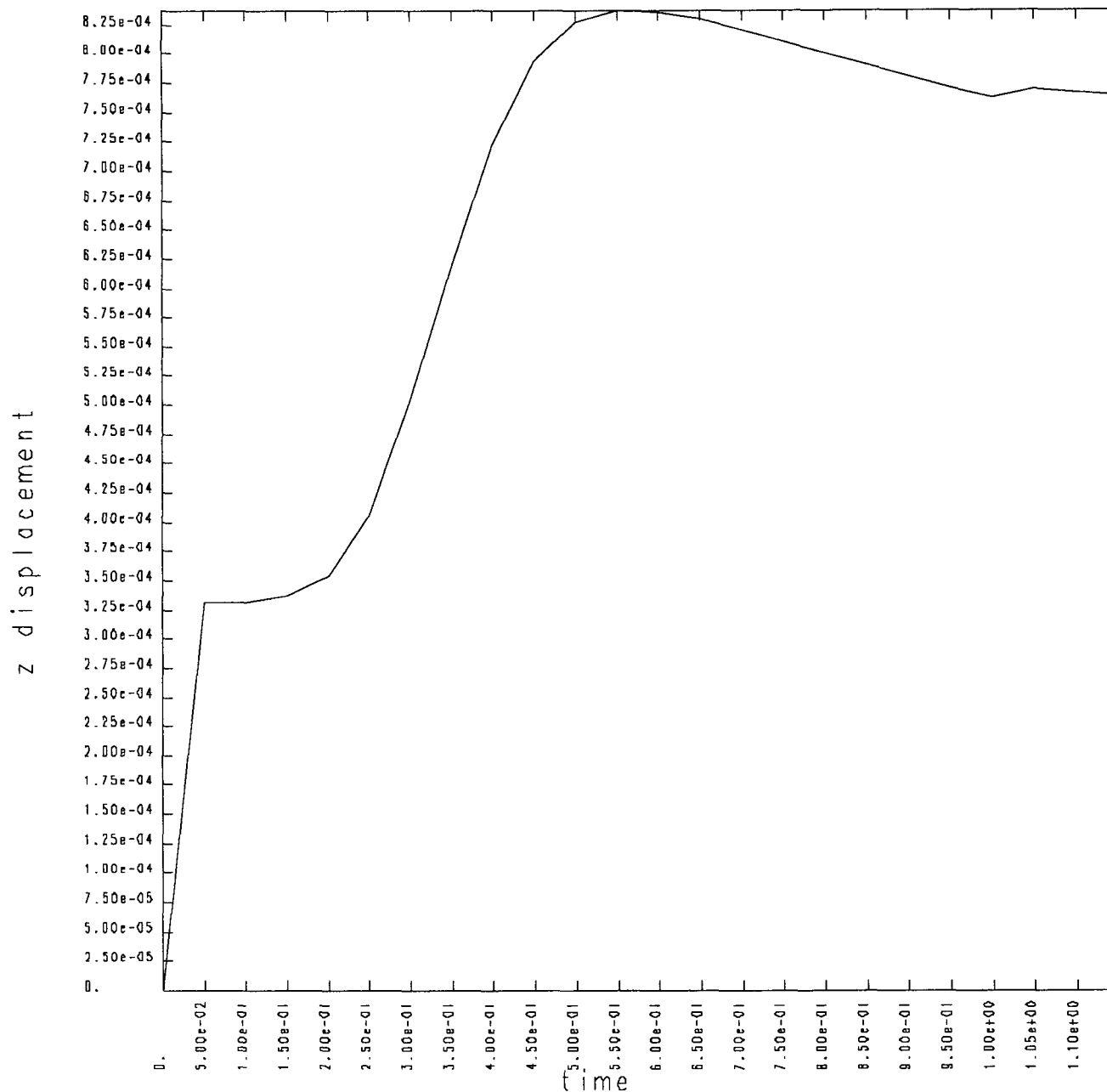
STRUCTURAL QUENCH/STEADY STATE OPERATION - AL. COLLAR 4-2-87



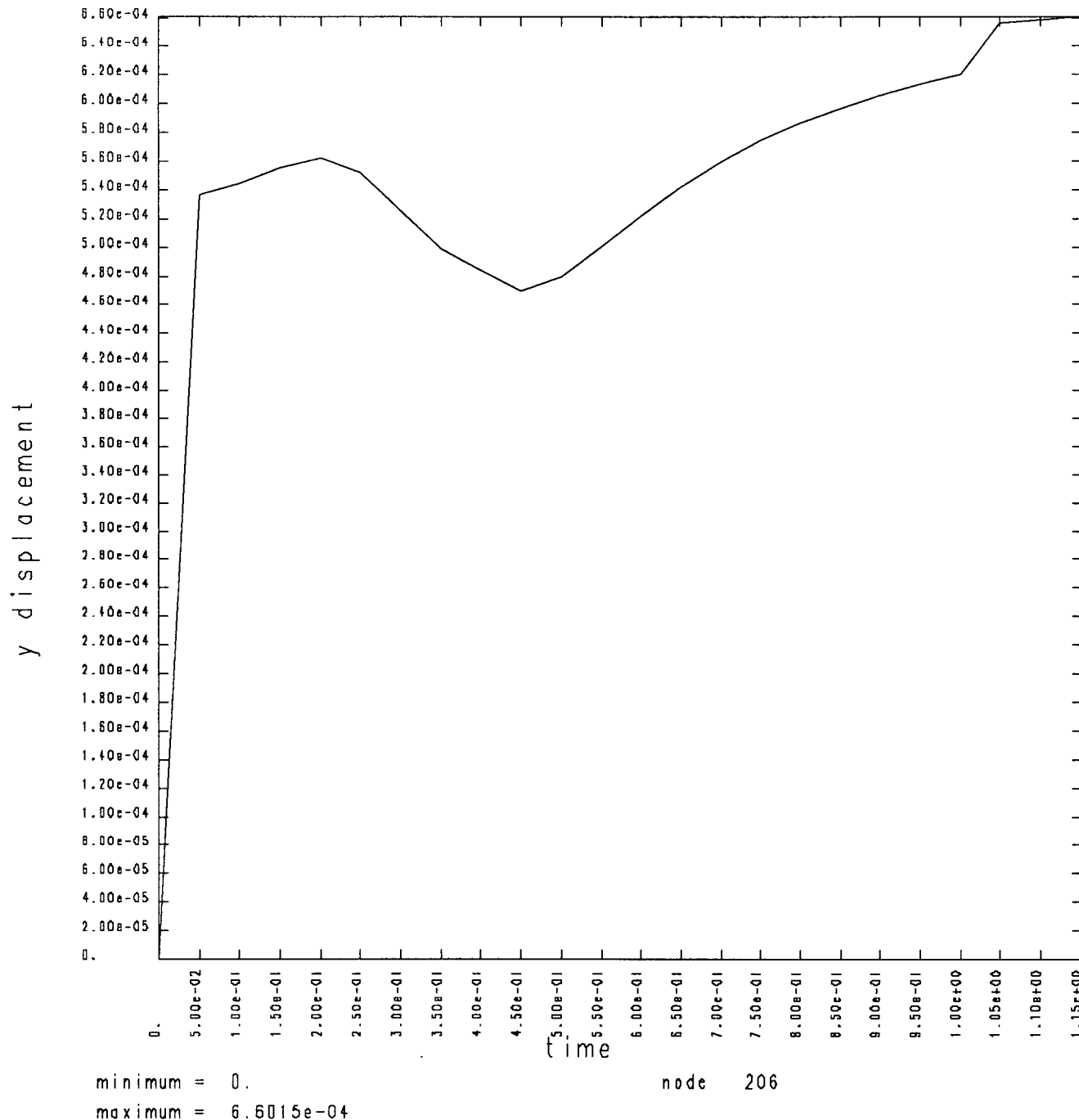
STRUCTURAL QUENCH/STEADY STATE OPERATION - AL. COLLAR 4-2-87



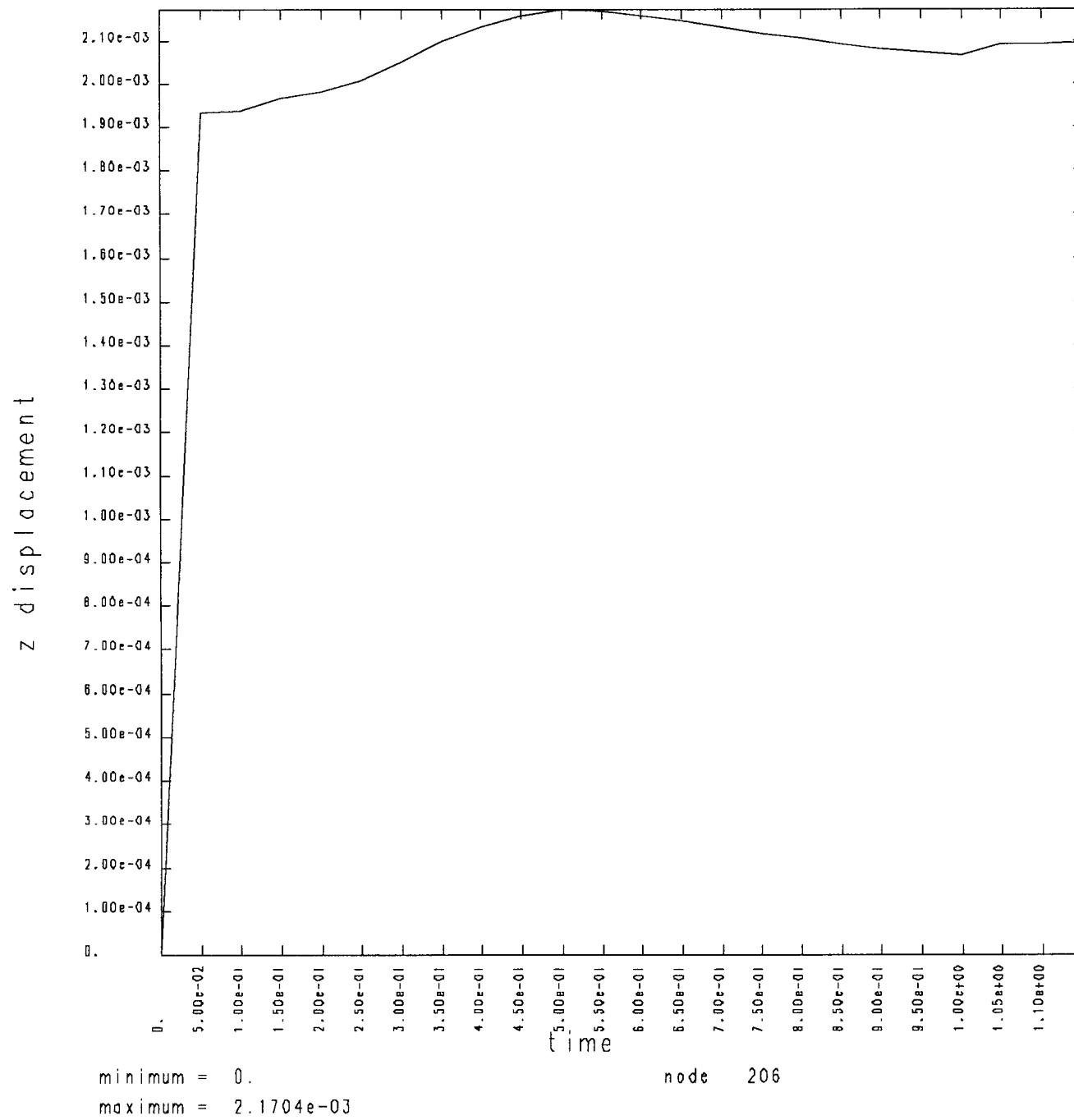
STRUCTURAL QUENCH/STEADY STATE OPERATION - AL. COLLAR 4-2-87



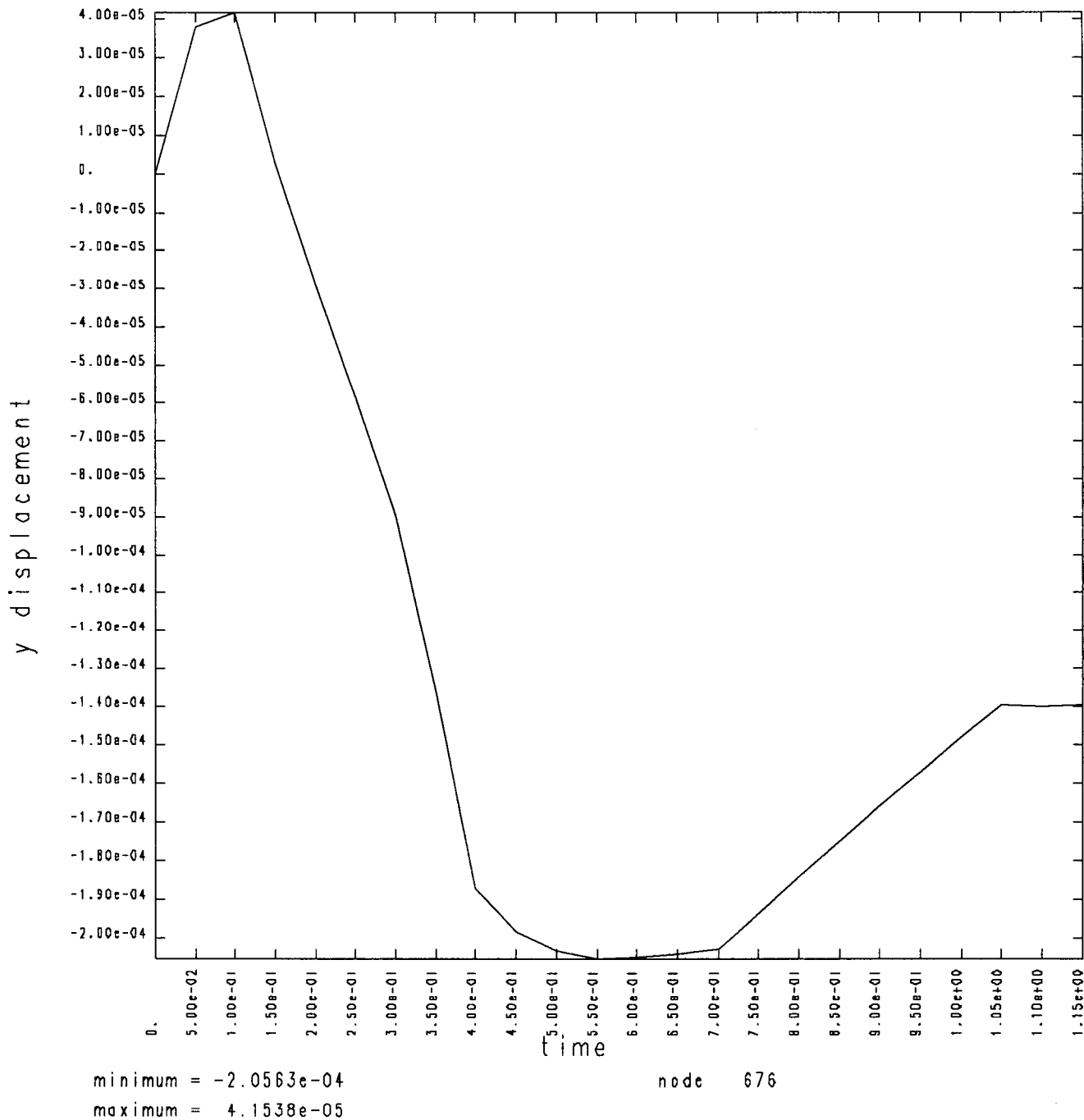
STRUCTURAL QUENCH/STEADY STATE OPERATION - AL. COLLAR 4-2-87



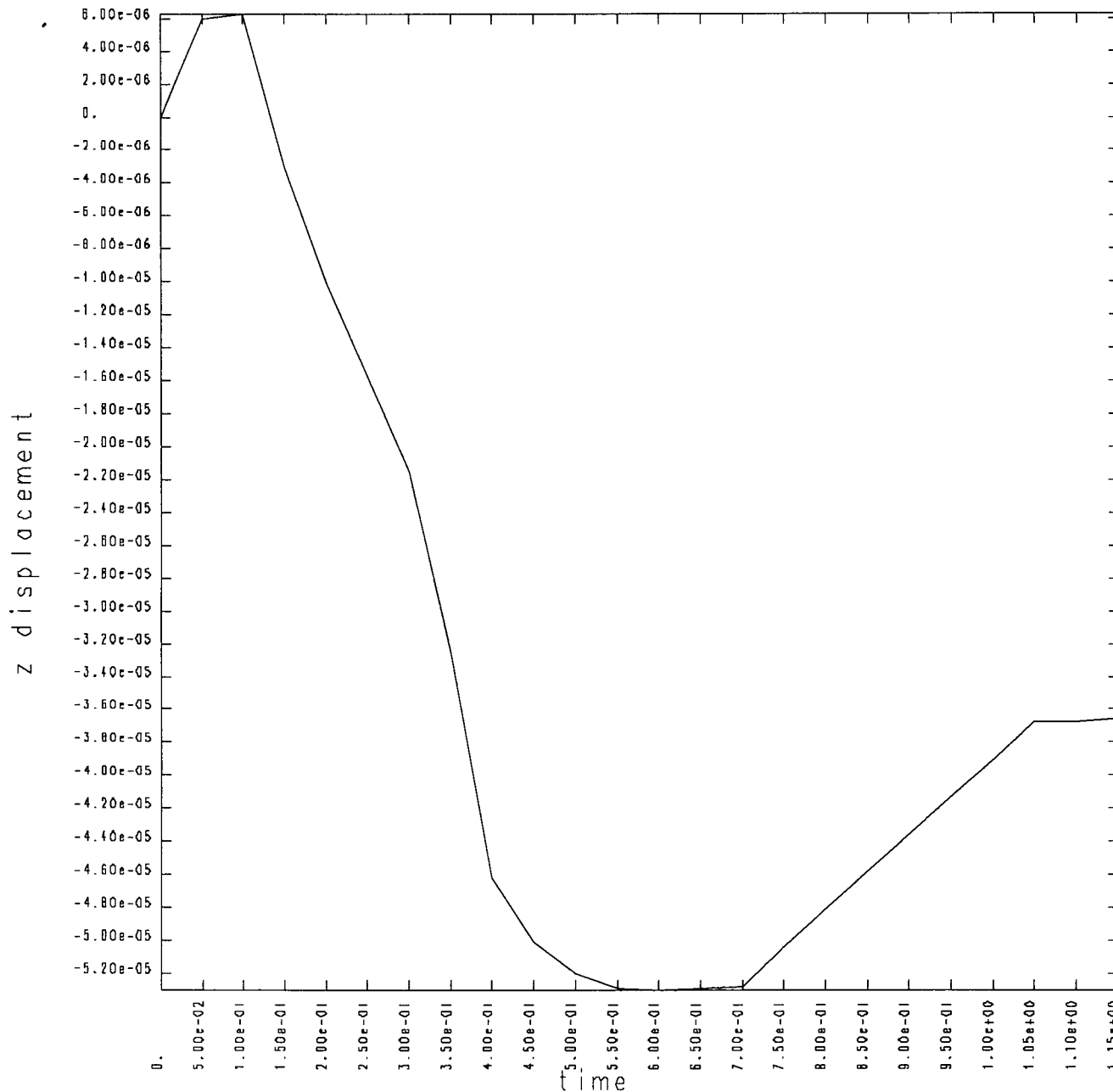
STRUCTURAL QUENCH/STEADY STATE OPERATION - AL. COLLAR 4-2-87



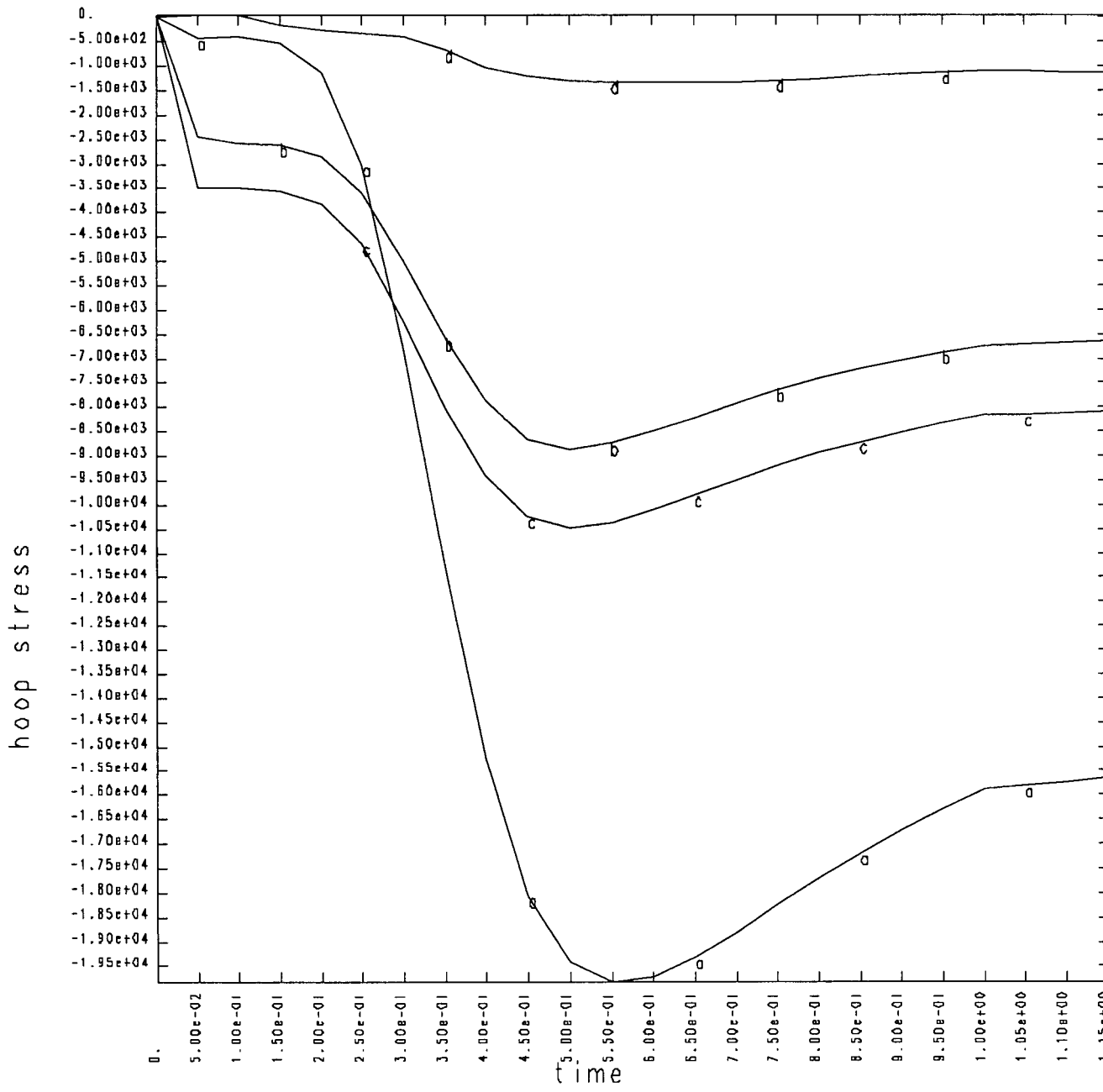
STRUCTURAL QUENCH/STEADY STATE OPERATION - AL. COLLAR 4-2-87



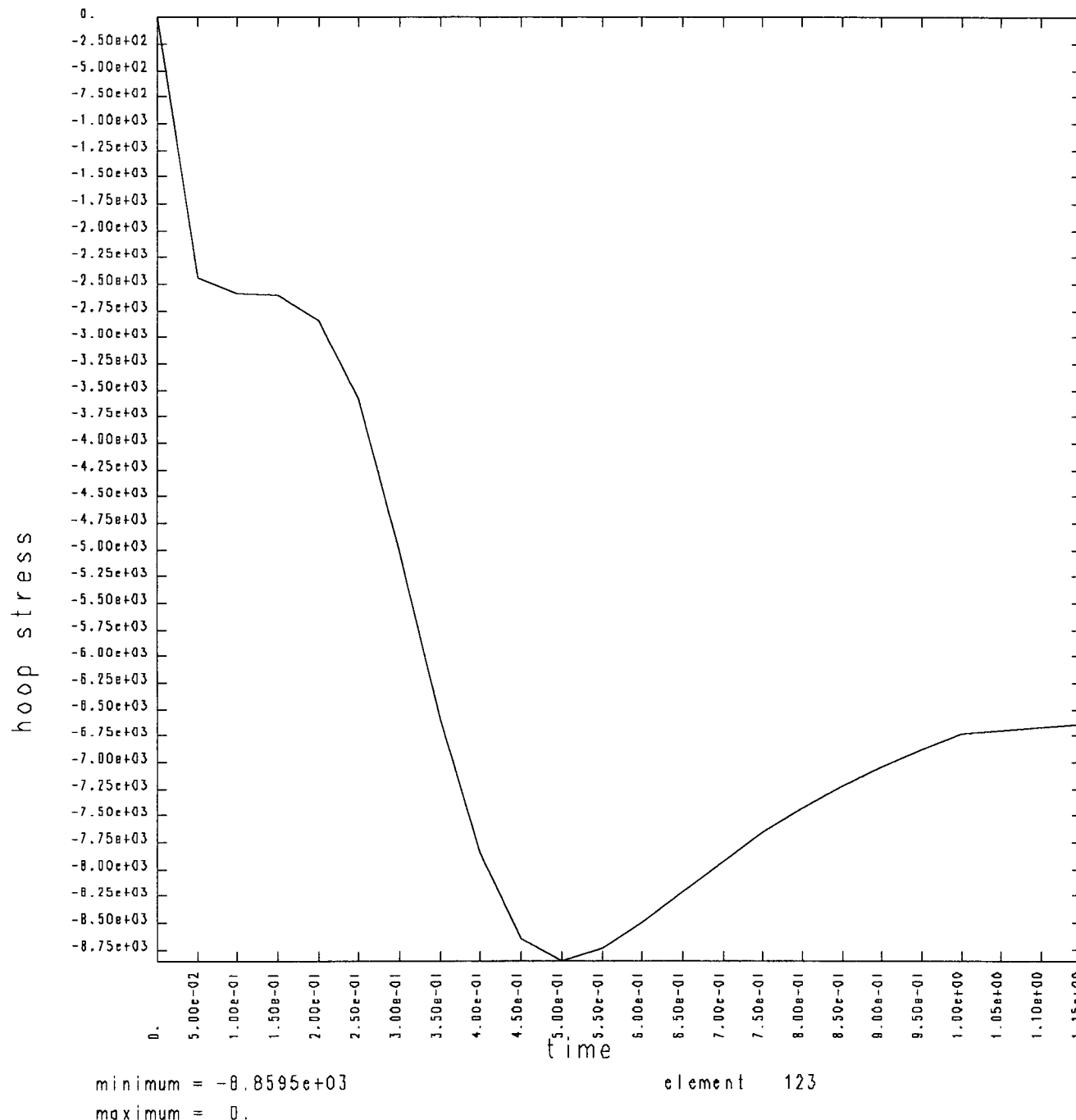
STRUCTURAL QUENCH/STEADY STATE OPERATION - AL. COLLAR 4-2-87



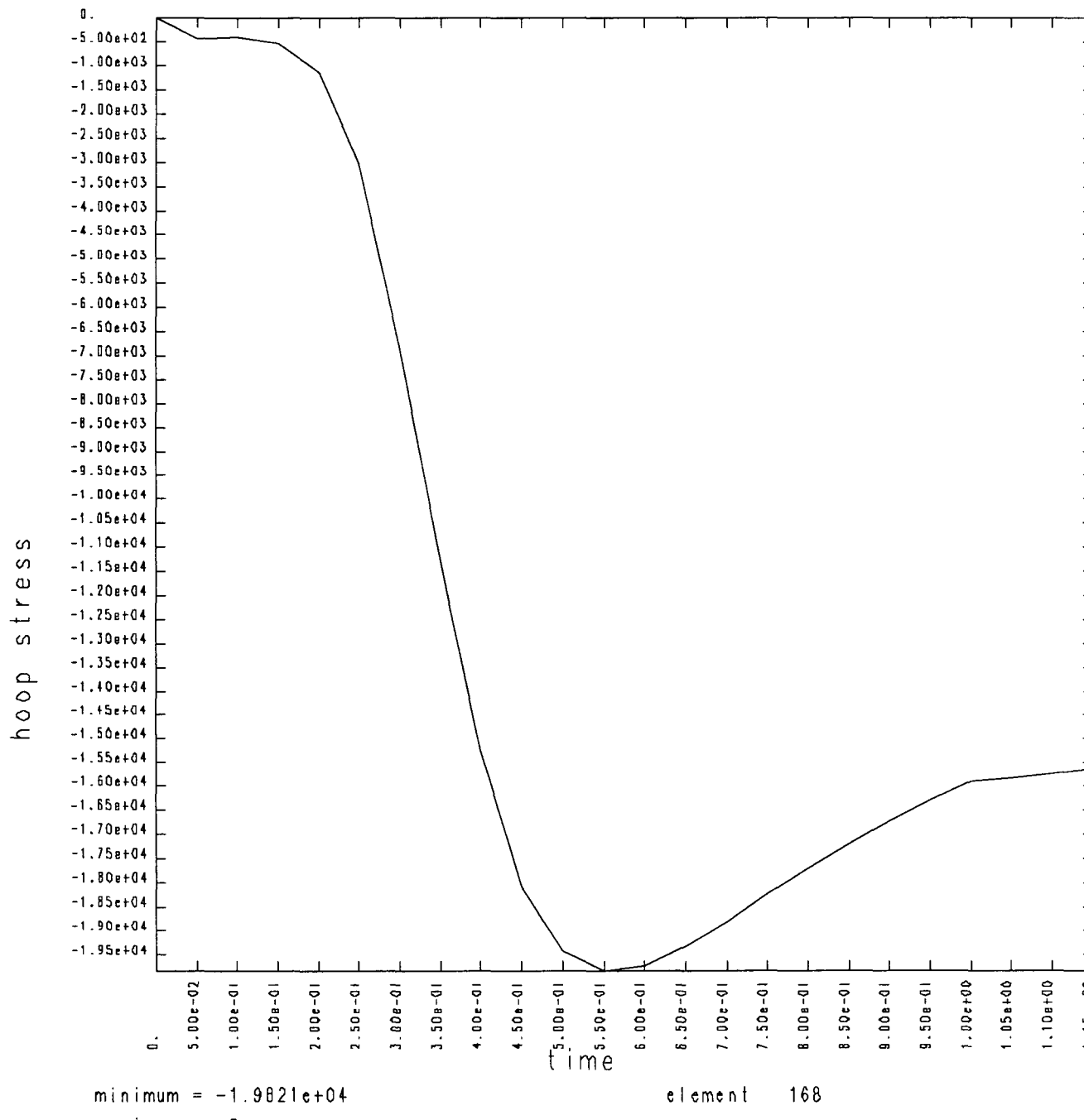
STRUCTURAL QUENCH/STEADY STATE OPERATION - AL. COLLAR 4-2-87



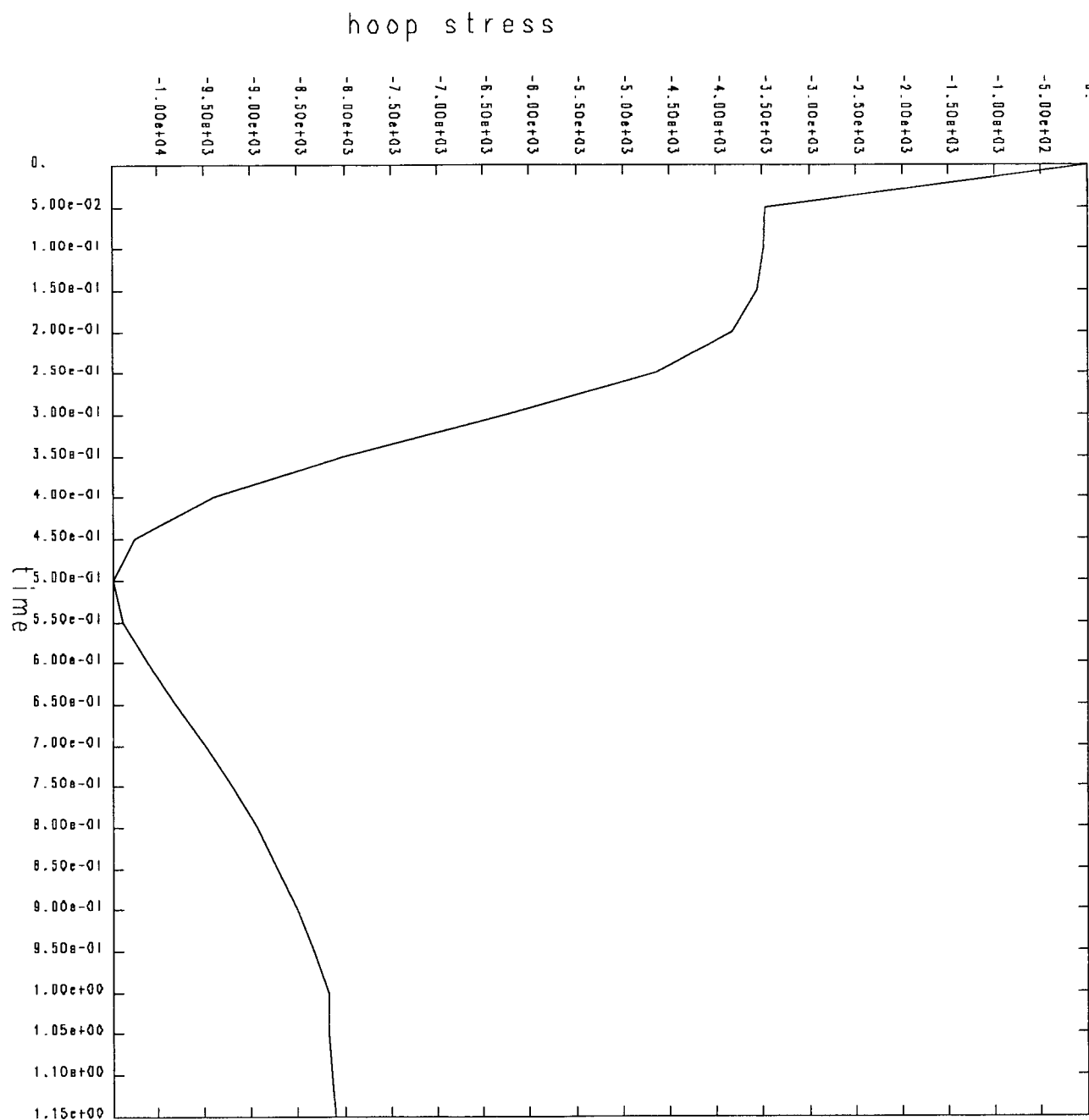
STRUCTURAL QUENCH/STEADY STATE OPERATION - AL. COLLAR 4-2-87



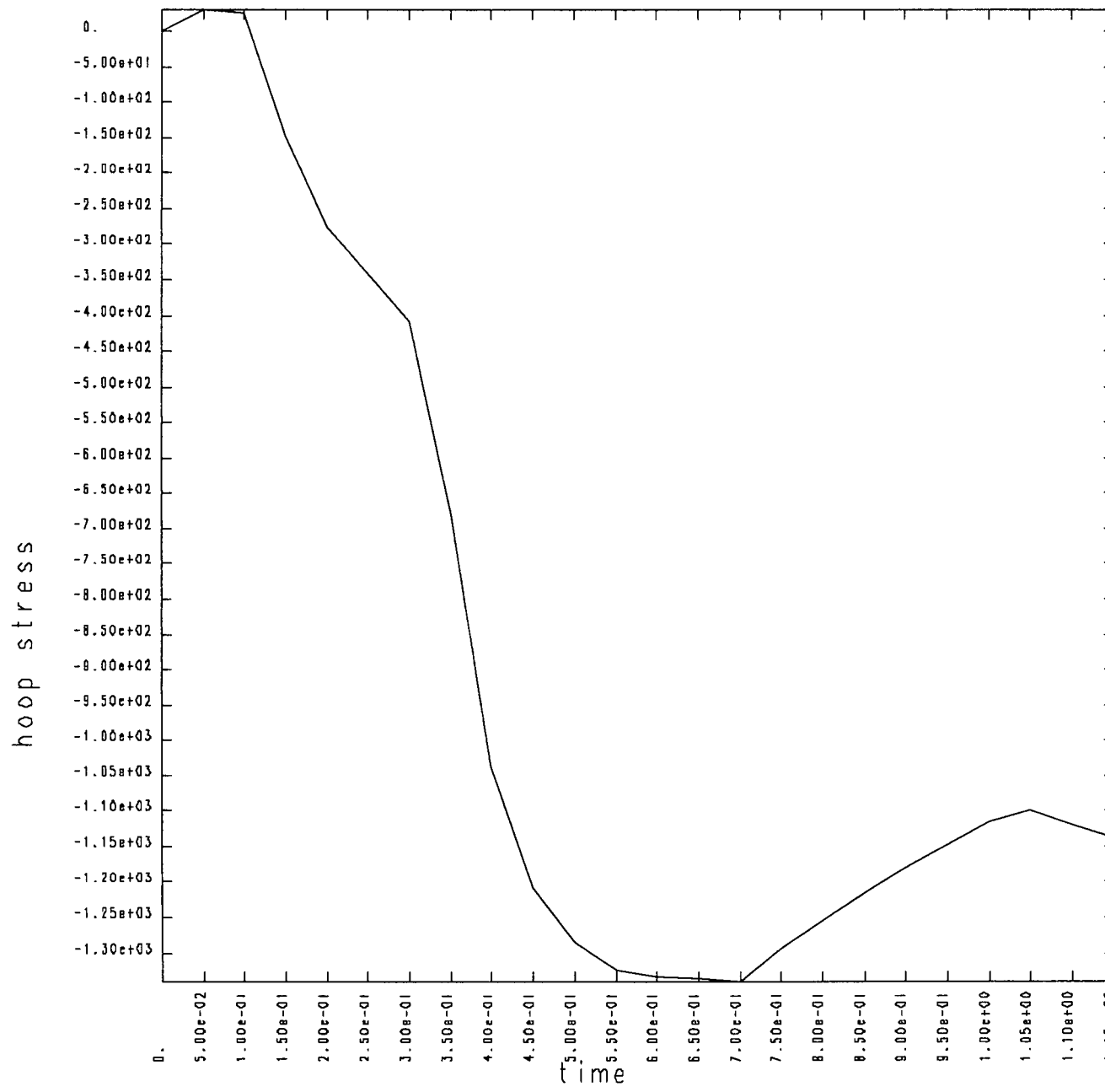
STRUCTURAL QUENCH/STEADY STATE OPERATION - AL. COLLAR 4-2-87



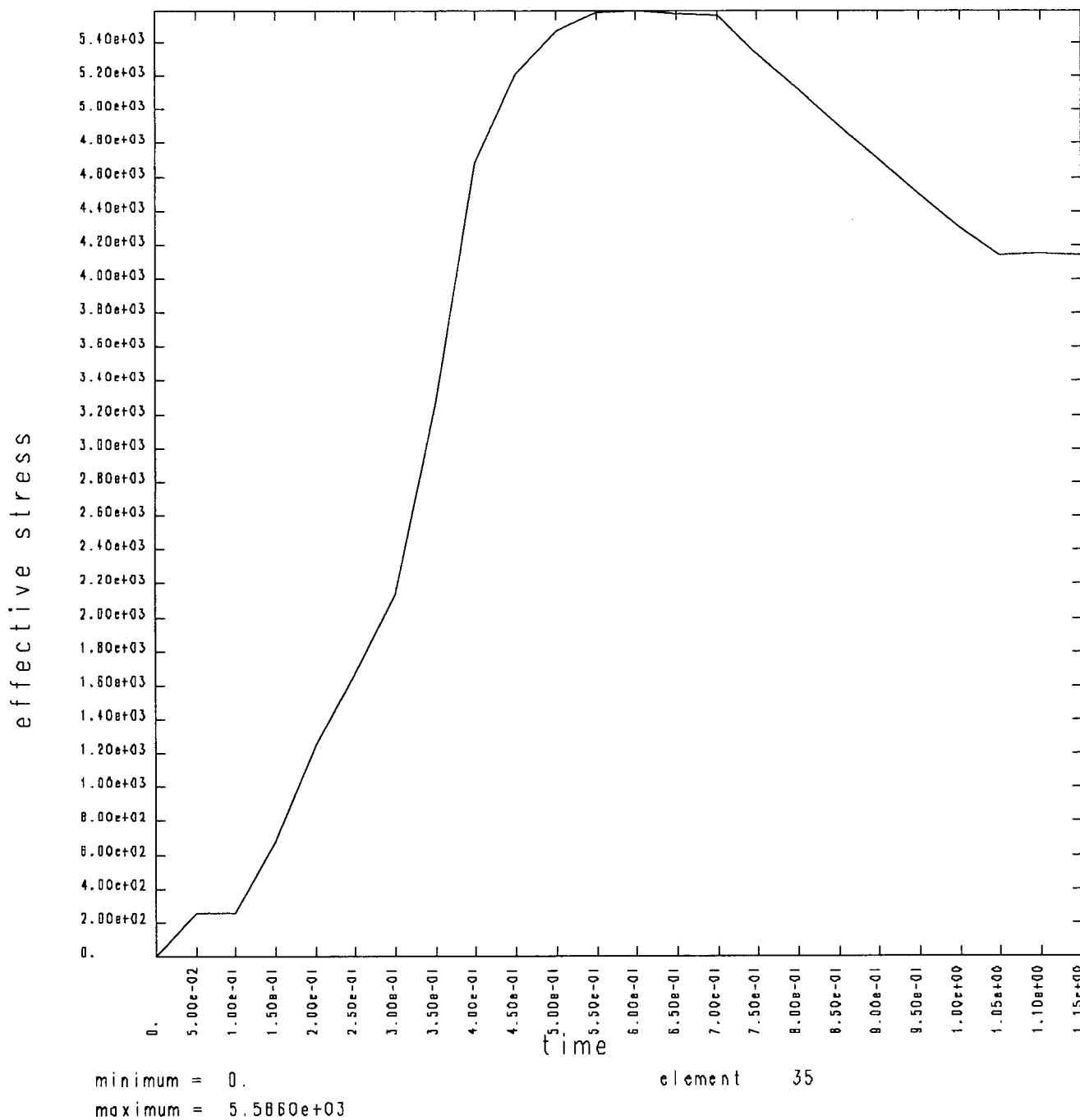
STRUCTURAL QUENCH/STEADY STATE OPERATION - AL. COLLAR 4-2-87



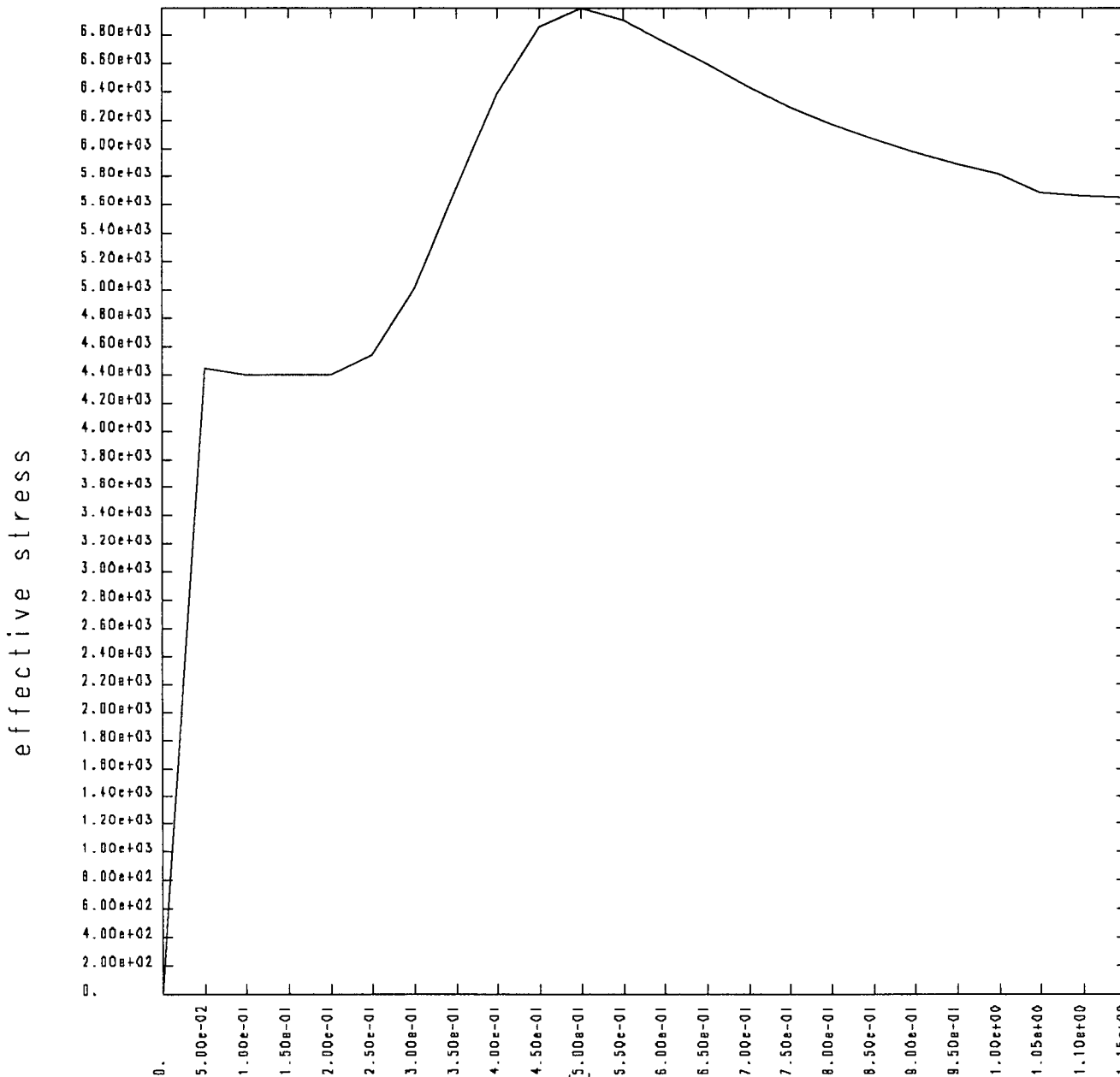
STRUCTURAL QUENCH/STEADY STATE OPERATION - AL. COLLAR 4-2-87



STRUCTURAL QUENCH/STEADY STATE OPERATION - AL. COLLAR 4-2-87



STRUCTURAL QUENCH/STEADY STATE OPERATION - AL. COLLAR 4-2-87

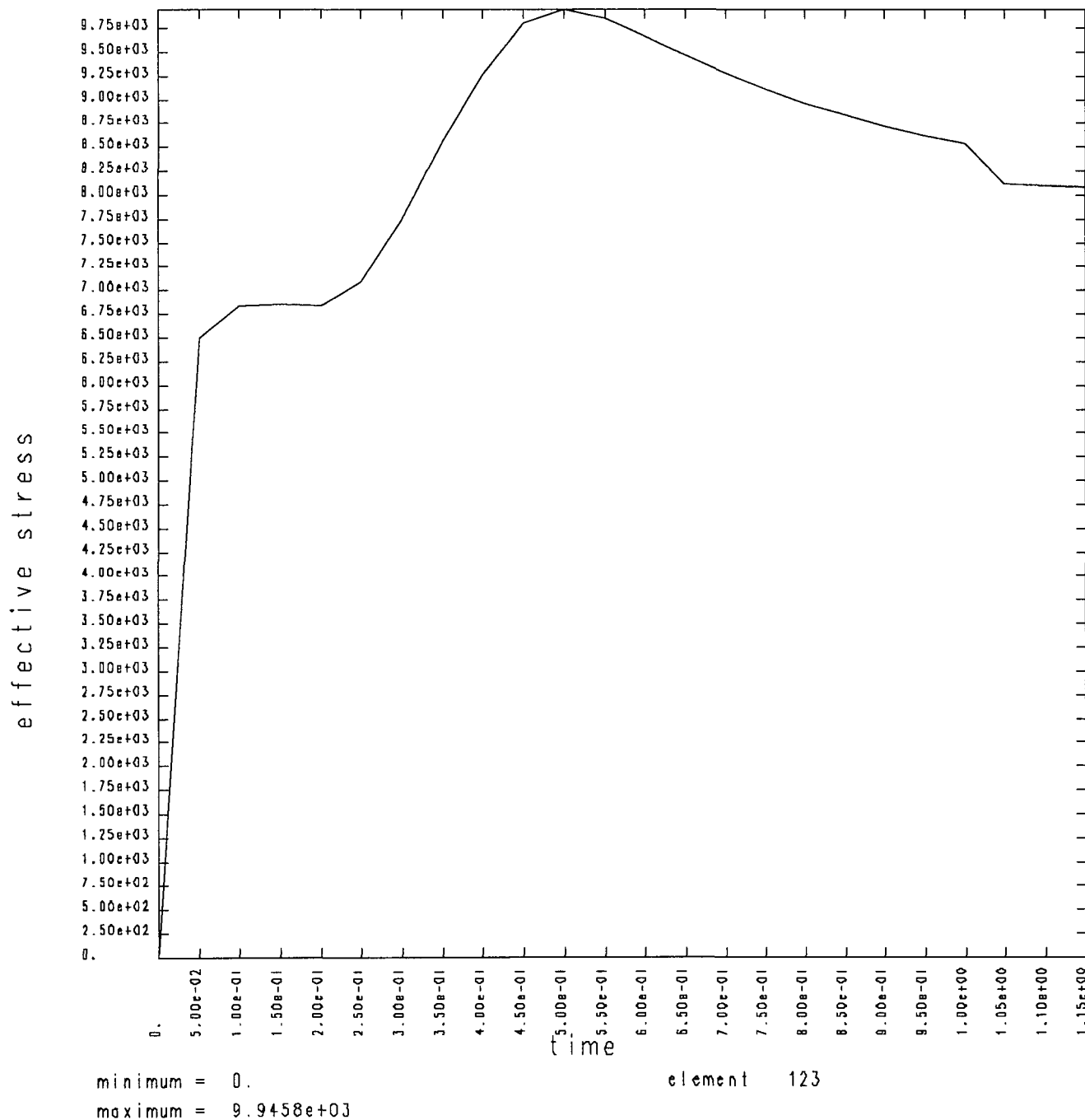


minimum = 0.

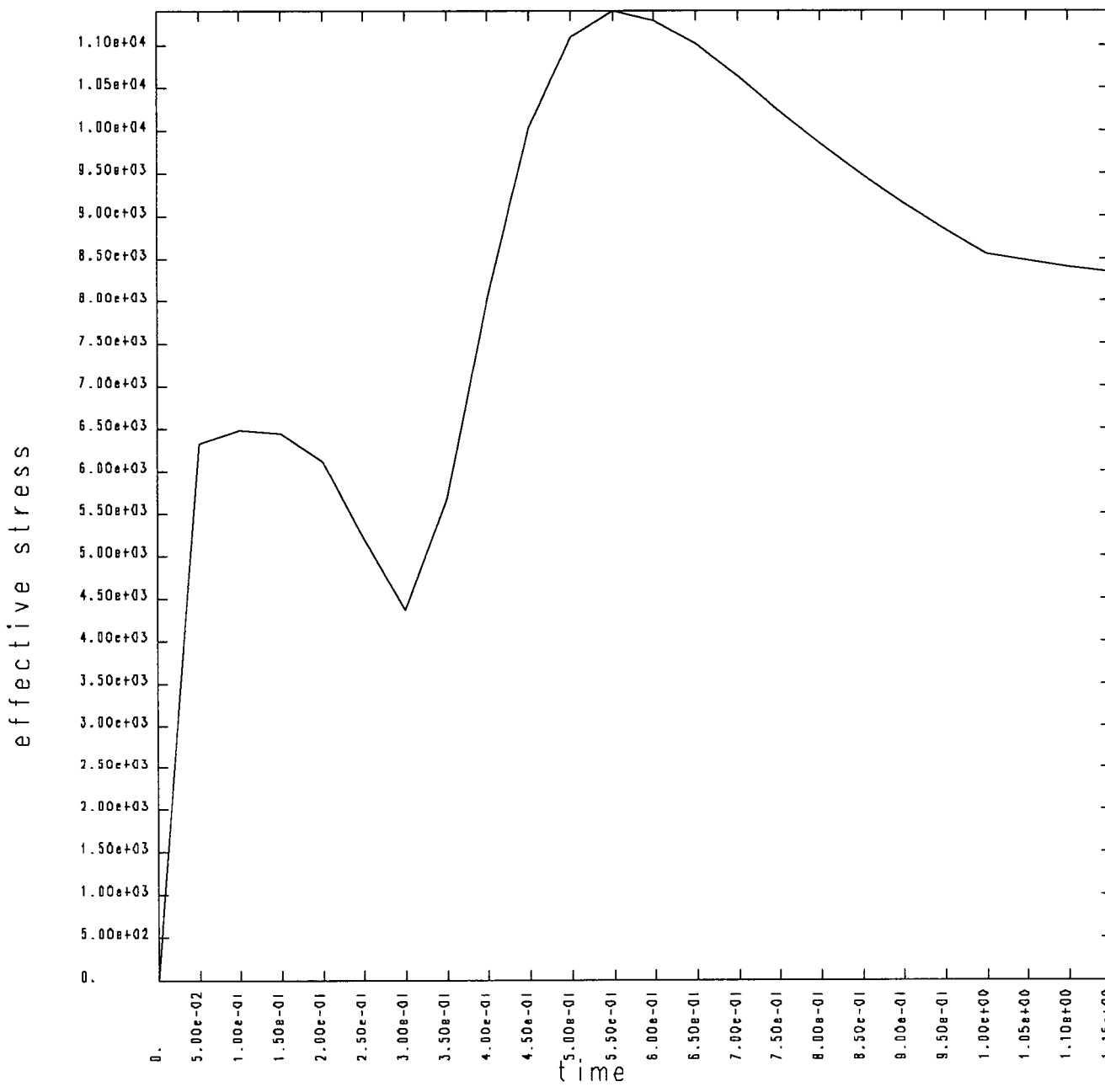
maximum = 6.9831e+03

element 142

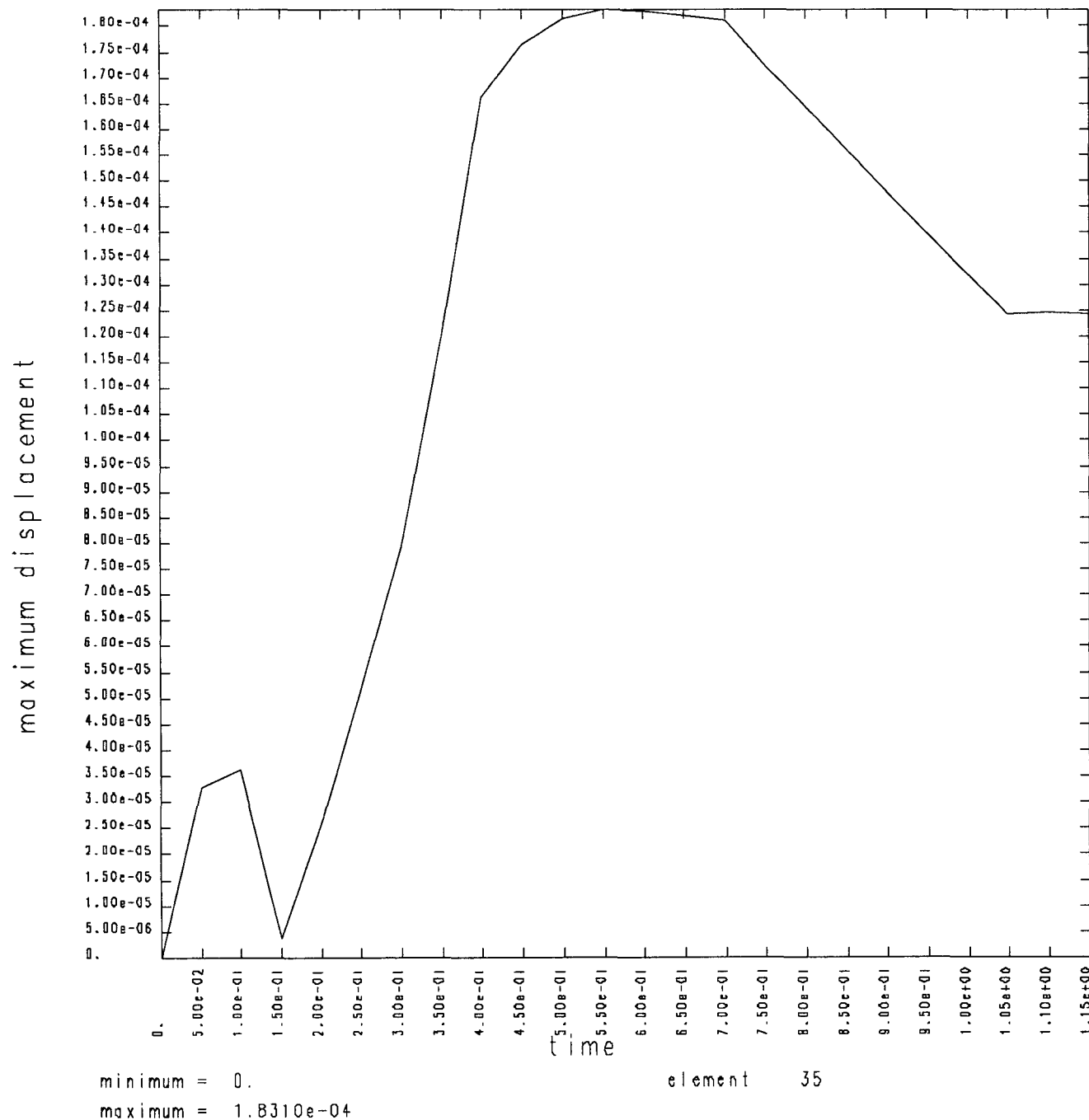
STRUCTURAL QUENCH/STEADY STATE OPERATION - AL. COLLAR 4-2-87



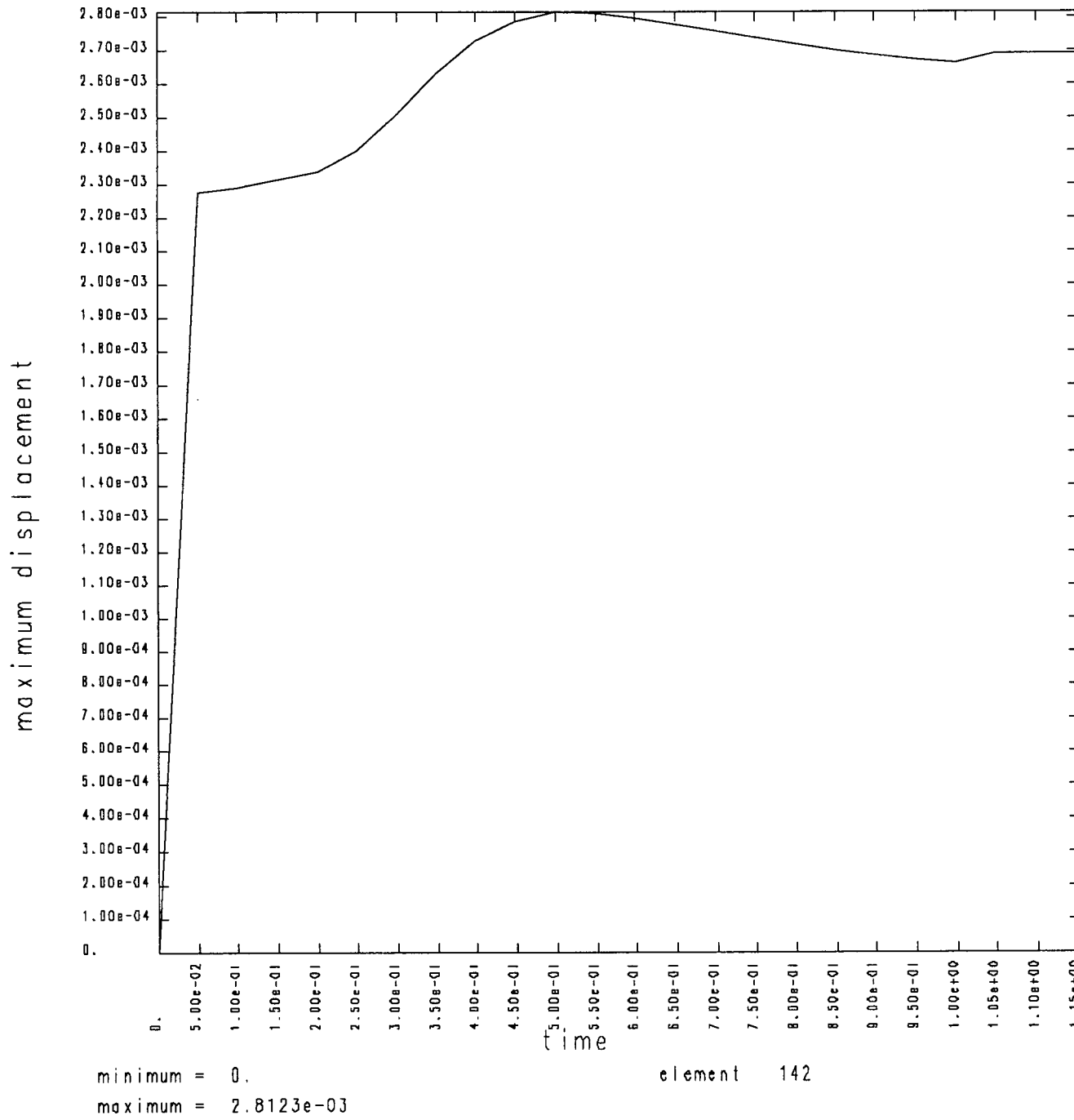
STRUCTURAL QUENCH/STEADY STATE OPERATION - AL. COLLAR 4-2-87



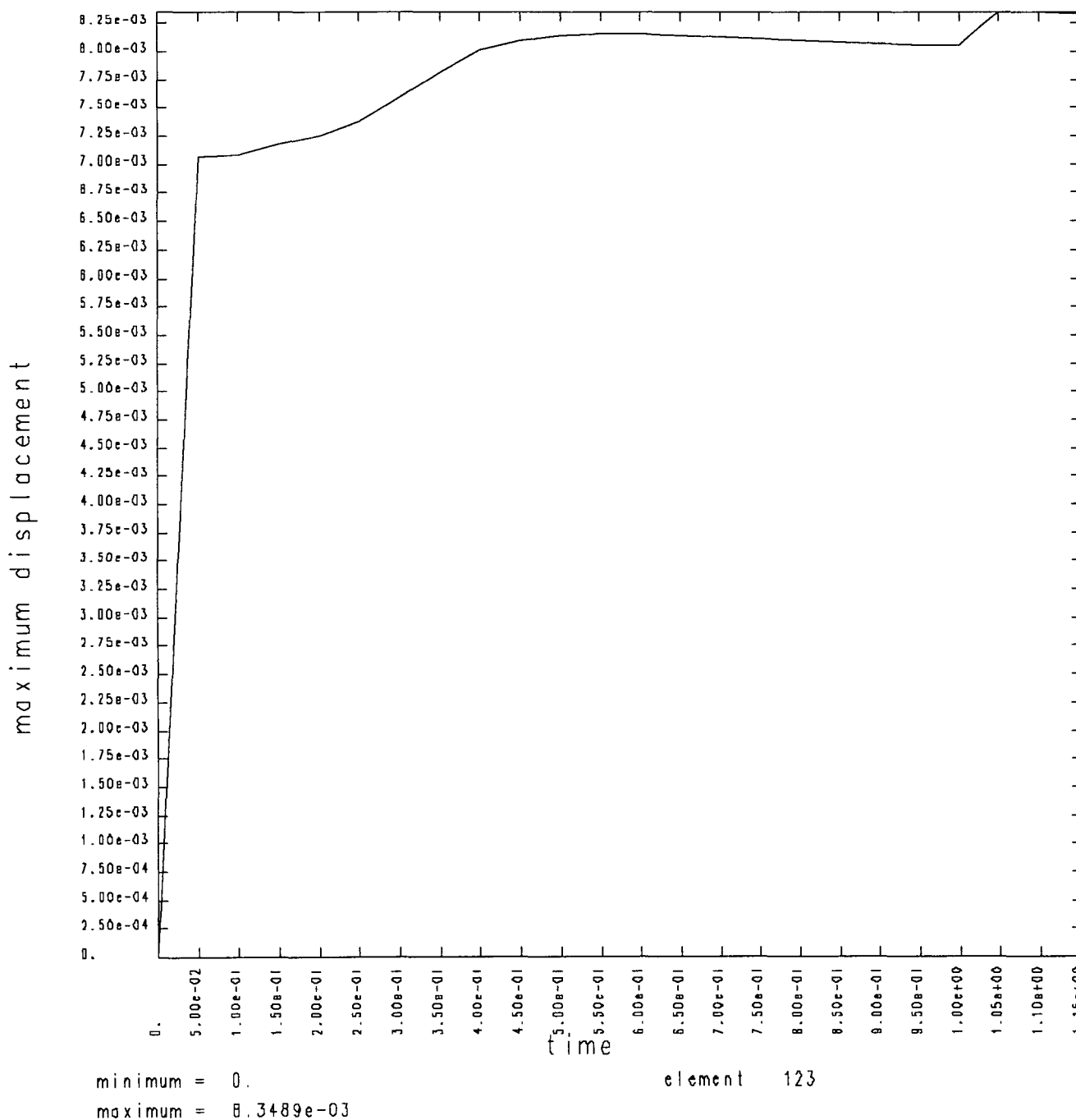
STRUCTURAL QUENCH/STEADY STATE OPERATION - AL. COLLAR 4-2-87



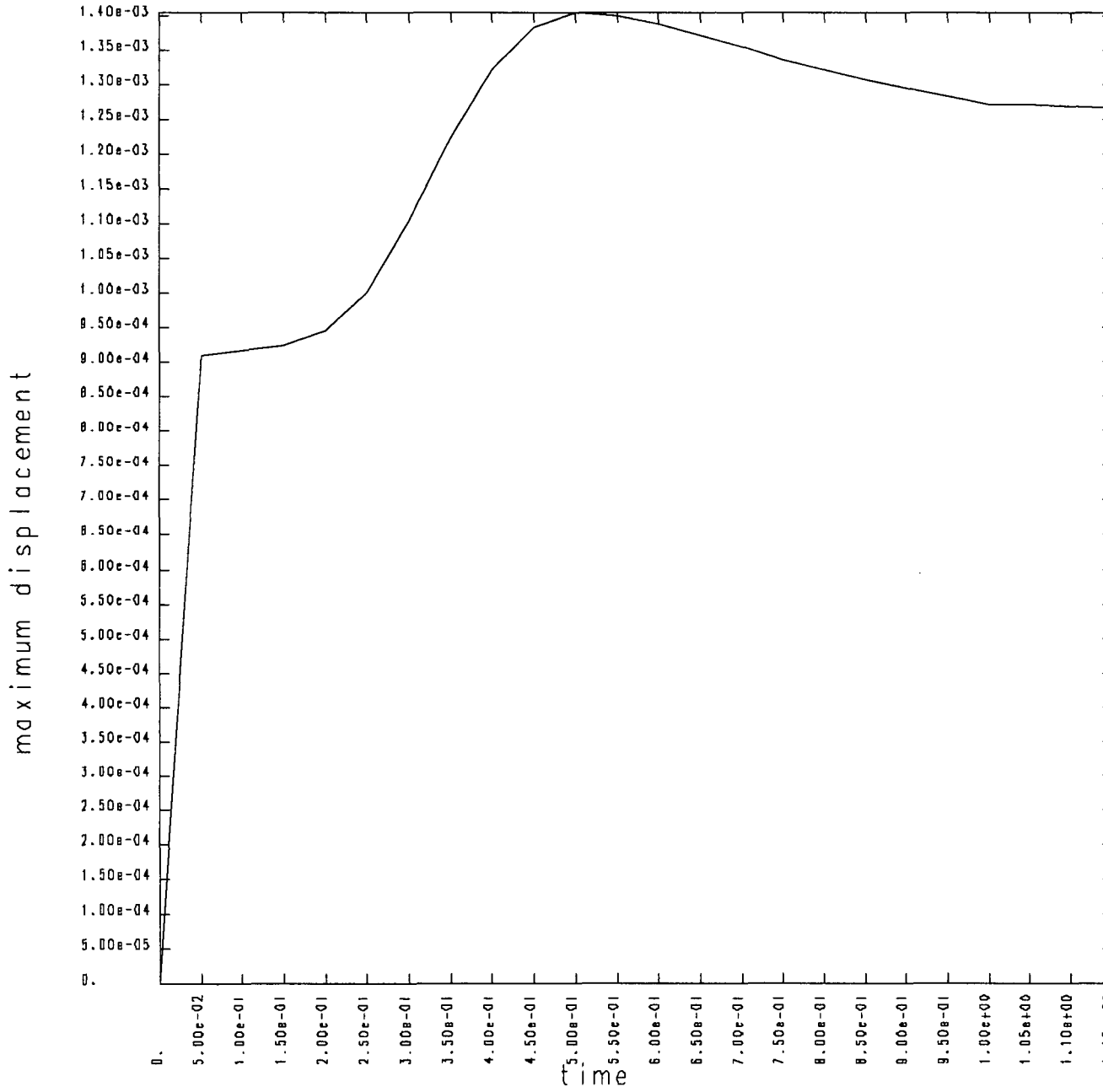
STRUCTURAL QUENCH/STEADY STATE OPERATION - AL. COLLAR 4-2-87



STRUCTURAL QUENCH/STEADY STATE OPERATION - AL. COLLAR 4-2-87



STRUCTURAL QUENCH/STEADY STATE OPERATION - AL. COLLAR 4-2-87



minimum = 0.

maximum = 1.4036e-03

element 168